NUCLEAR BINDING AND TRANSLATION REGULATION BY FMRP THROUGH NOVEL ASSOCIATED PROTEIN AND PUTATIVE RNA HELICASE MOV10

BY

MIRI KIM

DISSERTATION

Submitted in partial fulfillment of the requirements
for the degree of Doctor of Philosophy in Neuroscience
in the Graduate College of the
University of Illinois at Urbana-Champaign, 2013

Urbana, Illinois

Doctoral Committee:

Associate Professor Stephanie Ceman, Chair, Director of Research
Professor Lisa J. Stubbs
Professor Jie Chen
Associate Professor Su-A Myong

ABSTRACT

The work presented in this dissertation focuses primarily on the role of FMRP, the fragile X mental retardation protein and its role in translational regulation. More specifically, I began my studies trying to understand the role of FMRP in the nucleus. This work is novel and interesting because the nuclear role of FMRP has not been widely studied. FMRP is an RNA binding protein that is important for normal neuronal development and maturation as well as proper cognitive development as the lack of FMRP results in fragile X syndrome (FXS). I next move out of the nucleus and study the role of FMRP and translation in the cytoplasm. This work elaborates on a novel FMRP associated protein, putative RNA helicase MOV10

Chapter 1 begins with an introduction to fragile X syndrome as well as a current literature review of the fragile X field. I introduce the history of fragile X syndrome and the characteristics of the syndrome as well as introducing the key player: FMRP. FMRP is an interesting protein because it has several RNA binding domains as well as several post translational modifications. Despite all that is currently known about FMRP, there is still a large gap in understanding about how these modifications act as guides for specific RNA targeting and binding.

My first project outlined in Chapter 2 focuses on the role of FMRP in the nucleus. FMRP contains both a Nuclear Localization Sequence (NLS) as well as a Nuclear Export Sequence (NES), however how FMRP enters the nucleus is unclear because of its non-canonical NLS. I demonstrate that FMRP enters the nucleus and that it requires Tap/Nxf1 for efficient export from the nucleus. Additionally, I use the *Xenopus laevis* oocyte system to demonstrate that FMRP is indeed present along nascent mRNA transcripts suggesting that FMRP enters the nucleus and can target newly transcribed RNAs.

Next, in Chapter 3, I focus on a novel FMRP associated protein, MOV10. MOV10 is a putative RNA helicase that associates with FMRP. I demonstrate that MOV10 and FMRP associate in a salt and RNA dependent manner and that the two proteins exist in tissue in similarly sized granules suggesting a cellular interaction. We also determined that FMRP requires MOV10 to recruit a number of brain specific mRNAs and that both FMRP and MOV10 bind G quadruplex structures specifically. Using iClip, we identified MOV10 specific mRNA targets as well as identifying binding sites of MOV10. We also found that Ago2 binding sites

influenced the fate of MOV10 clip targets, suggesting a role of MOV10 acting as a facilitator or inhibitor of miRNA mediated regulation depending on proximity to Ago2 binding sites.

Chapter 4 develops a novel single molecule study directed towards understanding how MOV10 behaves as a helicase. I generated mRNA constructs to study G quadruplex forming RNA sequences at the single molecule level and establish that sc1and sc1 mutant RNAs behave different in salt solutions. In addition to studying sc1 and sc1 model RNAs, I expanded the study to encompass hASH1, a recently identified FMRP mRNA target that contained tandem GQ sequences near the 5' cap, and also PSD-95, a well established FMRP target. Through the efforts of this chapter, it will be possible to continue to further elucidate the behavior of MOV10 on target mRNAs identified through the iCLIP studies.

In Chapter 5, I explore the role of MOV10 in the 5'UTR of mRNA targets. Chapter 3 focused more on the role of the 3'UTR and miRNA mediated translational regulation and mRNA stability. From the data generated from the iCLIP studies, we found a number of genes that are bound by MOV10 in the 5'UTR. Using hASH1 as a model mRNA target based on previously published work on FMRP and hASH1 translation, we found that upregulation of hASH1 by FMRP is dependent on the presence of MOV10. These studies demonstate that MOV10 may also play a significant role in translation through the 5'UTR through a mechanism that is independent of the miRNA pathway.

ACKNOWLEDGEMENTS

First and foremost, I would like to thank my thesis advisor, mentor, and friend Dr. Stepahnie Ceman. You have been an inspirational, charismatic, enthusiastic scientist whose passion for research I hope to foster in the future. I cannot thank you enough for the privilege of joining your lab and also for giving me the opportunity to develop as a young scientist. Thank you for instilling in me a "fire for science" that will never die out. I will miss our coffee runs, random impromptu meetings in front of the chalk board, and I am glad that we were finaly able to get you the advisor of the year award!

I am also incredibly grateful to the members of my committee: Drs. Jie Chen, Sua Myong and Lisa Stubbs. Your suggestions, support and conversations have been so encouraging over the years and have truly guided many of the new and exciting directions of my project. Additionally, I am thankful for all the other mentors during the PhD: Drs. Maria Spies, Michel Bellini and Peter Jones for their support and constant enthusiasm just to name a few. I have only benefitted from your involvement in my graduate career.

Thank you to all the current and former members of the lab, to Drs. Anne Cheever, Tory Blackwell, and Claudia Winograd for welcoming me into the lab and tolerating all my (silly) first year questions. To soon to be PhDs Geena Skaria and Phil Kenny, thank you for all the random and interesting conversations, it has been an enormous pleasure mentoring you and also learning from you. I cannot wait to see what the future has in store for you. Thank you to my fantastic undergrads, especially Mohamed for patiently enduring the meandering path of research, in between my hectic schedule and moments of insanity.

I cannot even begin to thank all my friends and colleagues I have crossed paths with along the way, old friends and new friends, you have all helped me get through a challenging and interesting time in my life! June, Janet, Nat—you ladies have been fantastic and supportive and I have no idea what I would have done without you. We may be states and countries apart, but you are all near and dear to me. To Drs!!!!! Helen Hwang, Christine Yang, Sarah Holton, and Tracy Flood: I have no idea how I would have survived without you around to make things awesome. Vincent Chan, Song Jiang, Jaeyun Sung, and to so many others— thanks for being great friends and fantastic troubleshooting buddies. I enjoyed all our lunches and coffee breaks. Special thanks to David Jun for being supportive and understanding. I am so glad that we made each others graduate experiences exciting and I am thankful for the time we spent to help each other succeed.

Lastly, I want to thank my family for their endless support and patience as I ventured down this long and seemingly endless journey. Mom and dad, you guys have patiently tried to understand and be interested in my research and it has been fun trying to explain to you what I work on, but most of all, I am appreciative of all your unending love and care. Thank you for packing me so much food over the years and helping me around the house. Thanks to my sister and brother, Mihwa and Youngin, for all the random crazy adventures we have been on. I am looking forward to many many more adventures to come.

And Grandpa—I miss you.

TABLE OF CONTENTS

Chapter 1. Fragile X Mental retardation protein: Past, present and future

This chapter has been previously published in part as "Fragile X Mental Retardation protein: Past, present and future" (Curr Protein Pept Sci. 2012 Jun;13(4):358-71). Permission to reprint the material has been provided by the publisher.

1.1 Fragile X Syndrome

Fragile X Syndrome (FXS) was first described by Martin and Bell after characterizing families with males with intellectual disability [1]. In 1969, Herbert Lubs observed a constriction on the X chromosome in males with Martin-Bell syndrome. These constricted sites were called "fragile" sites on the X chromosome due to their propensity to break [2]. However, this constriction was not a reliable predictor of Martin-Bell syndrome until Southerland and colleagues described a way to increase the occurrence of the fragile site by using folate-deficient media [3]. The possibility that a gene existed within this fragile site led to the cloning and final discovery of the fragile X mental retardation gene, FMR1, in 1991. The source of the fragile site was a CGG repeat expansion in the 5' Untranslated Region (UTR) of the FMR1 gene [4]. The gene product of FMR1, the Fragile X Mental Retardation Protein FMRP, was characterized as an RNA binding protein soon after [5].

Expansion of the CGG repeat in the first exon of the FMR1 gene is the cause of FXS--one of the first trinucleotide repeat disorders described (reviewed in [6]). It is now known that there are several other disorders caused by trinucleotide repeat expansions in both UTRs, as in myotonic dystrophy, and in coding regions, such as Huntington's disease and a number of spinocerebellar ataxias [6]. The FMR1 gene is 38 kb in size, containing 17 exons and encoding a 4.4 kb mRNA transcript containing a G-quadruplex in the coding region [7]. The average CGG repeat length is 6-44 with a mode of 30 [8]. Repeats within that range are stably transmitted from generation to generation. Grey zone alleles with repeats between 45-54 and premutation alleles with 55-200 repeats are highly unstable and prone to expansion during maternal transmission [8].

Mechanisms of expansion

The CGG repeat expansion occurs predominantly during maternal meiosis, although the reason for this gender bias is currently unknown [8]. Three potential mechanisms for repeat expansion have been proposed including recombination, replication, and repair (reviewed in [9]). It is thought that the trinucleotide repeat forms a stable secondary structure during replication, causing the DNA polymerase to skip or stall during replication, leading to repeat expansion. The leading and lagging strands form hairpin structures with Watson Crick base pairing or mismatched pairing based on the sequence, which would ultimately result in compromised DNA repair [10-12]. Recently, a crystal structure of the CGG repeat has been solved, demonstrating the complex nature of the CG and GG base pairing and stacking to form a stable pseudo helix [13]. This highly stable structure may stall the DNA polymerase at the replication fork, causing problems with re-initiation and repair [11]. During DNA replication, the CGG repeat causes slipping of the three-way DNA junction, which causes the repair machinery in the cell to continuously add a few repeats, gradually expanding the repeat over time [10]. Once the number of repeats exceeds 200, the FMR1 gene is abnormally hypermethylated, causing chromatin condensation and subsequent gene silencing. Thus, individuals with FXS express no FMR1 mRNA and consequently, no FMRP.

Other causes of FXS

While repeat expansions are the most common cause of FXS, other mutations within the gene that compromise protein function or perturb gene expression will also lead to the syndrome. One of the most striking examples of fragile X syndrome due to a point mutation is the isoleucine to asparagine (I304N) substitution in the KH2 domain [14]. Recent studies by Collins and colleagues used massively parallel sequencing of developmentally delayed males without CGG repeat expansion to discover mutations in the *fmr1* promoter region as well as a novel variant, R138Q, present within the nuclear localization sequence of the protein [15]. Interestingly, this residue is highly conserved among many species. Additional studies by Collins and colleagues found a deletion in the *fmr1* gene beginning 220 bases upstream of the CGG repeat, spanning 355 bases into the second codon of the FMR1 coding sequence [16]. This mutation resulted in the absence of FMRP expression, thus resulting in FXS without repeat expansion. These mutations demonstrate the necessity for expression of a fully functional

protein--one that can shuttle and localize properly, as well as bind and recognize mRNA properly. The consequences of improper localization and RNA binding will be discussed in more detail below.

1.2 Fragile X premutation syndromes

The prevalence of premutation carriers in the population is about 1:130-250 for females and about 1:800 males [17]. While functional FMR1-encoded protein, FMRP, is produced in these individuals, premutation carriers are also expressing an FMR1 transcript with an expanded CGG repeat. Premutation alleles can produce two distinct syndromes including a parkinsonian-like tremor-ataxia referred to as fragile X-associated tremor/ataxia syndrome (FXTAS) and premature ovarian insufficiency, termed fragile X-associated premature ovarian insufficiency (FXPOI). FXTAS was first described in 2001 in male premutation carriers as a late onset neurodegenerative disorder (reviewed in [18]). Individuals diagnosed with FXTAS develop progressive intention tremor and cerebellar gait ataxia as well as memory deficits and emotional changes [19, 20]. Females generally present less frequently and with less severe clinical phenotypes than males who have FXTAS [21]. In FXPOI, up to 23% of women reach menopause prior to the age of 40, and even as early as in the teenage years, in contrast to the general population where the risk is about 1% [22]. The extent of ovarian dysfunction depends on the length of the repeat expansion as well as the age of the individual, increasing in severity with increasing repeat length and progressing age [23].

The mechanism behind how premutation alleles cause disease is not well understood. FMRP is expressed at slightly reduced levels; however, there is increased transcription of the FMR1 mRNA, suggesting a toxic gain of function [24]. Over-expression of the FMR1 mRNA may disrupt proper cellular function due to the expansion of the CGG repeat, causing RNA toxicity and the accumulation of intranuclear inclusions in neurons and astrocytes [24, 25]. One model is that the accumulation of CGG repeats in the mRNA sequesters proteins away from their designated tasks. Analysis of the protein content of intranuclear inclusions in FXTAS showed that hnRNPA2/B1, CUGBP1, and Sam68 were consistently found in these inclusion bodies [26-29]. Presumably, the paucity of these proteins from their normal sites of activity leads to development of either FXTAS or POI.

1.3 Features of FXS

FXS presents with characteristic behavioral and physical features. The incidence of FXS is 1 in 4000 males and is about half as frequent in females, who have varying degrees of FXS depending on compensatory levels of the unsilenced normal allele. FXS is characterized by developmental delays and intellectual disability. The average IQ in males is around 40 points and in females, around 70 or 80 points due to the X-linked nature of this syndrome. There is high co-morbidity with autism, as FXS is the most common monogenic cause of autism. Approximately 25% of fragile X males will qualify as fully autistic while a high majority will demonstrate some phenotypes that fall under the ASD umbrella. Females are less affected, with less than 7% with autism [30].

It is common for individuals with FXS to have language delays. During normal language acquisition, first words are usually uttered around 12 months of age. Fragile X individuals generally utter their first words between the ages of 18 months and 3 years [31]. Males generally acquire language later than fragile X females. FXS language deficits also include deficiencies in receptive language as well as expressive language. In studies of conversational skills, fragile X individuals took a reduced number of turns and had more difficulty maintaining extended communication [32]. Another interesting aspect of language development in FXS is the presence of repetitive language. Individuals demonstrate perseverative language, repeating words that have been said to them, as well as echolalia, which is repetition of words spoken by themselves [33-35].

In addition to their cognitive and behavioral patterns, individuals with fragile X syndrome have subtle yet distinct features (reviewed in [36]). FXS presents with mild craniofacial abnormalities and mild connective tissue abnormalities. These individuals are difficult to diagnose early in age as the features accumulate over time. Adult males have long faces with an enlarged head circumference and prominent forehead and jaw, large ears, as well as high arched palate. After puberty, FXS males develop macroorchidism, or enlarged testicular volume, in excess of 25 mL [37]. They also have features of a mild connective tissue disorder, which can include velvet-like skin, hyperextensible joints, flat feet and mitral valve prolapse [37-39].

FXS dendritic phenotype

All of these cognitive and behavioral differences suggest that at a cellular level, there are changes in the connectivity of neurons in the brain. Post mortem samples of FXS brains and also from Fmr1 KO mice have shown that there is an excess of long and immature dendritic spines compared to age matched normal controls. Filopodia are the precursor structure to developing dendritic spines, suggesting that FXS is a problem of proper dendritic maturation from the filopodia to mature spines. Studies done in *Drosophila* demonstrated that *dfmr1* mutants developed mushroom body neurons with an excess of branching, which is not usually observed in WT flies [40]. Conversely, overexpression of dFMRP resulted in the opposite morphology, yielding reduced complexity of dendritic branching and arborization [40].

Because FMRP is present in the dendrites, it is not surprising that in its absence, there is a neuronal phenotype. FMRP expression itself is dependent on synaptic stimulation [41]. In isolated synaptoneurosomes, FMRP was rapidly synthesized in response to metabotropic glutamate receptor (mGluR) signaling [42]. As synapse maturation is dependent on protein synthesis, FMRP plays an important role in the proper development and maintenance of synapses. In addition to the spine phenotype, Fmr1 knockout animals also demonstrate enhanced long term depression (LTD) in response to mGluR signaling when compared to wild type animals [43, 44] suggesting that FMRP functions as a regulator of translation at the synapse, and is especially important for mGluR signaling, which will be discussed in more detail below. FMRP also plays a role in regulating actin polymerization and also modulates MAP1B RNA translation in response to synaptic stimulation [45-47].

1.4 FMRP

FMRP belongs to a small family of RNA binding proteins, consisting of FMRP, FXR1P, and FXR2P. These proteins have about 70% sequence homology and each family member is capable of homo- or heterodimerization [48]. FMRP is expressed ubiquitously throughout the body, but not in muscle tissue [49]. FMRP has elevated expression in the brain and testes. In the brain, FMRP is highly expressed in cortex and hippocampus as well as abundantly expressed in the granule cell layer in the cerebellum [50, 51]. In neurons, FMRP is expressed throughout the cell, throughout the cell body and in the dendrites. FMRP is also present in axons, but at a lower

level [52]. Because FMRP contains several RNA binding domains as well as protein interacting domains, FMRP can form several messenger ribonucleoprotein particles (mRNPs) and associate with a large collection of proteins and RNA, allowing FMRP to take on many different roles as both a transport molecule as well as a regulatory molecule. The exact mechanism behind how FMRP specifically regulates its target mRNAs is still unknown and is a question of great interest. Some possibilities include binding mRNAs to expose start sites for translation, controlling localization, influencing mRNA stability, and also association with the microRNA (miRNA) pathway have been suggested and will be described in more detail below.

FMRP RNA binding domains

FMRP is an RNA binding protein containing three RNA binding domains consisting of two hnRNP K-protein homology domains (KH) as well as an Arg-Gly-Gly (RGG) box [53]. Currently, no specific RNA substrates have been identified for the KH1 domain while the KH2 domain binds a complex double stem loop structure called a kissing complex that was identified in SELEX experiments [54]. FMRP has been shown to co-immunoprecipitate with components of the miRNA pathway, including precursor miRNAs and a number of mature miRNAs [55, 56]. While the specific binding target of the KH domains has not yet been completely explored, it is of great interest to determine the miRNA binding capabilities of FMRP itself. The importance of the KH2 domain in normal FMRP function was underscored when an individual with extreme features of FXS was found to have a single point mutation in the KH2 domain, substituting an isoleucine to an asparagine (I304N) [14]. The I304N FMR protein does not associate with translating polyribosomes and is deficient in several tests of RNA binding, suggesting gross misfolding of the protein as well as inappropriate protein localization and RNA binding [57]. This mutation describes the necessary role of RNA binding as well as proper localization for FMRP to perform its designated tasks. Accordingly, an I304N knockin mouse has features similar to the Fmr1 knockout mouse [58].

In addition to the KH domains, FMRP and FXR1P contain an RGG box; however the FMRP RGG box has been demonstrated to be unique among the family members because of its ability to bind G-quadruplexes with high affinity [59-61]. G-quadruplexes are very stable secondary structures found in both RNA and DNA formed by the stacking of guanine (G) tetrads. Intramolecular G-quadruplexes in RNA are important regulators of translation that inhibit

ribosomal scanning. The RGG box is the high affinity RNA binding domain of FMRP [7, 60]. Accordingly, removal of the RGG box disrupts association of FMRP on translating polyribosomes, shifting the protein to the free protein fraction and lower polysome fractions [62, 63]. Further evidence that the association between FMRP and polyribosomes is RNA dependent is that FMRP--as well as the other fragile X family members—can be competed off polyribosomes by addition of the kissing complex RNAs [54]. The RGG box binds G-quadruplex structures and has been demonstrated to bind a G-quadruplex containing RNA, sc1, with nanomolar affinity; however, similar to the kissing complex RNA, the sc1 sequence per se has not been identified in an mRNA and was identified in SELEX experiments [54]. FMRP-associated mRNAs bear G-quadruplexes in their 5'UTRs, coding sequences and 3'UTRs. A number of the mRNAs bound by FMRP have been found to contain G-quadruplexes, such as its own mRNA message, FMR1, and other mRNAs such as MAP1b, PSD-95, and semaphorin 3A [47, 64, 65]. The interaction between FMRP and some of its target mRNAs has been biochemically confirmed to be mediated by G-quadruplexes by several groups [7, 64, 66]. Another well studied target is the amyloid precursor protein, APP. APP has a G-rich region located within the coding sequence and was also found to be regulated in an mGluR mediated manner [67]. A recent study demonstrated that mGluR activation resulted in the release of APP mRNA from an FMRP-containing mRNP, resulting in increased translation of APP [68]. FMRP binding to G-quadruplexes may help direct mRNAs bearing them to various locations throughout a neuron, or even within subcellular granules to facilitate translation or maintain an un-translated state of the mRNA.

FMRP also binds to uracil (U)-rich tracts along mRNA [46, 69, 70]. In a recently characterized mRNA target, the 5' UTR of human Achaete-scute, FMRP bound the U-rich region of the mRNA and also mediated translational upregulation of a reporter construct bearing the 5'UTR [70]. How FMRP increases the translation of this reporter is a question of great interest as FMRP is largely thought of as a translational repressor, although there is evidence for its role as an activator [71]. Another RNA motif that is bound and recognized by FMRP is a novel three stem loop structure called SoSLIP that is present in the 5'UTR of the Sod1 mRNA [72]. This mRNA forms a three-stem loop structure, SoSLIP, that negatively regulates translation until FMRP binds it to open the structure, which exposes the initiator codon of the

mRNA, thus increasing expression of Sod1. The region of FMRP that binds Sod1 has not yet been identified; however the C-terminal domain is thought to provide this function [72].

Several lists of FMRP-bound mRNAs have been generated over the years, using a variety of techniques to identify the associated mRNAs including microarrays, hybridization to RNA arrays, and high throughput sequencing [71, 73]. Over 400 targets have been identified by a number of groups, but only a small handful of mRNAs have been studied in depth. A recent paper published by Darnell et al identified FMRP-associated RNAs in brain using High throughput Sequencing and Cross-linked Immunoprecipitations (HITS-CLIP). 24% of the RNAs were also present in the list generated by Brown and colleagues, while a number of the novel RNAs found were involved in the pathogenesis of autism [74]. Interestingly, HITS-CLIP revealed that FMRP bound along the length of the mRNA, with a majority of FMRP associated with the coding region. Almost a third of the FMRP bound to RNA was found in the 3'UTR, and a small percentage of FMRP was found to be bound to the 5'UTRs. Given that the targets were selected from polyribosomal fractions, it is not surprising that the majority of FMRP is found along the coding region. FMRP was found to play a role in stalling ribosomes.

In addition to finding FMRP primarily bound to coding region, this study is also remarkable because of the lack of specificity demonstrated by FMRP in its ability to bind multiple sites in the coding region of an mRNA. G-quadruplexes were no more enriched in the FMRP-associated mRNAs than in the control immunoprecipitations. One explanation for this observation is that Darnell and colleagues chose to study FMRP-mRNAs isolated from polyribosomal fractions in the brains of adult mice instead of choosing from the entire pool of FMRP-associated mRNA complexes in the brain. It is possible that specificity in this fraction was limited because FMRP also associates with translating ribosomes, which would correlate well with the data showing FMRP enriched along the coding region of RNA. Significantly, FMRP is present in several other cellular components such as the nucleus, and contained within stress granules and processing bodies (P-bodies), which were not examined in this study. Perhaps the motifs that FMRP would recognize to recruit RNA to other cellular compartments would be different than the motifs that would recruit mRNA bound by FMRP to the translational machinery. In fact, FMRP has been shown to bind ribosomes, thus, its RNA binding specificity in this compartment might be minimized [75]. For example, because G-quadruplexes are translationally inhibitory structures in mRNA, FMRP may potentially bind G-quadruplexes to

localize quiescent mRNA to P-bodies for storage in a translationally silent state. Alternatively, FMRP binds some or all of its mRNAs in the nucleus [76]. Perhaps in that compartment, FMRP binds mRNAs through specific motifs. Since FMRP can directly bind ribosomes [75], isolating it from polysomes reflects a pool of FMRP that is associated with many different mRNAs. In addition, FMRP also plays an important role in neuronal differentiation and development throughout embryonic development into adulthood. The use of juvenile mice, as the Darnell group did, would also generate a significantly different population of bound mRNA than isolating FMRP-mRNA complexes from embryonic or adult animals.

Posttranslational modifications of FMRP

FMRP is a dynamic protein with many different functions. FMRP associates with a number of proteins and can form a diverse range of mRNA-containing particles. FMRP is also found in many different subcellular compartments such as the nucleus, stress granules, P-bodies, and also in various regions of a cell, which is especially significant in highly polarized cells like neurons. Appropriate localization of mRNA targets from the cell body to the dendrite or axon as well as activity-dependent translation of mRNAs upon stimulation is important for proper development and maintenance of synapses. Post-translational modifications offer an additional mechanism for regulating FMRP function (Table 1).

Methylation of FMRP

The chemical modification of methylation serves two very distinct roles in FMRP function and pathogenesis. DNA methylation is present in the full mutation of FXS, resulting in chromatin condensation and silencing of the FMR1 gene [77, 78]. At the protein level, FMRP is posttranslationally modified on arginines comprising the RGG box [79, 80]. These arginines are mono and asymmetrically dimethylated suggesting that specific protein arginine methyl transferases (PRMTs) act on FMRP, namely, PRMT1, PRMT3, PRMT4 and/or PRMT6 based on the pattern of methylation and localization in the cell [79].

RGG box arginines 533, 538, 543, and 545 are methylated on murine FMRP in cells, and it was demonstrated that arginine methylation reduced the affinity of FMRP for a subset of RNAs [63]. In a recent study, the arginine residues were substituted to examine their effect on

polysome association and binding to either the model G-quadruplex RNA sc1 or to AATYK, the second most common RNA immunoprecipitated with FMRP from brain [71] and that contains a putative G-quadruplex. Blackwell and colleagues found that arginines 533 and 538 were required for normal polysome association, suggesting that their substitution led to a disruption in RNA binding. In contrast, association with AATYK did not require arginines at positions 533 and 538. In addition, methylation of 533 and 538 inhibited binding to sc1 but their methylation had no effect on binding to AATYK [63]. These results suggest that differential methylation of FMRP can confer binding specificity for different RNA molecules. To further support the importance of these specific residues for RNA binding, a recent study by Phan and colleagues examined the binding requirements of the minimal FMRP RGG box to sc1 and obtained an NMR structure. Residues 533 and 538 were important for coordinating residues in the sc1 quadruplex stemloop junction while other arginine residues in the RGG box may be important for binding different types of G-quadruplex structures [63, 81].

Phosphorylation

In addition to methylation, FMRP is phosphorylated in cells [82]. A conserved phosphorylation site on FMRP is present in both human and *Drosophila* FMR proteins at serine 500 and serine 406 respectively [82, 83]. These serine residues act as the primary phosphorylation site on FMRP, triggering the phosphorylation of flanking serines [82]. The primary phosphorylation site of FMRP is about 30 amino acids N-terminal to the RGG box however, phosphorylation of FMRP does not influence RNA binding abilities [82]. Rather, phosphorylation seems to act as a switch between actively translating polyribosomes and stalled untranslating polyribosomes, suggesting that phosphorylation regulates the step of elongation where removal of the phosphate group signals to resume translation. In studies using point mutations of FMRP such that it mimics constitutively phosphorylated FMRP and unphosphorylated FMRP, it was found that phosphorylated FMRP was more resistant to ribosomal runoff than unphosphorylated FMRP suggesting that unphosphorylated FMRP is associated with actively translated polyribosomes [74, 82]. Phosphorylated FMRP was studied using the constitutively phosphorylated and dephosphorylated serine mutants, S500A and S500D respectively [84]. While the presence of constitutively phosphorylated FMRP had no effect on synapse strength or function, dephosphorylated FMRP showed a decrease in synapse strength as

well as a reduction in synapse number suggesting that WT FMRP exists in a dephosphorylated state in hippocampal slice cultures and was important as a post synaptic regulator at the synapse [84]. To evaluate the role of phosphorylation *in vivo,* Coffee and colleagues substituted human FMRP into an Fmr1 knockout strain in *Drosophila* to evaluate protein function. Interestingly, S500D was found to restore the protein levels as well as neural architecture at the neuromuscular junction while S500A did not [85]. Phosphomimic FMRP also rescued associative learning performance in *Drosophila* [85]. Based on these studies, postsynaptic FMRP is important for proper synaptic pruning and normal function. In recent studies using HITS-CLIP, it was found that FMRP bound along coding region of mRNA transcripts. This suggests that somehow, FMRP associated with ribosomes can consistently be found stalled and associated with coding regions within mRNA.

What then, are the implications of FMRP phosphorylation on mRNA targets? In hippocampal neurons, it was found that ribosomal protein S6 kinase (S6K1) is a major kinase of FMRP while PP2A is the major phosphatase [86, 87]. FMRP is phosphorylated and de-phosphorylated in an activity dependent manner. FMRP is rapidly dephosphorylated immediately after group1 mGluR stimulation by DHPG but is then rapidly re-phosphorylated within minutes of stimulation. One well-studied example of a dendritically localized mRNA regulated by FMRP is SAP90/PSD-95-associated protein 3 (SAPAP3). Loss of S6K1 resulted in an overall increase in FMRP target SAPAP3. Cells expressing the alanine substituted FMRP showed a similar increase in SAPAP3, while mRNA levels remained constant [86]. Thus, by an unknown mechanism, phosphorylation acts as in inhibitor of translation.

FMRP localized to the synapse plays an important role in the regulation of translation, and phosphorylation may play a pivotal role in managing the balance of translated and repressed mRNAs. Upon mGluR stimulation of the synapse, FMRP is rapidly synthesized. Additionally, FMRP that is already localized to the synapse is rapidly dephosphorylated, resulting in a burst of translation. Minutes after stimulation, FMRP is then rapidly phosphorylated. Protein translation-dependent synaptic strengthening such as LTP and mGluR LTD is perturbed in fragile X knockout mice. Perhaps the presence of the FMRP complex at the synapse is poised to rapidly regulate translation of its associated mRNAs upon the appropriate signal.

Phosphorylation of FMRP, and miRNAs at the synapse

Post-synaptic density protein 95 (PSD-95) is a prime example of how translation of an FMRP-associated mRNA is regulated by post-translational modifications at the synapse. The 3'untranslated region of PSD-95 contains a miR-125a binding site that is buried within a G-quadruplex region that is bound and recognized by FMRP [88]. PSD-95 expression is mGluR stimulation-dependent, such that treatment with DHPG results in an increase of translation. Binding of miR-125a to PSD-95 inhibits translation, while mutating the seed sequence lifted miRNA-mediated inhibition of the mRNA. Using mutants of FMRP that mimic constitutively phosphorylated or unphosphorylated FMRP, it was found that constitutively phosphorylated FMRP inhibited PSD-95 translation while unphosphorylated FMRP was a permissive signal for translation. In addition to translational suppression by FMRP, Argonaute 2 association with PSD-95 mRNA was increased in the presence of phosphorylated FMRP. The model proposed by Muddashetty and colleagues is that phosphorylated FMRP associates with Argonaute 2 and the RISC machinery in a suppressive state on PSD-95. However upon mGluR stimulation with DHPG, FMRP is rapidly de-phosphorylated, causing the RISC machinery to dissociate from the mRNA, liberating PSD-95 from the suppressed state to an actively translating state [56]. Because phosphorylation is reversible, soon after stimulation, FMRP may be rephosphorylated, thereby returning PSD-95 mRNA to a translationally silent state once again. Thus, phosphorylation of FMRP works as a reversible switch to permit or inhibit translation of PSD-95.

While FMRP associates with RISC machinery on an mRNA, FMRP also associates with other components of the miRNA machinery. Phosphorylation inhibited association of Dicer with FMRP, leading to accumulation of an RNA the size of a precursor microRNAs. This observation suggests that phosphorylation of FMRP may regulate association with Dicer and consequently processing of pre-miRNAs to miRNAs [89].

Ubiquitination

In addition to methylation and phosphorylation, FMRP is also ubiquitinated. In neurons, LTP and LTD both require the synthesis of specific proteins to maintain the longevity of the response. The ubiquitin-proteasome pathway is important for cellular degradation of proteins. Expression of FMRP increases in the soma and proximal dendrites after DHPG stimulation, with a notable increase of nuclear FMRP [90]. The presence of nuclear FMRP is interesting especially

after a burst of FMRP synthesis. Newly synthesized FMRP maybe triggered to enter the nucleus and bind target mRNA before targeting it to specific destinations. After an initial burst of FMRP expression, the levels of FMRP returned to a basal state after 10 minutes which suggested a mechanism by which FMRP protein levels were rapidly modulated [90]. FMRP was found to be degraded by the 26S proteasome, where blocking proteasomal activity with MG132 resulted in sustained levels of FMRP after DHPG stimulation. Blocking degradation of FMRP resulted in the inhibition of mGluR mediated LTD, which is consistent with the exaggerated LTD in Fmr1 knockout mice. Thus, ubiquitin serves as a mechanism to modulate the steady-state levels of FMRP at the synapse.

1.5 FMRP and the fate of progenitor cells

Neurogenesis is a complex series of events that takes place throughout life. Striking the proper balance between forming neurons versus supporting glial cells and then forming cells that can be integrated into a functional circuit is a challenging task that the brain must perform [91]. Developmentally, FMRP plays an important role in dictating the fate of precursor cells in the developing brain. FMRP also plays a role in the regulation of cell cycle and neural progenitor proliferation [92]. A recent review by Callan and Zarnescu elegantly summarizes the effects of FMRP on progenitor cells and neurogenesis [93]. The loss of FMRP altered the ratio of neurons to glia in both embryonic and developing cells and also even in adult tissues [94]. Loss of FMRP in embryonic cells resulted in increased development of neurons with a decrease in glia. This was found to be due to reduced viability of glial cells which would suggest that in early development, FMRP plays an important role in the maintenance of glia [94]. Interestingly, the role of FMRP in progenitor cell differentiation takes on a reverse role in adult cells. Developmental timing of differentiation as well as the different mRNA targets during neuronal development may skew progenitor differentiation to favor glial development in developmentally older animals [92]. Comparison of WT to Fmr1 knockout mice showed that knockout mice had decreased levels of neurogenesis with an increase in astrocytes, predominantly in the adult hippocampus of mice.

1.6 FMRP localization in cells

FMRP is present throughout the neuron, and with the number of posttranslational modifications that are present on FMRP, cellular localization also adds another element of translational control and regulation of bound mRNAs (Figure 1).

Nuclear FMRP

At a cellular level, FMRP is generally cytoplasmic, however, a small amount of FMRP has been described in the nucleus at steady state. Early stages of *Xenopus* and zebrafish development, 2 and 3 hours post fertilization, respectively, have shown that FMRP is primarily nuclear, suggesting an important role for FMRP in the nucleus during specific points in development [95, 96]. Further, FMRP has been found along nascent transcripts in the lampbrush chromosomes of *Xenopus laevis* oocytes suggesting that FMRP enters the nucleus to bind its nascent mRNA targets before being exported to the cytoplasm and properly localized for translational regulation [76]. Exactly how FMRP finds its mRNA target while in the nucleus is still not yet clear, but it can be speculated that specific RNA motifs such as RNA G-quadruplexes and arginine methylation of FMRP may help to guide and facilitate RNA binding. Upon stimulation by DHPG, the localization of FMRP in the hippocampus was found to be increased in the nucleus and also throughout the dendritic arbor suggesting rapid transport into the nucleus to bind mRNA cargo and also rapid synthesis in response to stimulation at the site of regulation [90].

Immunogold labeling showed FMRP in the nucleoplasm and associated with the nuclear pores of neurons but not in astrocytes or glia [97]. FMRP has a non-canonical nuclear localization sequence encoded by exons 5, 6, and part of 7 that contains lysines and arginines but does not contain a canonical importin alpha binding sequence [98, 99]. Thus, it is unclear how FMRP enters the nucleus. In addition to its RNA binding domains, FMRP has a leucine-rich nuclear export sequence (NES) encoded by exon 14 that is alternatively spliced. Accordingly, a splice variant of FMRP lacking exon 14 was found to be primarily nuclear in localization. The leucine-rich NES in FMRP is similar to the Rev regulatory protein of HIV1 and was proposed to bind CRM1 [100]. However, FMRP has additional mechanisms for exiting the nucleus.

Blocking the primary mRNA exporter, Tap/Nxf1, increased the nuclear localization of FMRP suggesting that the export of FMRP is mediated by its bound mRNA [76].

FMRP association with the translation machinery

FMRP associates with mRNAs bound to multiple ribosomes, termed polyribosomes, in the cell body and in synaptoneurosomes suggesting a role in translation regulation at the synapse [41, 97, 101]. Despite the extensive studies done to understand FMRP and its effects on translation, a clear mechanism behind how FMRP regulates translation of its bound mRNAs has yet to be elucidated. One model of FMRP mediated translation regulation begins at the step of translation initiation. Translation begins by assembling a number of proteins at the 5'methyl guanosine cap including eIF4E and eIF4G, which assemble into the translationally competent eIF4F complex. Formation of this complex is inhibited by 4F binding proteins, 4FBP. FMRP may act as an inhibitor of initiation through its association with CYFIP, which was recently described as a 4FBP [102]. CYFIP has been shown to contain no RNA binding ability, therefore its localization and function in an mRNP would be mediated by protein-protein interactions. CYFIP interacts with a region encoded by exon 7 in FMRP which is also the region of interaction between FMRP and its family members, FXR1P and FXR2P [103]. The ability of all of these proteins to bind the same domain in FMRP suggests a complex form of regulation where association with CYFIP may inhibit translation while association with other proteins such as the fragile X family members may activate translation.

In addition to translational machinery, FMRP is found associated with many RISC proteins in both *Drosophila* and mammals. As mediators of translational suppression, it comes as no surprise that FMRP would be closely associated with RISC proteins. While FMRP does not seem to be necessary for proper function of the RISC machinery [104], it seems evident that FMRP can serve as a vehicle to localize mRNA to the RISC machinery. FMRP associates with a number of neuron specific miRNAs. A recent paper by Edbauer and colleagues described FMRP and its role in modulating the effect of mi-125b and miR-132 where miR-125b overexpression resulted in more immature dendritic phenotypes [55]. Not only was FMRP found to be associated with miRNAs, a novel target, the NMDA receptor subunit, NR2A was also found to be regulated by miR-125b in an FMRP-dependent manner [55]. The specific mechanism behind how FMRP can guide miRNAs to target mRNAs is still unknown.

FMRP in translationally silent granules

Subcellular RNA containing granules called processing bodies (P-bodies) and stress granules (SG) are present throughout the cytoplasm, harboring mRNA molecules sequestered from translationally active machinery (reviewed in [105]). These two translationally silent compartments are very similar and contain many regulatory molecules however their presence is dependent on cellular conditions such as the translational state of the cell as well as the presence of various stressors such as oxidative stress.

P-bodies are another subcellular compartment where non-translated mRNA is kept for transient storage or degradation [106-108]. Several proteins associated with nonsense-mediated decay such as Dcp1 and Upf1 are present in P-bodies in addition to components of the RISC machinery [109, 110]. mRNAs targeted for degradation or sequestration may be localized to P-bodies for storage by FMRP until a signal for translation activation is triggered. Upon exiting the P-bodies, the mRNA is then actively translated [110, 111]. APP, a known binding target of FMRP is recruited to P-bodies to silence translation in competition with hnRNP C [68]. By this mechanism, FMRP may physically sequester a bound mRNA to cellular compartments that are not regions of active translation.

Cellular stress triggers a complex response from the cell such that translation is rapidly reduced as a means for the cell to survive the duration of the stressor. Triggers such as oxidative stress, UV irradiation, heat shock, and other extreme conditions result in the organization and accumulation of stress granules in the cytoplasm [112-115]. FMRP localizes to stress granules where it is thought to bind quiescent transcripts that are targeted for degradation or storage. Interestingly, formation of stress granules results in a shift of mRNA away from the translational machinery into aggregates of protein that also contain a double stranded RNA binding protein, Staufen, which is thought to facilitate ribosome stalling [116]. FMRP, which associates with stalled nontranslating polyribosomes in a phosphorylated state, also associates with Trdr3 and Staufen which may suggest that these two proteins coordinate a stress granule assembly response [117]. In cells lacking FMRP, it was found that stress granule assembly was altered while RISC activity remained intact suggesting that FMRP is a component of stress granule assembly [104]. The association of FMRP with these stress granule and P-body components greatly underscores the important role of FMRP in mRNA regulation.

FMRP and mRNA transport

Important for translational regulation is the proper localization of mRNAs to cellular targets. This targeting mechanism is especially important in highly polarized cells such as neurons. FMRP associates with a number of molecular motors such as dynein and kinesins, with mammalian FMRP associating with neuron-specific kinesin, KIF3C, and mRNA targets such as CamKII and Arc/arg [118, 119]. Interestingly, the RNA transport granules that contain FMRP also contain RNA helicases, Poly-A binding proteins, splicing factors and nuclear/cytoplasmic shuttling factors. Upon mGluR stimulation, FMRP and RNA-containing granules demonstrate bi-directional movement suggesting that FMRP may play a role as a localization protein such that bound mRNA can be translated at the site of stimulation [120]. In studies using neuron culture, CamKII alpha was used as a regulated cargo. After mGluR stimulation, FMRP was found to be rapidly colocalized to spines containing group 1 mGluRs within 20 minutes [120]. Additionally, FMRP targeted CamKII alpha to the spines for rapid translation. In studies done using dFMR1, the motility, speed, and distance of specific FMRP target mRNA granules was altered after DHPG stimulation. FMRP also affects cellular localization of some, but not all target mRNAs [73, 121]. In the absence of FMRP, some mRNAs are mislocalized and absent from synapses perhaps due to a lack of transport from the soma to respective cellular compartments.

A small amount of FMRP has also been found in axons along developing growth cones, suggesting an important role in regulating the translation of mRNAs in the axons, which is especially important in developing proper neural circuitry during development [122]. Expression of dFMRP mutants demonstrated more complex branching of axons, appearing to encroach on inappropriate brain areas [40]. dFMRP in the mushroom bodies of *Drosophila* was found to regulate the complexity of axonal branching during development. Activity-dependent pruning of axons is an important role of dFMRP in the developing mushroom body [123]. On a molecular level, FMRP and mRNA containing granules were located in the axonal growth cones, and out in the axonal filopodia with Map1b mRNA [124-126]. Proper development of neural circuitry requires the appropriate localization of mRNAs that are capable of responding to external stimulation such as growth cone regulation and translational regulation in response to signals such as netrin-1 and Sema3a [127]. FMRP in the axon is proposed to play an important role in managing protein synthesis and localization in the growth cone [52].

FMRP at the synapse

Synaptic activity can create changes in the stability of synapses, such that they can be strengthened in the case of LTP, allowing new connections to be maintained. Conversely, LTD can result in the destabilization and elimination of synapses. These long-term responses require the activation of post-synaptic protein translation of mRNAs already present in the synapse in response to group 1 mGluRs, which include mGluR1 and mGluR5 [44]. Several interesting observations were made by Huber and colleagues where the absence of FMRP somehow resulted in exaggerated LTD in neurons which ultimately resulted in the development of the mGluR theory [43]. Dysregulated signaling through over-active group 1 mGluRs results in many characteristic features such as developmental delay and long thin spines, which are also distinct characteristics of fragile X syndrome. Since then, the interaction between FMRP and the response to metabotropic glutamate receptor stimulation has sparked an immense interest in the role of FMRP at the level of the synapse.

1.7 mGluR theory of FXS

The connection between FMRP and the group 1 mGluRs has been of great interest, leading to many new ideas regarding the role of FMRP and translation at the synapse. Proteins that are thought to stabilize LTD are synthesized in the synapse in response to mGluR stimulation, and along with this milieu of proteins, FMRP is also coordinately synthesized [41, 44, 128]. Activation of mGluR5 triggers a cascade of signaling molecules along the MAPK and ERK pathways. mRNAs already present at the synapse are rapidly translated, resulting in a burst of protein synthesis upon group 1 mGluR stimulation [65, 129]. Along with this burst of translation, after prolonged stimulation, surface AMPA receptors are rapidly internalized [130]. The mGluR theory proposes that FMRP acts as a brake, to inhibit further synthesis of LTD proteins. Therefore Fmr1 knockout mice have continuously dysregulated synthesis of LTD proteins. Because of this exaggerated mGluR signaling, synaptogenesis is perturbed, especially during critical periods of development.

1.8 Current therapies for FXS

Understanding the role of FMRP at the synapse has led to several therapeutic avenues in an attempt to tackle the dysregulated signaling in FXS (Figure 2). Several therapeutic agents

have been developed to ameliorate the downstream effects in patients with FXS. While it would seem that targeting downstream signaling would be an ideal method to treat FXS, the effects of perturbing universal signaling cascades must also be taken into consideration. One such example would be to target the MAPK/mTOR/ERK cascade with the use of general inhibitors. While this approach would address the dysregulated signaling in neurons, this signaling cascade is involved in many other cellular processes such as cell cycle regulation.

Negative modulators or antagonists of mGluRs are a promising target for managing FXS, as exaggerated mGluR signaling is a major proposed mechanism of disease phenotype [43, 131]. MPEP (2-methyl-6-phenylethynyl pyridine hydrochloride) is a strong negative regulator of mGluR5 receptors [132]. In mice and *Drosophila*, MPEP significantly improved behavior and reversed the fragile X phenotype, showing marked improvement in courting behavior in *Drosophila* and reduced hyperactivity and audiogenic seizure induction in mice [133-135]. Additionally, at the cellular level, AMPA receptor internalization was also reduced [136]. While this molecule was promising in animals, the use of MPEP in humans was too toxic [137]. A different specific blocker of mGluR5 was used in clinical trials called fenobam. Single treatment of fenobam showed marked reduction in hyperactive behaviors and anxiety, however longer term studies were not performed [138]. Other mGluR5 modulators and antagonists that are in clinical trials are AFQ056 (Novartis) and RO4917523 (Hoffman La Roche),which have progressed into Phase II of clinical trials (clinicaltrials.gov).

One aspect of FXS is the excessive internalization of AMPA receptors from the cell surface [130, 136]. Targeting AMPA internalization by using AMPA receptor modulators (ampakines) is another potential avenue for therapy. Ampakines essentially trigger BDNF signaling and stimulate mRNA translation such that LTD is facilitated [139]. CX516 is a weak ampakine that was used in a few clinical trials, however there were few significant improvements in cognitive and behavior results [140] .

Lithium has been used to treat neurological disorders for several years, and in a recent study, it was found that lithium treatment in Fmr1 knockout mice improved hyperactive and social behaviors [141]. In cells, lithium inhibited excessive protein synthesis by blocking inositol phosphate signaling pathways [142, 143]. In human clinical trials, there were minimal major side effects and some improved behaviors on the irritability and adaptive behavior scales [143]. Interestingly, lithium treatment also showed that ERK1/2 phosphorylation, which is overactive in

FXS, in the lymphocytes of the human subjects were reduced [144]. These studies are still incomplete and pose a promising avenue for FXS therapy, however the long term effects of systemic lithium treatment are a concern. Developing a more targeted and effective method to administer and regulate lithium is an area that requires more study.

Minocycline, in addition to being used to treat acne and other bacterial infections, has been used in clinical trials as a target of a specific dysregulated downstream, matrix metalloprotease 9, MMP9. Minocycline is a tetracycline analog that has been used as a therapeutic agent in several other neurodegenerative disorders such as multiple sclerosis, autism and stroke [145]. Studies using Fmr1 knockout mice showed that minocycline treatment improved the behavioral phenotype and also showed changes in the immature dendritic phenotype to a more mature phenotype [145]. In human clinical trials, 20 individuals given minocycline demonstrated improved behavior without major side effects [146]. Other studies showed marked improvements in behavior, language, and attention [147]. While this study still requires more investigation, it is a promising therapeutic agent that has already been demonstrated to be useful for other health purposes. One concern, however, was the timing of administration. There was a high risk of yellowing or browning of permanent teeth in children who were given minocycline before the age of 12, therefore finding an optimal window for treatment is a necessary study [148].

Arbaclofen is another molecule that has been considered for FXS therapy. Arbaclofen is the right-handed enantiomer of baclofen, and is a potent GABA b agonist (reviewed in [137]). As a GABAergic agonist, it has been used in patients who have spasticity due to stroke and also in children with cerebral palsy (reviewed in [149, 150]). The GABA system in Fmr1 knockout mice is dysregulated, showing downregulation in activity, therefore using this drug for human trials seemed promising. Arbaclofen indirectly modulates mGluR signaling by lowering glutamate that is available at the synapse [137]. Clinical trials showed improvements in aggression and irritability, and further testing is still necessary.

Several other small molecules are being used in clinical trials, many of which have a broad range of effects along many points leading to dysregulated signaling. In the future, perhaps a combinatorial drug treatment will be useful or development of more specific and targeted drug therapies.

1.9 MOV10

MOV10 was identified in an insertional mutation study of the Moloney leukemia virus (MOV). Insertion number 10 was then identified to be within a gene encoding a 110 kDA *putative* GTP binding protein/RNA helicase [151, 152]. Introductory studies showed that there was developmental control of expression, and that MOV10 was expressed in a number of tissues, including the brain and testes [152]. In the early 2000s, MOV10 re-emerged as a protein of interest as small RNAs caught the eye of the scientific community. MOV10 was bioinformatically determined to be a homolog of SDE3, a superfamily 1 RNA helicase required for gene silencing in Arabidopsis [153]. SDE3 and MOV10 displayed similar helicase domain homology to UPF1 and SMG-2, which are required for nonsense mediated decay (NMD) in yeast and C. elegans.

To this day, MOV10 remains largely uncharacterized. It has been found to have sequence homology to other superfamily 1 helicases such as UPF1 [154]. SDE3 in Arabidopsis, armitage in *Drosophila*, and also sequence homology to the MOV10 like protein, specific to cardiac muscle [153-155]. However, despite the little that is known about the enzymatic function of MOV10 itself, the protein has been published to participate in a number of important cellular functions such as the miRNA pathway. MOV10 plays an important role in RNA virus replication and infectivity and has also been found to be involved in the miRNA pathway, which will be discussed in the sections below.

MOV10 and RNA viruses

Hepatitis D virus and HIV are both retroviral viruses that require the assistance of host proteins to replicate their genetic material and also package and secrete more virus particles. Hepatitis D virus is the smallest known virus, encoding a single protein, the hepatitis delta antigen. Knockdown of MOV10 inhibited replication of the HDV genome [156]. A proposed mechanism by which MOV10 is thought to influence genome replication is through modification of viral RNA of HDV which mimic small RNA hairpins to form a transcriptionally competent RNP [156].

In 2010, several labs demonstrated that increased expression of MOV10 inhibited HIV replication and infectivity [157-159]. In the case of HIV, MOV10 plays a complex role in HIV

genome replication and also virus infectivity. The exact mechanism by which MOV10 inhibits HIV is still under investigation. MOV10 significantly reduced HIV infectivity compared to other RISC protein components such as Ago1 and 2 and TRBP [157]. In studies of P-body related proteins, MOV10 but not DCP1 or 2 inhibited HIV replication. Interestingly, MOV10 was also packaged with the virus particles and subsequently impaired virus infectivity [158]. A point mutation in the helicase domains of MOV10 showed that HIV infectivity was not affected suggesting an important role in the N terminal region of the protein [159]. In a similar study, however, all domains of MOV10 except for domain V, typically involved in ATP hydrolysis [160] were found to be required for HIV packaging function [161]. The various roles of MOV10 in RNA virus biology suggest a complex function for MOV10— ranging from secondary structure binding to facilitating protein interactions.

MOV10 in the miRNA pathway

With 30-40% sequence homology to SDE3 in *Arabidopsis thaliana* and armitage in *Drosophila melanogaster*, MOV10 is implicated in small RNA processes based on conservation of function. Armitage is required for RISC maturation by facilitating siRNA incorporation into the complex [155]. In 2005, Meister *et al*. purified Ago1 and 2 containing complexes to determine what protein components were present. In addition to Gemin 3 and 4 and Dicer, TNRC6B, MOV10, and PRMT5 were found in the Ago2 containing complex [162]. MOV10 and Ago2 co-localize in cytoplasmic granules, which stained positively for P-body markers. Isolated complexes of MOV10 demonstrated no Dicer activity suggesting that MOV10 acts downstream of Dicer processing and only transiently associates with RISC assembly. MOV10 was required for miRNA mediated mRNA cleavage. Knockdown of MOV10 relieved miRNA mediated silencing of reporter constructs in studies using miR21 and let-7b [162, 163].

In other studies of RISC protein components, TRBP containing complexes generally exist in a 500 kDa complex, however larger complexes in the 2 mDa range also exist [163]. This mega-dalton sized complex was found to contain large subunit components of the ribosome, eIF6, and also MOV10. While the association of these proteins were not as robust as the core RISC components, Ago2 and Dicer, miRNA mediated silencing of let-7b targeted luciferase reporters were impaired when eIF6 and MOV10 were knocked down [163].

MOV10 at the synapse

Translation at the synapse is important for plasticity, learning and memory. MOV10 is expressed in a number of tissue types, including the brain. Banerjee et al. showed MOV10 present at the synapse in neurons. Interestingly, KCl stimulation, which activates NMDA receptors resulted in rapid degradation of MOV10 containing granules. Furthermore, this degradation was proteasome and activity dependent. mRNAs known to be associated with RISC, namely CamKII and LimK1, were found to be actively translated upon stimulation. LimK1 is a target of brain enriched microRNA, miR138, suggesting that MOV10 degradation relieved translational silencing through the RISC complex [164].

These studies have sparked great interest in the role of MOV10 in translation regulation, however very little is known about how MOV10 functions in the cell, and the specific role in regulation that the protein performs.

1.10 Figures and Tables.

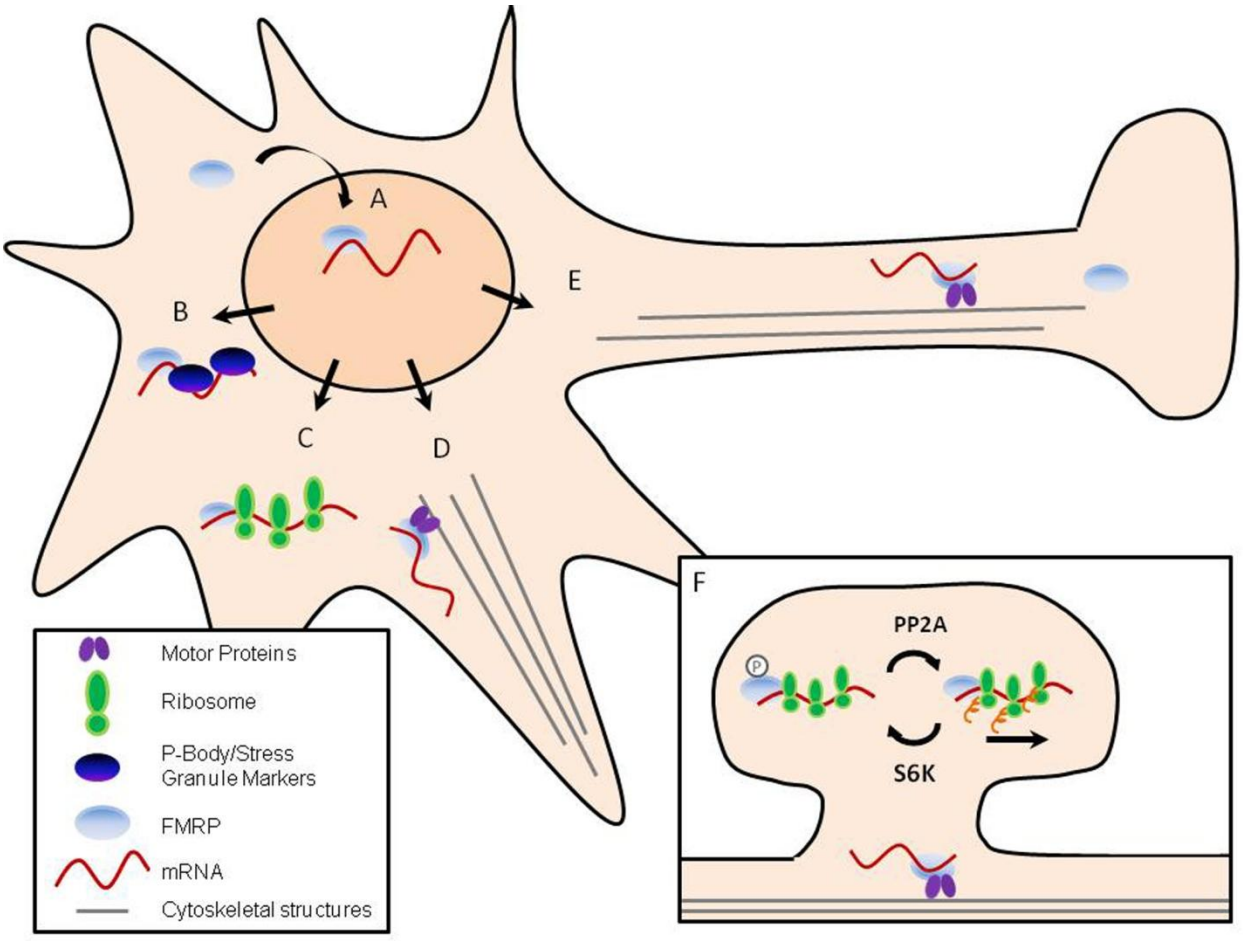

Figure 1.1. Cellular localization of FMRP. A. FMRP enters the nucleus and binds nascent mRNA transcripts, which facilitate its export from the nucleus to the cytoplasm. B. Translationally silent FMRP-containing granules that harbor mRNA in P-body or Stress Granule type compartments. C. FMRP can associate with translationally competent mRNA, found along actively translating polyribosomes. D. FMRP associates with motor proteins to localize mRNAs to the dendrite or E. localize mRNAs to the axon to regulate translation of bound mRNA. F. In response to mGluR stimulation, postsynaptic FMRP is rapidly dephoshorylated and subsequently rephosphorylated such that regulation of protein synthesis is tightly regulated.

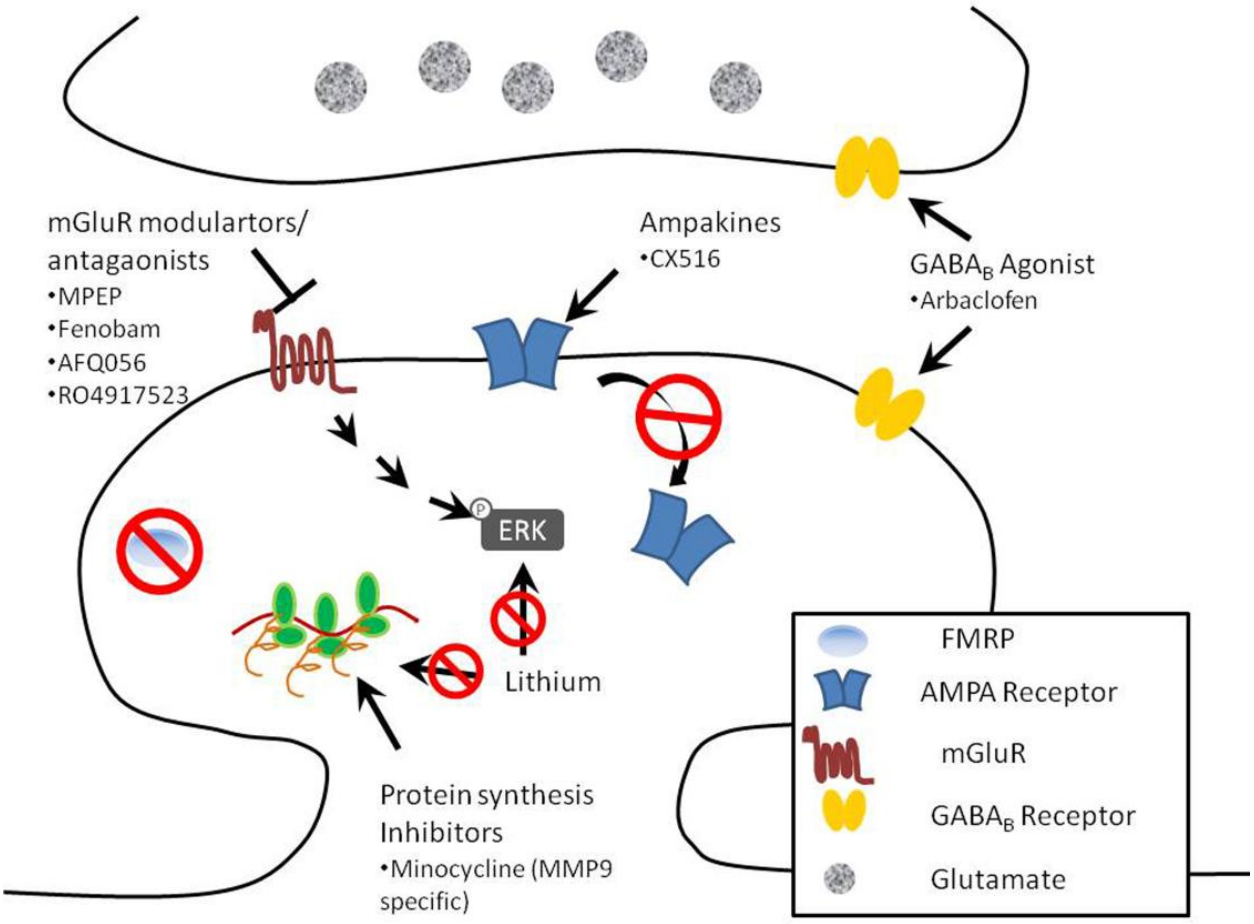

Figure 1.2. Drug targets at the Fragile X synapse. Loss of FMRP affects many different aspects of proper synaptic function from protein synthesis to proper downstream signaling and also receptor endocytosis. Several drug candidates have been used in drug trials and animal models including mGluR antagonists such as MPEP, Fenobam, AFQ056, RO4917523. Other targets are AMPA receptor agonists through the actions of ampakines, GABAb B agonists present on both the pre and post synaptic terminals to regulate glutamate availability at the synapse. Other small molecules such as Lithium and minocycline act to regulate signaling cascades and protein translation targets.

Table 1.1. Modifications of FMRP and effects on translation			
Modification	**Effect on FMRP**	**Effect on Translation**	**Reference**
Phosphorylation	P-FMRP associates with stalled untranslating polyribosomes, P-FMRP does not associate with Dicer P-FMRP associates with RISC	Inhibits translation	51, 85, 86
Methylation	Alters mRNA binding specificity	Unknown	59, 68, 78
Ubiquitnation	Triggers FMRP for degradation at the synapse	Increases translation	87
Splicing	Changes exon composition of FMRP	Alters FMRP localization	97

1.11 References

1. Martin, J.P. and J. Bell, *A pedigree of mental defect showing sex linkage.* Journal of Neurology and Neurosurgical psychiatry, 1943. **6**: p. 154-157.
2. Lubs, J.A., Jr., *A marker X chromosome.* Am. J. Hum. Genet., 1969. **21**: p. 231-244.
3. Sutherland, G.R., *Fragile sites on human chromosomes: demonstration of their dependence on the type of tissue culture medium.* Science, 1977. **197**: p. 265-266.
4. Verkerk, A.J., et al., *Identification of a gene (FMR-1) containing a CGG repeat coincident with a breakpoint cluster region exhibiting length variation in fragile X syndrome.* Cell, 1991. **65**(5): p. 905-14.
5. Ashley, C.T.J., et al., *FMR1 protein: conserved RNP family domains and selective RNA binding.* Science, 1993. **262**(5133): p. 563-66.
6. McMurray, C.T., *Mechanisms of trinucleotide repeat instability during human development.* Nat Rev Genet. **11**(11): p. 786-99.
7. Schaeffer, C., et al., *The fragile X mental retardation protein binds specifically to its mRNA via a purine quartet motif.* Embo J, 2001. **20**(17): p. 4803-13.
8. Fu, Y.-H., et al., *Variation of the CGG repeat at the fragile X site results in genetic instability: resolution of the Sherman paradox.* Cell, 1991. **67**: p. 1047-1058.
9. Mirkin, S.M., *Toward a unified theory for repeat expansions.* Nat Struct Mol Biol, 2005. **12**(8): p. 635-7.
10. Pearson, C.E., et al., *Slipped-strand DNAs formed by long (CAG)*(CTG) repeats: slipped-out repeats and slip-out junctions.* Nucleic Acids Res, 2002. **30**(20): p. 4534-47.
11. Mirkin, S.M., *DNA structures, repeat expansions and human hereditary disorders.* Curr Opin Struct Biol, 2006. **16**(3): p. 351-8.
12. Mirkin, S.M., *Expandable DNA repeats and human disease.* Nature, 2007. **447**(7147): p. 932-40.
13. Kiliszek, A., et al., *Crystal structures of CGG RNA repeats with implications for fragile X-associated tremor ataxia syndrome.* Nucleic Acids Res. **39**(16): p. 7308-15.
14. De Boulle, K., et al., *A point mutation in the FMR-1 gene associated with fragile X mental retardation.* Nat. Genet., 1993. **3**(1): p. 31-35.
15. Collins, S.C., et al., *Identification of novel FMR1 variants by massively parallel sequencing in developmentally delayed males.* Am J Med Genet A. **152A**(10): p. 2512-20.
16. Collins, S.C., et al., *Array-based FMR1 sequencing and deletion analysis in patients with a fragile X syndrome-like phenotype.* PLoS One. **5**(3): p. e9476.
17. Tassone, F., et al., *Transcription of the FMR1 gene in individuals with fragile X syndrome.* Am J Med Genet, 2000. **97**(3): p. 195-203.
18. Garcia-Arocena, D. and P.J. Hagerman, *Advances in understanding the molecular basis of FXTAS.* Hum Mol Genet. **19**(R1): p. R83-9.
19. Leehey, M.A., et al., *Progression of tremor and ataxia in male carriers of the FMR1 premutation.* Mov Disord, 2007. **22**(2): p. 203-6.
20. Leehey, M.A., *Fragile X-associated tremor/ataxia syndrome: clinical phenotype, diagnosis, and treatment.* J Investig Med, 2009. **57**(8): p. 830-6.
21. Hagerman, R.J., et al., *Fragile-X-associated tremor/ataxia syndrome (FXTAS) in females with the FMR1 premutation.* Am J Hum Genet, 2004. **74**(5): p. 1051-6.

22. Coulam, C.B., S.C. Adamson, and J.F. Annegers, *Incidence of premature ovarian failure.* Obstet Gynecol, 1986. **67**(4): p. 604-6.
23. Hunter, J.E., et al., *Fragile X-associated primary ovarian insufficiency: evidence for additional genetic contributions to severity.* Genet Epidemiol, 2008. **32**(6): p. 553-9.
24. Tassone, F., C. Iwahashi, and P.J. Hagerman, *FMR1 RNA within the intranuclear inclusions of fragile X-associated tremor/ataxia syndrome (FXTAS).* RNA Biol, 2004. **1**(2): p. 103-5.
25. Jacquemont, S., et al., *Penetrance of the fragile X-associated tremor/ataxia syndrome in a premutation carrier population.* JAMA, 2004. **291**(4): p. 460-9.
26. Dreyfuss, G., V. Narry Kim, and N. Kataoka, *Messenger-RNA-binding proteins and the messages they carry.* Nature Reviews Molecular Cell Biology, 2002. **3**: p. 195-205.
27. Jin, P., et al., *Pur alpha binds to rCGG repeats and modulates repeat-mediated neurodegeneration in a Drosophila model of fragile X tremor/ataxia syndrome.* Neuron, 2007. **55**(4): p. 556-64.
28. Sofola, O.A., et al., *RNA-binding proteins hnRNP A2/B1 and CUGBP1 suppress fragile X CGG premutation repeat-induced neurodegeneration in a Drosophila model of FXTAS.* Neuron, 2007. **55**(4): p. 565-71.
29. Sellier, C., et al., *Sam68 sequestration and partial loss of function are associated with splicing alterations in FXTAS patients.* EMBO J. **29**(7): p. 1248-61.
30. Abrahams, B.S. and D.H. Geschwind, *Advances in autism genetics: on the threshold of a new neurobiology.* Nat Rev Genet, 2008. **9**(5): p. 341.
31. Brady, N., et al., *Communication in young children with fragile X syndrome: a qualitative study of mothers' perspectives.* Am J Speech Lang Pathol, 2006. **15**(4): p. 353-64.
32. Finestack, L.H., E.K. Richmond, and L. Abbeduto, *Language Development in Individuals with Fragile X Syndrome.* Top Lang Disord, 2009. **29**(2): p. 133-148.
33. Abbeduto, L., N. Brady, and S.T. Kover, *Language development and fragile X syndrome: profiles, syndrome-specificity, and within-syndrome differences.* Ment Retard Dev Disabil Res Rev, 2007. **13**(1): p. 36-46.
34. Abbeduto, L. and R. Hagerman, *Language and communication in FXS.* Mental Retardation and Developmental
Disabilities Research Reviews, 1997. **3**: p. 313-322.
35. Murphy, M.M. and L. Abbeduto, *Language and communication in fragile X syndrome. . International review of research*
in mental retardation, ed. L. Abbeduto. Vol. 27. 2003: New York: Academic Press. 83-119.
36. Visootsak, J., et al., *Fragile X Syndrome: An Update and Review for the Primary Pediatrician.* Clinical Pediatrics %R 10.1177/000992280504400501, 2005. **44**(5): p. 371-381.
37. Lachiewicz, A.M., D.V. Dawson, and G.A. Spiridigliozzi, *Physical characteristics of young boys with fragile X syndrome: reasons for difficulties in making a diagnosis in young males.* Am J Med Genet, 2000. **92**(4): p. 229-36.
38. Hagerman, R.J., K. Amiri, and A. Cronister, *Fragile X checklist.* Am. J. Med. Genet, 1991. **38**: p. 283-287.
39. Loehr, J.P., et al., *Aortic root dilatation and mitral valve prolapse in the fragile-X syndrome.* Am. J. Med. Genet., 1986. **23**: p. 189-194.

40. Zhang, Y.Q., et al., *Drosophila fragile X-related gene regulates the MAP1B homolog Futsch to control synaptic structure and function.* Cell, 2001. **107**(5): p. 591-603.
41. Weiler, I.J. and W.T. Greenough, *Metabotropic glutamate receptors trigger postsynaptic protein synthesis.* Proc Natl Acad Sci U S A, 1993. **90**(15): p. 7168-71.
42. Weiler, I.J., et al., *Fragile X mental retardation protein is translated near synapses in response to neurotransmitter activation.* Proc Natl Acad Sci U S A, 1997. **94**(10): p. 5395-400.
43. Huber, K.M., et al., *Altered synaptic plasticity in a mouse model of fragile X mental retardation.* Proc Natl Acad Sci U S A, 2002. **99**(11): p. 7746-50.
44. Huber, K.M., M.S. Kayser, and M.F. Bear, *Role for rapid dendritic protein synthesis in hippocampal mGluR-dependent long-term depression.* Science, 2000. **288**(5469): p. 1254-7.
45. Menon, L., S.A. Mader, and M.R. Mihailescu, *Fragile X mental retardation protein interactions with the microtubule associated protein 1B RNA.* RNA, 2008. **14**(8): p. 1644-55.
46. Chen, L., et al., *The fragile x mental retardation protein binds and regulates a novel class of mRNAs containing u rich target sequences.* Neurosci., 2003. **120**(4): p. 1005-1017.
47. Lu, R., et al., *The fragile X protein controls microtubule-associated protein 1B translation and microtubule stability in brain neuron development.* Proc Natl Acad Sci U S A, 2004. **101**(42): p. 15201-6.
48. Kirkpatrick, L.L., K.A. McIlwain, and D.L. Nelson, *Comparative genomic sequence analysis of the FXR gene family: FMR1, FXR1, and FXR2.* Genomics, 2001. **78**(3): p. 169-77.
49. Hinds, H.L., et al., *Tissue specific expression of FMR-1 provides evidence for a functional role in fragile X syndrome.* Nat Genet, 1993. **3**(1): p. 36-43.
50. Devys, D., et al., *The FMR-1 protein is cytoplasmic, most abundant in neurons, and appears normal in carriers of the fragile X premutation.* Nat Genet, 1993. **4**(4): p. 335-40.
51. Hinds, H., et al., *Tissue specific expression of FMR-1 provides evidence for a functional role in fragile X syndrome.* Nat Genet, 1993. **3**(1): p. 36-43.
52. Li, C., G.J. Bassell, and Y. Sasaki, *Fragile X Mental Retardation Protein is Involved in Protein Synthesis-Dependent Collapse of Growth Cones Induced by Semaphorin-3A.* Front Neural Circuits, 2009. **3**: p. 11.
53. Siomi, H., et al., *The protein product of the fragile X gene, FMR1, has characteristics of an RNA-binding protein.* Cell, 1993. **74**(2): p. 291-8.
54. Darnell, J.C., et al., *Kissing complex RNAs mediate interaction between the Fragile-X mental retardation protein KH2 domain and brain polyribosomes.* Genes Dev, 2005. **19**(8): p. 903-18.
55. Edbauer, D., et al., *Regulation of Synaptic Structure and Function by FMRP-Associated MicroRNAs miR-125b and miR-132.* Neuron, 2010. **65**(3): p. 373.
56. Muddashetty, R.S., et al., *Reversible inhibition of PSD-95 mRNA translation by miR-125a, FMRP phosphorylation, and mGluR signaling.* Mol Cell. **42**(5): p. 673-88.
57. Feng, Y., et al., *FMRP associates with polyribosomes as an mRNP, and the I304N mutation of severe fragile X syndrome abolishes this association.* Mol Cell, 1997. **1**(1): p. 109-18.

58. Zang, J.B., et al., *A mouse model of the human Fragile X syndrome I304N mutation.* PLoS Genet, 2009. **5**(12): p. e1000758.
59. Darnell, J.C., et al., *Discrimination of common and unique RNA-binding activities among Fragile-X mental retardation protein paralogs.* Hum Mol Genet, 2009. **18**(17): p. 3164-77.
60. Darnell, J.C., et al., *Fragile X mental retardation protein targets G quartet mRNAs important for neuronal function.* Cell, 2001. **107**(4): p. 489-99.
61. Darnell, J.C., S.T. Warren, and R.B. Darnell, *The fragile X mental retardation protein, FMRP, recognizes G-quartets.* Ment Retard Dev Disabil Res Rev, 2004. **10**(1): p. 49-52.
62. Mazroui, R., et al., *Fragile X Mental Retardation protein determinants required for its association with polyribosomal mRNPs.* Hum Mol Genet, 2003. **12**(23): p. 3087-96.
63. Blackwell, E., X. Zhang, and S. Ceman, *Arginines of the RGG box regulate FMRP association with polyribosomes and mRNA*
Human Molecular Genetics, 2010. **19**(7): p. 1314-23.
64. Menon, L. and M.R. Mihailescu, *Interactions of the G quartet forming semaphorin 3F RNA with the RGG box domain of the fragile X protein family.* Nucleic Acids Res, 2007. **35**(16): p. 5379-92.
65. Todd, P.K., K.J. Mack, and J.S. Malter, *The fragile X mental retardation protein is required for type-I metabotropic glutamate receptor-dependent translation of PSD-95.* Proc Natl Acad Sci U S A, 2003. **100**(24): p. 14374-8.
66. Menon, R.P., T.J. Gibson, and A. Pastore, *The C Terminus of Fragile X Mental Retardation Protein Interacts with the Multi-domain Ran-binding Protein in the Microtubule-organising Centre.* Journal of Molecular Biology, 2004. **343**(1): p. 43.
67. Westmark, C.J. and J.S. Malter, *FMRP mediates mGluR5-dependent translation of amyloid precursor protein.* PLoS Biol, 2007. **5**(3): p. e52.
68. Lee, E.K., et al., *hnRNP C promotes APP translation by competing with FMRP for APP mRNA recruitment to P bodies.* Nat Struct Mol Biol. **17**(6): p. 732-9.
69. Brown, V., et al., *Purified Recombinant Fmrp Exhibits Selective RNA Binding as an Intrinsic Property of the Fragile X Mental Retardation Protein.* J Biol Chem, 1998. **273**(25): p. 15521-15527.
70. Fahling, M., et al., *Translational Regulation of the Human Achaete-scute Homologue-1 by Fragile X Mental Retardation Protein.* J. Biol. Chem. , 2009. **284**(7): p. 4255-4266.
71. Brown, V., et al., *Microarray identification of FMRP-associated brain mRNAs and altered mRNA translational profiles in fragile X syndrome.* Cell, 2001. **107**(4): p. 477-87.
72. Bechara, E.G., et al., *A novel function for fragile X mental retardation protein in translational activation.* PLoS Biol, 2009. **7**(1): p. e16.
73. Miyashiro, K.Y., et al., *RNA cargoes associating with FMRP reveal deficits in cellular functioning in Fmr1 null mice.* Neuron, 2003. **37**(3): p. 417-31.
74. Darnell, J.C., et al., *FMRP stalls ribosomal translocation on mRNAs linked to synaptic function and autism.* Cell. **146**(2): p. 247-61.
75. Siomi, M.C., et al., *Specific Sequences in the Fragile X Syndrome Protein FMR1 and the FXR Proteins Mediate Their Binding to 60S Ribosomal Subunits and the Interactions Among Them.* Mol. Cell. Biol, 1996. **16**(7): p. 3825-3832.
76. Kim, M., M. Bellini, and S. Ceman, *Fragile X mental retardation protein FMRP binds mRNAs in the nucleus.* Mol Cell Biol, 2009. **29**(1): p. 214-28.

77. Pieretti, M., et al., *Absence of expression of the FMR-1 gene in fragile X syndrome.* Cell, 1991. **66**: p. 817-822.
78. Coffee, B., et al., *Histone modifications depict an aberrantly heterochromatinized FMR1 gene in fragile x syndrome.* Am J Hum Genet, 2002. **71**(4): p. 923-32.
79. Stetler, A., et al., *Identification and characterization of the methyl arginines in the fragile X mental retardation protein Fmrp.* Hum Mol Genet, 2006. **15**(1): p. 87-96.
80. Denman, R.B., *Methylation of the arginine-glycine-rich region in the fragile X mental retardation protein FMRP differentially affects RNA binding.* Cell Mol Biol Lett, 2002. **7**(3): p. 877-83.
81. Phan, A.T., et al., *Structure-function studies of FMRP RGG peptide recognition of an RNA duplex-quadruplex junction.* Nat Struct Mol Biol. **18**(7): p. 796-804.
82. Ceman, S., et al., *Phosphorylation influences the translation state of FMRP-associated polyribosomes.* Hum Mol Genet, 2003. **12**(24): p. 3295-305.
83. Siomi, M., et al., *Casein Kinase II Phosphorylates the Fragile X Mental Retardation Protein and Modulates Its Biological Properties.* Mol Cell Biol, 2002. **22**(24): p. 8438-8447.
84. Pfeiffer, B.E. and K.M. Huber, *Fragile X mental retardation protein induces synapse loss through acute postsynaptic translational regulation.* J Neurosci, 2007. **27**(12): p. 3120-30.
85. Lane Coffee, R., Jr., et al., *In vivo neuronal function of the fragile X mental retardation protein is regulated by phosphorylation.* Hum Mol Genet.
86. Narayanan, U., et al., *S6K1 phosphorylates and regulates fragile X mental retardation protein (FMRP) with the neuronal protein synthesis-dependent mammalian target of rapamycin (mTOR) signaling cascade.* J Biol Chem, 2008. **283**(27): p. 18478-82.
87. Narayanan, U., et al., *FMRP phosphorylation reveals an immediate-early signaling pathway triggered by group I mGluR and mediated by PP2A.* J Neurosci, 2007. **27**(52): p. 14349-57.
88. Zalfa, F., et al., *A new function for the fragile X mental retardation protein in regulation of PSD-95 mRNA stability.* Nat Neurosci, 2007. **10**(5): p. 578-87.
89. Cheever, A. and S. Ceman, *Phosphorylation of FMRP inhibits association with Dicer.* RNA, 2009. **15**(3): p. 362-9.
90. Hou, L., et al., *Dynamic Translational and Proteasomal Regulation of Fragile X Mental Retardation Protein Controls mGluR-Dependent Long-Term Depression.* Neuron, 2006. **51**(4): p. 441-54.
91. Götz, J., et al., *Amyloid-induced neurofibrillary tangle formation in Alzheimer's disease: insight from transgenic mouse and tissue-culture models.* Int J Dev Neurosci, 2004. **22**(7): p. 453-65.
92. Luo, Y., et al., *Fragile X Mental Retardation Protein Regulates Proliferation and Differentiation of Adult Neural Stem/Progenitor Cells.* PLoS Genet. **6**(4): p. e1000898.
93. Callan, M.A. and D.C. Zarnescu, *Heads-up: new roles for the fragile X mental retardation protein in neural stem and progenitor cells.* Genesis. **49**(6): p. 424-40.
94. Castrén, M., et al., *Altered differentiation of neural stem cells in fragile X syndrome.* PNAS %R 10.1073/pnas.0508995102, 2005. **102**(49): p. 17834-17839.
95. Blonden, L., et al., *Two members of the Fxr gene family, Fmr1 and Fxr1, are differentially expressed in Xenopus tropicalis.* Int. J. Dev. Biol., 2005. **49**(4): p. 437-41.

96. van 't Padje, S., et al., *Characterisation of Fmrp in zebrafish: evolutionary dynamics of the fmr1 gene.* Development Genes and Evolution, 2005. **215**(4): p. 198.
97. Feng, Y., et al., *Fragile X mental retardation protein: nucleocytoplasmic shuttling and association with somatodendritic ribosomes.* J Neurosci, 1997. **17**(5): p. 1539-47.
98. Eberhart, D.E., et al., *The fragile X mental retardation protein is a ribonucleoprotein containing both nuclear localization and nuclear export signals.* Hum Mol Genet, 1996. **5**(8): p. 1083-91.
99. Bardoni, B., et al., *Analysis of Domains affecting intracellular localization of the FMRP protein.* Neurobiol. Dis., 1997. **4**: p. 329-336.
100. Fridell, R.A., et al., *A nuclear role for the Fragile X mental retardation protein.* Embo J, 1996. **15**(19): p. 5408-14.
101. Willemsen, R., et al., *Association of FMRP with ribosomal precursor particles in the nucleolus.* Biochem Biophys Res Commun, 1996. **225**(1): p. 27-33.
102. Napoli, I., et al., *The Fragile X Syndrome Protein Represses Activity-Dependent Translation through CYFIP1, a New 4E-BP.* Cell, 2008. **134**(6): p. 1042.
103. **Schenck,** A., et al., *A highly conserved protein family interacting with the **fragile** X mental retardation protein (FMRP) and displaying selective interactions with FMRP-related proteins FXR1P and FXR2P.* Proc. Natl. Acad. Sci. USA, 2001. **98**(15): p. *8844-9*.
104. Didiot, M.-C., et al., *Cells Lacking the Fragile X Mental Retardation Protein (FMRP) have Normal RISC Activity but Exhibit Altered Stress Granule Assembly.* Mol. Biol. Cell %R 10.1091/mbc.E08-07-0737, 2009. **20**(1): p. 428-437.
105. Thomas, M.G., et al., *RNA granules: the good, the bad and the ugly.* Cell Signal. **23**(2): p. 324-34.
106. Parker, R. and U. Sheth, *P bodies and the control of mRNA translation and degradation.* Mol Cell, 2007. **25**(5): p. 635-46.
107. Eulalio, A., I. Behm-Ansmant, and E. Izaurralde, *P bodies: at the crossroads of posttranscriptional pathways.* Nat Rev Mol Cell Biol, 2007. **8**: p. 9 - 22.
108. Barbee, S.A., et al., *Staufen- and FMRP-containing neuronal RNPs are structurally and functionally related to somatic P bodies.* Neuron, 2006. **52**(6): p. 997-1009.
109. Teixeira, D., et al., *Processing Bodies require RNA for assembly and contain nontranslating mRNAs.* RNA, 2005. **11**: p. 371-82.
110. Bhattacharyya, S., et al., *Relief of microRNA-mediated Translational Repression in Human Cells Subjected to Stress.* Cell, 2006. **125**: p. 1111-24.
111. Brengues, M., D. Teixeira, and R. Parker, *Movement of eukaryotic mRNAs between polysomes and cytoplasmic processing bodies.* Science, 2005. **310**(5747): p. 486-9.
112. Kedersha, N. and P. Anderson, *Mammalian Stress Granules and Processing Bodies.* Methods Enzym, 2007. **431**: p. 61-81.
113. Kedersha, N., et al., *Stress granules and processing bodies are dynamically linked sites of mRNP remodeling.* J. Cell Biol. %R 10.1083/jcb.200502088, 2005. **169**(6): p. 871-884.
114. Kedersha, N.L., et al., *RNA-binding proteins TIA-1 and TIAR link the phosphorylation of eIF-2 alpha to the assembly of mammalian stress granules.* J Cell Biol, 1999. **147**(7): p. 1431-42.
115. Pothof, J., et al., *MicroRNA responses and stress granule formation modulate the DNA damage response.* Cell Cycle, 2009. **8**(21): p. 3462-8.

116. Thomas, M.G., et al., *Mammalian Staufen 1 is recruited to stress granules and impairs their assembly.* J Cell Sci, 2009. **122**(Pt 4): p. 563-73.
117. Linder, B., et al., *Tdrd3 is a novel stress granule-associated protein interacting with the Fragile-X syndrome protein FMRP*. Hum. Mol. Genet. %R 10.1093/hmg/ddn219, 2008. **17**(20): p. 3236-3246.
118. Kanai, Y., N. Dohmae, and N. Hirokawa, *Kinesin Transports RNA Isolation and Characterization of an RNA-Transporting Granule* Neuron, 2004. **43**(4): p. 513-525
119. Davidovic, L., et al., *The Fragile X Mental Retardation Protein is a molecular adaptor between the neurospecific KIF3C kinesin and dendritic RNA granules.* Hum Mol Genet, 2007.
120. Kao, D.I., et al., *Altered mRNA transport, docking, and protein translation in neurons lacking fragile X mental retardation protein.* Proc Natl Acad Sci U S A. **107**(35): p. 15601-6.
121. Muddashetty, R.S., et al., *Dysregulated metabotropic glutamate receptor-dependent translation of AMPA receptor and postsynaptic density-95 mRNAs at synapses in a mouse model of fragile X syndrome.* J Neurosci, 2007. **27**(20): p. 5338-48.
122. Hengst, U., et al., *Functional and selective RNA interference in developing axons and growth cones.* J Neurosci, 2006. **26**(21): p. 5727-32.
123. Tessier, C.R. and K. Broadie, *Drosophila fragile X mental retardation protein developmentally regulates activity-dependent axon pruning.* Development, 2008. **epub ahead of print**.
124. Antar, L.N., et al., *Localization of FMRP-associated mRNA granules and requirement of microtubules for activity-dependent trafficking in hippocampal neurons.* Genes Brain Behav, 2005. **4**(6): p. 350-9.
125. Antar, L.N., et al., *Local functions for FMRP in axon growth cone motility and activity-dependent regulation of filopodia and spine synapses.* Mol Cell Neurosci, 2006. **32**(1-2): p. 37-48.
126. Christie, S.B., et al., *The FXG: a presynaptic fragile X granule expressed in a subset of developing brain circuits.* J Neurosci, 2009. **29**(5): p. 1514-24.
127. Campbell, D.S., et al., *Semaphorin 3A elicits stage-dependent collapse, turning, and branching in Xenopus retinal growth cones.* J Neurosci, 2001. **21**(21): p. 8538-47.
128. Weiler, I.J. and W.T. Greenough, *Synaptic synthesis of the Fragile X protein: possible involvement in synapse maturation and elimination.* Am J Med Genet, 1999. **83**(4): p. 248-52.
129. Job, C. and J. Eberwine, *Localization and translation of mRNA in dendrites and axons.* Nat Rev Neurosci, 2001. **2**(12): p. 889-98.
130. Snyder, E.M., et al., *Internalization of ionotropic glutamate receptors in response to mGluR activation.* Nat Neurosci, 2001. **4**(11): p. 1079-85.
131. Bear, M.F., K.M. Huber, and S.T. Warren, *The mGluR theory of fragile X mental retardation.* Trends Neurosci, 2004. **27**(7): p. 370-7.
132. Gasparini, F., et al., *2-Methyl-6-(phenylethynyl)-pyridine (MPEP), a potent, selective and systemically active mGlu5 receptor antagonist.* Neuropharmacology, 1999. **38**(10): p. 1493.
133. Chuang, S.C., et al., *Prolonged epileptiform discharges induced by altered group I metabotropic glutamate receptor-mediated synaptic responses in hippocampal slices of a fragile X mouse model.* J Neurosci, 2005. **25**(35): p. 8048-55.

134. Yan, Q.J., et al., *Suppression of two major Fragile X Syndrome mouse model phenotypes by the mGluR5 antagonist MPEP.* Neuropharmacology, 2005. **49**(7): p. 1053.
135. McBride, S.M., et al., *Pharmacological rescue of synaptic plasticity, courtship behavior, and mushroom body defects in a Drosophila model of fragile X syndrome.* Neuron, 2005. **45**(5): p. 753-64.
136. Nakamoto, M., et al., *Fragile X mental retardation protein deficiency leads to excessive mGluR5-dependent internalization of AMPA receptors.* Proc Natl Acad Sci U S A, 2007. **104**(39): p. 15537-42.
137. Wang, L.W., E. Berry-Kravis, and R.J. Hagerman, *Fragile X: leading the way for targeted treatments in autism.* Neurotherapeutics. **7**(3): p. 264-74.
138. Berry-Kravis, E., et al., *A pilot open label, single dose trial of fenobam in adults with fragile X syndrome.* J Med Genet, 2009. **46**(4): p. 266-71.
139. Jourdi, H., et al., *Positive AMPA receptor modulation rapidly stimulates BDNF release and increases dendritic mRNA translation.* J Neurosci, 2009. **29**(27): p. 8688-97.
140. Berry-Kravis, E., et al., *Effect of CX516, an AMPA-modulating compound, on cognition and behavior in fragile X syndrome: a controlled trial.* J Child Adolesc Psychopharmacol, 2006. **16**(5): p. 525-40.
141. Liu, Z.H., D.M. Chuang, and C.B. Smith, *Lithium ameliorates phenotypic deficits in a mouse model of fragile X syndrome.* Int J Neuropsychopharmacol. **14**(5): p. 618-30.
142. Hagerman, R.J., et al., *Advances in the Treatment of Fragile X Syndrome.* Pediatrics %R 10.1542/peds.2008-0317, 2009. **123**(1): p. 378-390.
143. Berry-Kravis, E., et al., *Open-label treatment trial of lithium to target the underlying defect in fragile X syndrome.* J Dev Behav Pediatr, 2008. **29**(4): p. 293-302.
144. Weng, N., et al., *Early-phase ERK activation as a biomarker for metabolic status in fragile X syndrome.* Am J Med Genet B Neuropsychiatr Genet, 2008. **147B**(7): p. 1253-7.
145. Bilousova, T.V., et al., *Minocycline promotes dendritic spine maturation and improves behavioural performance in the fragile X mouse model.* J Med Genet, 2009. **46**(2): p. 94-102.
146. Paribello, C., et al., *Open-label add-on treatment trial of minocycline in fragile X syndrome.* BMC Neurol. **10**: p. 91.
147. Owen, R., et al., *Aripiprazole in the treatment of irritability in children and adolescents with autistic disorder.* Pediatrics, 2009. **124**(6): p. 1533-40.
148. Utari, A., et al., *Side effects of minocycline treatment in patients with fragile X syndrome and exploration of outcome measures.* Am J Intellect Dev Disabil. **115**(5): p. 433-43.
149. Dvorak, E.M., N.C. Ketchum, and J.R. McGuire, *The underutilization of intrathecal baclofen in poststroke spasticity.* Top Stroke Rehabil. **18**(3): p. 195-202.
150. Pin, T.W., et al., *Use of intrathecal baclofen therapy in ambulant children and adolescents with spasticity and dystonia of cerebral origin: a systematic review.* Dev Med Child Neurol. **53**(10): p. 885-95.
151. Jaenisch, R., et al., *Chromosomal position and activation of retroviral genomes inserted into the germ line of mice.* Cell, 1981. **24**(2): p. 519.
152. Mooslehner, K., et al., *Structure and expression of a gene encoding a putative GTP-binding protein identified by provirus integration in a transgenic mouse strain.* Mol Cell Biol, 1991. **11**(2): p. 886-93.
153. Dalmay, T., et al., *SDE3 encodes an RNA helicase required for post-transcriptional gene silencing in Arabidopsis.* EMBO J, 2001. **20**: p. 2069–2077.

154. Ueyama, T., et al., *Csm, a cardiac-specific isoform of the RNA helicase Mov10l1, is regulated by Nkx2.5 in embryonic heart.* J Biol Chem, 2003. **278**(31): p. 28750-7.
155. Tomari, Y., et al., *RISC Assembly Defects in the Drosophila RNAi Mutant armitage.* Cell, 2004. **116**(6): p. 831.
156. Haussecker, D., et al., *Capped small RNAs and MOV10 in human hepatitis delta virus replication.* Nat Struct Mol Biol, 2008. **15**(7): p. 714-21.
157. Wang, X., et al., *Moloney leukemia virus 10 (MOV10) protein inhibits retrovirus replication.* J Biol Chem. **285**(19): p. 14346-55.
158. Burdick, R., et al., *P Body-Associated Protein Mov10 Inhibits HIV-1 Replication at Multiple Stages.* J. Virol. , 2010. **84**(19): p. 10241-53.
159. Furtak, V., et al., *Perturbation of the P-Body Component Mov10 Inhibits HIV-1 Infectivity.* PLoS ONE, 2010. **5**(2): p. e9081.
160. Schutz, P., et al., *Comparative structural analysis of human DEAD-box RNA helicases.* PLoS One, 2010. **5**(9).
161. Abudu, A., et al., *Identification of molecular determinants from Moloney leukemia virus 10 homolog (MOV10) protein for virion packaging and anti-HIV-1 activity.* J Biol Chem. **287**(2): p. 1220-8.
162. Meister, G., et al., *Identification of novel argonaute-associated proteins.* Curr Biol, 2005. **15**(23): p. 2149-55.
163. Chendrimada, T.P., et al., *MicroRNA silencing through RISC recruitment of eIF6.* Nature, 2007. **447**(7146): p. 823-8.
164. Banerjee, S., P. Neveu, and K.S. Kosik, *A Coordinated Local Translational Control Point at the Synapse Involving Relief from Silencing and MOV10 Degradation.* Neuron, 2009. **64**(6): p. 871.

Chapter 2. FMRP binds mRNAs in the nucleus

This chapter has been published in Molecular Cellular Biology

Mol. Cell. Biol. January 2009 vol. 29 no. 1 214-228

2.1 Abstract

The fragile X mental retardation protein FMRP is an RNA binding protein that associates with a large collection of mRNAs. Since FMRP was previously shown to be a nucleocytoplasmic shuttling protein, we examined the hypothesis that FMRP binds its cargo mRNAs in the nucleus. The enhanced green fluorescent protein-tagged FMRP construct (EGFP-FMRP) expressed in Cos-7 cells was efficiently exported from the nucleus in the absence of its nuclear export sequence and in the presence of a strong nuclear localization sequence (the simian virus 40 [SV40] NLS), suggesting an efficient mechanism for nuclear export. We hypothesized that nuclear FMRP exits the nucleus through its bound mRNAs. Using silencing RNAs to the bulk mRNA exporter Tap/NXF1, we observed a significantly increased number of cells containing EGFP-FMRP in the nucleus, which was further augmented by removal of FMRP's nuclear export sequence. Nuclear-retained SV40-FMRP could be released upon treatment with RNase. Further, Tap/NXF1 coimmunoprecipitated with EGFP-FMRP in an RNA-dependent manner and contained the FMR1 mRNA. To determine whether FMRP binds pre-mRNAs cotranscriptionally, we expressed hemagglutinin-SV40 FMRP in amphibian oocytes and found it, as well as endogenous Xenopus FMRP, on the active transcription units of lampbrush chromosomes. Collectively, our data provide the first lines of evidence that FMRP binds mRNA in the nucleus.

2.2 Introduction

Fragile X syndrome is one of the most common forms of inherited mental retardation, affecting approximately 1/4,000 males and 1/8,000 females (reviewed in reference 34). Fragile X syndrome is caused by the loss of expression of the fragile X mental retardation protein FMRP (32, 40, 64, 77, 84), which is a highly conserved RNA binding protein with two KH domains and an RGG box (6, 70, 71). The N terminus (2, 86), KH1 domain (1), KH2 domain (17), and the

RGG box (12, 18, 69) have all been reported to bind RNA. FMRP is estimated to associate with approximately 4% of brain mRNAs (6, 12), and two large collections of associated mRNAs have been described (12, 58).

FMRP is primarily cytoplasmic by both immunostaining and biochemical fractionation (22, 30); however, it contains a functional, nonclassical nuclear localization sequence (NLS) near its N terminus (7, 24, 73). Immunogold studies have shown that FMRP is present in the neuronal nucleoplasm and within nuclear pores (30). In addition, the presence of FMRP in the nucleus is regulated temporally, such that at specific times during development, FMRP is predominantly nuclear. Studies in Xenopus tropicalis embryos showed that FMRP was largely nuclear 2 h postfertilization (stage 6), suggesting a special nuclear function during this developmental period (9). Zebrafish embryos also demonstrated predominantly nuclear FMRP staining very early in development, 3 h postfertilization (81). Interestingly, these time points coincide with times in development when no zygotic transcription is taking place (62), providing indirect evidence that FMRP export from the nucleus might depend on mRNA synthesis.

FMRP has been speculated to enter the nucleus to bind its mRNAs (25, 46, 78), although there is no evidence to support this assertion other than the fact that FMRP has an NLS and is occasionally nuclear. Some RNA binding proteins do enter the nucleus to associate with their mRNA cargoes and facilitate export to the cytoplasm, for example, the zipcode binding protein ZBP1 (43), hnRNP A2 (reviewed in reference 28), and Drosophila proteins Sqd (35, 38) and Y14/Tsunagi (37, 50, 53).

The nuclear protein Tap/NXF1 was originally characterized as the exporter of retroviral RNAs bearing the constitutive transport element (CTE) (11, 36, 49). Since then, Tap/NXF1 has been identified as the primary exporter of cellular mRNAs (reviewed in references 15, 44, 56, 61, and 80) by binding mRNAs directly through CTE-like elements (10, 55) or indirectly through association with other RNA binding proteins. Tap/NXF1 has been demonstrated to interact with proteins bound to the mature mRNA like the SR proteins (41, 42) and proteins in the exon junction complex, like Aly/Ref (68), supporting the idea that mRNA export is tightly coupled to splicing (reviewed in references 46 and 47).

To begin to understand how FMRP identifies and binds its collection of mRNAs, it was critical to establish where mRNA binding occurs. We hypothesized that this association takes place in the nucleus. We show here that FMRP functionally interacts with the bulk mRNA

exporter Tap/NXF1, suggesting that these proteins associate through mRNAs bound in the nucleus. Further, we demonstrate that FMRP associates with the active transcription units of the lampbrush chromosomes (LBCs) in amphibian oocytes. Taken together, we provide the first direct evidence that FMRP binds mRNAs in the nucleus.

2.3 Results

FMRP requires an efficient nuclear export mechanism in addition to its NES.

In order to test whether FMRP binds its cargo mRNAs in the nucleus, we strove to develop an experimental system in which a significant amount of FMRP would be nuclear. We used an EGFP-FMRP construct, described previously (75), for the direct visualization of FMRP cellular trafficking. Importantly, it was previously shown that EGFP-FMRP has RNA binding properties and transport characteristics indistinguishable from the native protein (3, 19, 21, 75). EGFP-FMRP was found to localize primarily within the cytoplasm of transfected cells (Fig. 1A), as described before (22), while only ~0.4% of the cells displayed predominantly nuclear EGFP-FMRP (Fig. 1F).

FMRP has an NES encoded within exon 14 that was defined by deletion analysis: its removal increased the localization of FMRP ΔNES (hereafter referred to as ΔNES) to the nucleus (5, 24, 73). The NES of FMRP is similar to the Rev/protein kinase A inhibitor-type NES and can even function in place of the Rev NES in an export assay (31). Further, treatment with leptomycin B, which blocks the nuclear export of proteins containing leucine-rich NESs by inhibiting interaction with CRM1/exportin 1 (33, 65, 74), resulted in some nuclear accumulation of FMRP (78). Accordingly, we found that the removal of the NES from EGFP-FMRP resulted in an increased nuclear accumulation of ΔNES (Fig. 1B, arrows) but not in all cells (Fig. 1F). To show that ΔNES was indeed in both the nucleus and the cytoplasm, we obtained optical sections through cells transfected with ΔNES and confirmed that the distribution of FMRP was between both the nucleus and the cytoplasm (Fig. 1C). One major conclusion is that the majority of the transfected cells exhibit cytoplasmic EGFP-FMRP even in the absence of the NES (Fig. 1B, C, and F). There are at least three possible explanations for this result. The first is that the NES is inactive in these cells. We do not suspect that this is the case because the NES was functionally defined in Cos-7 cells by conjugating it to bovine serum albumin and then showing that the nuclear injected fusion protein could be exported (24). The second possibility is that there are

two distinct populations of FMRP, with the majority being exclusively cytoplasmic. The third possibility is that FMRP is efficiently exported out of the nucleus by a mechanism that is independent of its NES.

The NLS of FMRP is not a classical NLS (39); thus, the molecular requirements for its activation are not well understood. To address the possibility that only a fraction of the FMRP enters the nucleus, we attempted to direct all of the expressed EGFP-FMRP to the nucleus by adding the autonomous NLS of the SV40 large T antigen (47, 48) to the N terminus of FMRP. Surprisingly, while the SV40 NLS is a strong nuclear import signal, it did not significantly increase the amount of steady-state nuclear SV40-FMRP (Fig. 1D and F), and the percentage of cells with primarily nuclear SV40-FMRP was essentially unchanged (Fig. 1F). The SV40 NLS was effective because the removal of the NES from SV40-FMRP resulted in an increased number of cells in which the newly expressed protein was evenly distributed between the cytoplasm and the nucleus (Fig. 1E [arrows] and F). However, the percentage of cells where SV40-FMRP ΔNES (SV40-ΔNES) was exclusively nuclear only increased to 12% (Fig. 1F). The same results were obtained when the constructs were expressed in HeLa cells (data not shown). Together, these data strongly suggest the existence of an efficient mechanism—distinct from the NES-dependent export pathway—that is primarily responsible for the nuclear export of FMRP.

Tap/NXF1 knockdown increases the nuclear accumulation of FMRP.

FMRP binds a large collection of mRNAs (12, 58) and has been estimated to associate with approximately 4% of brain mRNAs (6). We hypothesized that if FMRP enters the nucleus to bind mRNAs, then the bound mRNAs themselves might direct export through their association with the bulk mRNA exporter Tap/NXF1. To determine whether Tap/NXF1 is involved in the export of FMRP from the nucleus, we developed four siRNAs against Tap/NXF1 that were specific for Tap/NXF1 by a BLAST search (data not shown). Administered as a cocktail of all four siRNAs (Fig. 2A, lane All) or individually (Fig. 2A, lanes 1 to 4), the Tap/NXF1 siRNAs greatly reduced Tap/NXF1 expression in cells by 67 to 91% compared to that of the mock-treated cells, based on densitometry (Fig. 2A). Further, serial dilutions of the mock-treated cell extracts shown on the right in Fig. Fig.2A2A verify that all of the Tap/NXF1 siRNA treatments did indeed reduce Tap/NXF1 expression levels by more than 70%.

To examine the role of Tap/NXF1 in the export of FMRP from the nucleus, we treated EGFP- or SV40-FMRP-expressing cells with these siRNAs. Treatment with the irrelevant siRNA resulted in very few cells showing predominantly nuclear expressions of FMRP (Fig. (Fig. 2B and the first bars of E and F, respectively). Approximately 0.4% of the EGFP-FMRP-expressing cells and 2% of the SV40-FMRP-expressing cells were primarily nuclear. In contrast, the treatment of EGFP-FMRP-expressing cells with pooled siRNAs or the individual siRNAs significantly increased the number of cells with nuclear EGFP-FMRP to nearly 5%, which was a 10-fold increase over treatment with an irrelevant siRNA (Fig. 2E). The treatment of cells expressing SV40-FMRP with Tap siRNAs also resulted in a 10-fold increase in the number of cells expressing predominantly nuclear FMRP (Fig. 2C, D, and F). Because more SV40-FMRP was directed to the nucleus, the percentage of cells expressing primarily nuclear FMRP after Tap siRNA treatment was as high as 34.5% (Fig. 2F). Similarly to the results observed in Fig. 1F, the SV40 NLS was much more efficient at directing FMRP into the nucleus than the native protein (compare Fig. 2E and F). However, both populations of transfected cells showed a significant increase in the number of cells expressing FMRP in the nucleus after the reduction of Tap/NXF1 expression, underscoring the importance of this protein in the nuclear export of FMRP.

SV40-FMRP is localized in the nucleus.

To ensure that SV40-FMRP was indeed localized inside the nucleus and not on the outer nuclear membrane, we live imaged transfected cells using confocal microscopy. Figure Figure2G2G shows the nuclear expression of SV40-FMRP in Tap 2 siRNA-treated cells that were counterstained with the cytoplasmic stain BODIPY that labels endoplasmic reticula, Golgi bodies, and mitochondria, leaving the nuclei unstained (4, 82). SV40-FMRP is present in the nuclei and, in some cases, subnuclear structures (Fig. 2G). Thus, under conditions of reduced Tap/NXF1 expression, FMRP accumulates in the nucleus, suggesting that FMRP binds mRNAs in the nucleus and that the complex is exported by Tap/NXF1.

The endogenous NLS directs a significant amount of FMRP into the nucleus.

To examine the efficacy of the endogenous NLS, we examined the effects of removing both the NES- and the Tap/NXF1-mediated export pathways. We found that about 5% of the cells expressing ΔNES were nuclear and 39% had ΔNES evenly distributed between the nucleus

and the cytoplasm (Fig. 3, middle bars). When the ΔNES-expressing cells were treated with Tap/NXF1 siRNA, the number of cells with primarily nuclear expression of ΔNES increased to 7.6% and there was a further increase in the fraction of cells showing an even distribution of ΔNES between the nucleus and the cytoplasm from 39% to 57% (Fig. 3, right bars). Thus, blocking both nuclear export pathways led to the redistribution of FMRP from its primarily cytoplasmic distribution to one where the majority of cells (57%) expressed ΔNES evenly between the nucleus and the cytoplasm and 7.6% of the cells expressed ΔNES primarily in the nucleus. We conclude that a significant amount of FMRP enters the nucleus using the endogenous NLS.

Removal of the NLS leads to compromised RNA binding

If the endogenous NLS were indeed required for nuclear entry leading to subsequent RNA binding, we reasoned that its removal should result in a loss of FMRP from polyribosomes. We removed the 40 amino acid NLS from FMRP (ΔNLS), which is encoded within exon 5, and examined whether association with polyribosomes was affected, as evidence for a functional association with mRNAs (Fig. 4B). The removal of the NLS led to a 50% loss of FMRP from polyribosomes to the messenger RNP fractions compared to that of EGFP-FMRP (compare Fig. 4A and B). Initially, this result seemed like indirect evidence that FMRP bound mRNAs in the nucleus. However, we wanted to establish that ΔNLS had not lost the ability to bind RNAs because of the deletion. When we compared the ability of in vitro-synthesized EGFP-FMRP and ΔNLS to bind a G quartet bearing RNA (sc1) through the distal, C-terminal RNA binding domain, the RGG box (encoded within exon 15), we found ΔNLS to be severely compromised (Fig. 4C), suggesting that the ΔNLS protein is partially misfolded. Further, ΔNLS is unable to associate with the known binding partner autosomal paralog FXR1 in cells (Fig. 4D), whose binding site is encoded by exon 7 (72). Thus, the removal of the NLS in the N-terminal part of the protein led to a reduced ability to bind RNAs and FXR1, whose interaction sites are more distally located, suggesting that amino acids 110 to 151 are critical for the normal folding and function of FMRP.

Tap/NXF1 knockdown increases the nuclear accumulation of SV40-ΔNES.

To examine the combined effects of the NES and Tap/NXF1 on cells in which all of the FMRP is directed to the nucleus, we examined the effect of Tap reduction on nuclear localization using cells expressing SV40-ΔNES. As shown earlier, most of the cells expressing SV40-ΔNES had FMRP evenly distributed between the nucleus and the cytoplasm (55%). To verify that indeed the SV40-ΔNES cells were expressing FMRP in both the nuclear and cytoplasmic compartments, we also performed confocal microscopy on the cells (Fig. 5B). We also found that approximately 12% of the SV40-ΔNES-expressing cells treated with an irrelevant siRNA were primarily nuclear (Fig.1 and 5A and B). In contrast, treatment with either Tap 1 or Tap 2 siRNAs greatly increased the number of cells expressing primarily nuclear FMRP to 42% and 51%, respectively (Fig. 5C, D, and E). Accordingly, the amount of cells expressing SV40-ΔNES primarily in the cytoplasm decreased from 33% to 10% after Tap siRNA treatment (Fig. 5E, middle bars). Thus, FMRP can exit the nucleus through its NES, as well as by a Tap-mediated export pathway—presumably through its bound mRNAs—supporting our hypothesis for two mechanisms of export: one encoded by the NES of FMRP and the other by the bulk mRNA exporter Tap/NXF1.

Validation of the cell scoring method by directly quantifying the intracellular fluorescence.

To verify that quantifying the percentage of cells expressing EGFP-FMRP as nuclear, cytoplasmic, or evenly distributed was consistent, we determined the ratio of total nuclear fluorescence to total cellular fluorescence on a significant number of cells from each treatment type (Fig. 5F). For cells that were scored as cytoplasmic (Fig. 5F), approximately 13% of the total fluorescence was in the nucleus, and none of the treatment groups were significantly different from one another, with the exception of the cytoplasmic cells in the SV40-ΔNES Tap/NXF1, which had an increased amount of fluorescence in the nucleus (17%). For cells that were scored as nuclear (Fig. 5F), approximately 38% of the fluorescence was in the nucleus, which was significantly different from both the cytoplasmic and evenly distributed cells. All cells expressing EGFP-FMRP primarily in the nucleus had the same percentage of their fluorescence in the nucleus, regardless of the type of treatment and were not significantly different from one another. For cells that were described as evenly distributed, which were only observed when the NES was removed (Fig. 5F), approximately 24% of the fluorescence was

found in the nucleus. Thus, this quantification shows that the scoring of cells as nuclear, evenly distributed, or cytoplasmic represents distinct and reproducible subpopulations of cells in these experiments.

The nuclear association of FMRP is RNA mediated.

Our hypothesis is that FMRP enters the nucleus to bind mRNAs, which then facilitate the export of the complex through the Tap/NXF1 pathway. Therefore, in the absence of Tap/NXF1, SV40-FMRP retained in the nucleus should be bound to RNA. To test this prediction, Cos-7 cells transfected with SV40-FMRP and Tap 2 siRNA were treated with RNase A, which can freely diffuse into the nucleus of permeabilized cells. We then examined the number of cells expressing nuclear SV40-FMRP. The permeabilization of the cytoplasmic membrane in the absence of RNase A did not alter the nuclear or cytoplasmic localization of SV40-FMRP (Fig. 6A). Although the Triton X-100 treatment did moderately affect the morphology of the nucleus (Fig. 6A, top panels), it did not influence the percentage of cells expressing nuclear SV40-FMRP compared to that of CSK buffer-treated cells (Fig. 6C). In contrast, RNase A treatment significantly reduced the number of cells expressing SV40-FMRP primarily in the nucleus from 36.6% to 11.9% (Fig. 6B and C). RNase A treatment did not affect SV40-FMRP-containing granules in the cytoplasm (Fig. 6B). Our data show that in the absence of Tap/NXF1, SV40-FMRP is retained in the nucleus in an RNA-dependent manner.

Using siRNAs directed to Tap/NXF1, we have established a functional relationship between Tap/NXF1 and FMRP. To determine if FMRP associates with Tap/NXF1 in an RNA-dependent manner, we immunoprecipitated EGFP-FMRP or SV40-FMRP with 7G1-1, an antibody that robustly recognizes murine FMRP (12). The immunoprecipitated complex was then treated with RNase to disrupt any RNA-mediated complexes and examined for the presence of endogenous Tap/NXF1. We found that Tap/NXF1 did indeed coimmunoprecipitate with EGFP-FMRP and SV40-FMRP in an RNA-dependent manner (Fig. 6D).

To eliminate the possibility of the postlysis association of FMRP and Tap/NXF1, we chemically cross-linked mock-transfected cells or cells expressing Flag-Tap with one of the following constructs: EGFP-FMRP, SV40-FMRP, or the FMR point mutation I304N (20). The expression of the transgenes is shown in Fig. 6E (left panel) because both the Tap/NXF1 and FMRP constructs contain the Flag epitope. Upon the immunoprecipitation with the 7G1 antibody,

we found that EGFP-FMRP, SV40-FMRP, and I304N all associate with Tap/NXF1 (Fig. 6E, right panel). Like FMRP, Tap/NXF1 is also found on polyribosomes (45). The I304N mutant shuttles rapidly between the nucleus and cytoplasm more so than EGFP-FMRP (78), likely because it is not captured on polyribosomes. Since I304N is present in the nucleus but not on polyribosomes (29), the association of Tap/NXF1 with I304N provides evidence that Tap/NXF1 interaction with FMRP does not occur on polyribosomes.

Only proteins within close proximity to one another are cross-linked, as we were unable to find eIF5, an abundant but nonassociated protein, in the immunoprecipitations (data not shown). We conclude that Tap/NXF1 and FMRP do associate in cells and that this interaction does not occur on polyribosomes.

Tap/NXF1 associates with FMRP in a complex with FMR1 mRNA.

Our hypothesis is that FMRP enters the nucleus to associate with its cargo mRNAs, which then facilitate the export of the FMRP-mRNA complex through association with the bulk mRNA exporter Tap/NXF1. Although two large lists of FMRP mRNA cargoes have been described (12, 58), the association with FMR1 mRNA has been the most extensively characterized (3, 6, 13, 69). In fact, just recently FMRP was described as modulating the splicing of its own mRNA (23). To determine whether the FMRP-Tap/NXF1-FMR1 mRNA complex exists, we undertook the sequential immunoprecipitation strategy shown in Fig. 7A to capture the FMRP-Tap/NXF1 complex. After cross-linking mock-transfected Cos-7 cells or Cos-7 cells either expressing EGFP-FMRP or cotransfected with both EGFP-FMRP and Flag-Tap (Fig. 7B), we immunoprecipitated EGFP-FMRP with the 7G1-1 antibody. After being extensively washed, the FMRP-containing complexes were eluted using the FMRP peptide that is recognized by 7G1-1 (12). The released FMRP-containing complexes were then reimmunoprecipitated with the anti-Tap antibody that immunoprecipitates Tap/NXF1 (Fig. 7C) to isolate EGFP-FMRP-Flag-Tap/NXF1 complexes. RNA was isolated from the FMRP-Tap/NXF1 complex and found to contain FMR1 mRNA (Fig. 7D), which was also present in the peptide elution from the EGFP-FMRP immunoprecipitation but not from the mock immunoprecipitation. We conclude that FMRP associates with Tap/NXF1 in a complex that contains FMR1 mRNA that is known to bind FMRP, providing further evidence that FMRP and Tap/NXF1 associate in an mRNA-dependent complex.

Nuclear EGFP-SV40-Flag-FMRP is not recognized efficiently by the anti-FMRP antibody 1a by immunostaining.

In the studies presented here, all of the cellular assays were done with EGFP-FMRP. We also tried to examine the effect of Tap/NXF1 knockdown on endogenous FMRP localization in Cos-7 cells. To our surprise, we found that the anti-FMRP antibody 1a, which has effectively been used for immunostaining (22) and Western blotting, including the detection of the FMRP encoded by the constructs used here (75), did not consistently identify nuclear FMRP by immunostaining. We first attempted to immunostain endogenous FMRP in Tap/NXF1 siRNA-treated Cos-7 cells and saw only cytoplasmic staining (data not shown). To be sure that we were using the optimal staining conditions for the nuclear FMRP, we stained Tap/NXF1 siRNA-treated, SV40-FMRP-expressing cells with either the Flag antibody (Fig. 8B, red), which recognizes nuclear SV40-FMRP, or with the 1a antibody (Fig. 8A, red), which shows cytoplasmic staining. That SV40-FMRP is indeed in the nucleus is shown by the EGFP staining (green in Fig. 8A and B). Thus, unlike the N-terminal Flag epitope, perhaps the 1a epitope is inaccessible or buried in the nucleus.

FMRP associates with nascent transcripts in amphibian oocytes.

At this point, our data suggest that FMRP binds mRNAs in the nucleus because of a functional and RNA-mediated association with Tap/NXF1. To directly ask whether FMRP binds nascent mRNAs, we adopted the most tractable system for examining messenger RNP formation on transcripts: the LBCs of amphibian oocytes. LBCs are extended bivalent chromosomes, characterized by the presence of numerous lateral loops along the length of each homolog (reviewed in reference 60). Each chromosomal loop is composed of a DNA axis that is actively transcribed by RNA polymerase II and from which are elongating, tightly packed, nascent ribonucleoprotein (RNP) fibrils. We transcribed the HA-SV40-WT FMR1 mRNA in vitro, injected the RNA into the cytoplasm of stage V oocytes, and monitored the fate of the newly made HA-SV40-FMRP by indirect immunofluorescence on nuclear spreads. We found that HA-SV40-FMRP associates with nascent RNP fibrils on LBCs (Fig. 9B). We used the rat monoclonal antibody 3F10 because its high-affinity binding precludes nonspecific recognition (8, 66). Interestingly, the labeling of any given loop does not correspond to a homogenous signal over its length, as is usually the case for many other RNPs (8). Rather, the signal appears

discontinuous and specific for granular complexes on the loops (Fig. 9B and D). Overall, HA-SV40-FMRP staining was generally weak but specific compared to LBCs from uninjected control oocytes (Fig.9F), possibly due to the fact that this is a heterologous system where murine FMRP is bound to Xenopus proteins and transcripts. We also observed the presence of HA-SV40-FMRP in the nucleoli and Cajal bodies, with a general preference for association with Cajal bodies (data not shown).

To determine whether endogenous Xenopus FMRP is also present on LBCs, we stained nuclear spreads of uninjected oocytes with an antibody directed against Xenopus FMRP (9). Figure 10B and D show that anti-FMRP labeled the chromosomal loops, strongly suggesting that endogenous FMRP associates with nascent transcripts. A control stain using a preimmune serum showed no staining above the background (Fig. 10F), suggesting that the FMRP staining was specific for endogenous FMRP.

We used two independent approaches to examine whether FMRP associates with mRNAs in the nucleus. First, we showed that reduction of the primary mRNA exporter resulted in a significantly higher number of cells expressing EGFP-FMRP and SV40-FMRP in the nucleus and that both EGFP-FMRP and SV40-FMRP associate with Tap/NXF1 in an mRNA-containing complex. Second, using two different antibodies, we showed that HA-SV40 FMRP and endogenous Xenopus FMRP are present on nascent transcripts on LBCs. Together, these data provide the first evidence that FMRP binds mRNAs in the nucleus.

2.4 Discussion

Role of Tap/NXF1 on the export of FMRP from the nucleus.

Tap/NXF1 was originally characterized as the exporter of retroviral RNAs bearing a CTE (11, 36, 49). Tap/NXF1 has since been identified as the primary exporter of mRNAs (reviewed in references 15, 44, 56, 61, and 80). Although Tap/NXF1 has an RNA binding domain, it is of relatively low affinity (49). Thus, there are two mechanisms by which Tap/NXF1 is proposed to export mRNAs: the first is by directly binding the CTE-like elements in the mRNAs themselves; the second is by directly interacting with proteins bound to the mature mRNA (41, 42). At this time, we are not certain through which of these mechanisms Tap/NXF1 mediates the export of FMRP-mRNA complexes. CTEs have been found in mammalian genes, specifically, in the Tap/NXF1 gene itself (55) and in the Wilms' tumor gene (10). It is possible that some of the

RNAs bound by FMRP contain a CTE; alternatively, and probably more likely, the mRNAs bound by FMRP are also bound by proteins associated with mature splicing like the exon junction complex component Aly/Ref (52, 53), which directly associate with Tap/NXF1 (76).

Although we observed that both the NES and Tap/NXF1 were critical for the export of FMRP from the nucleus, we were unable to identify a condition where all of the cells expressed exclusively nuclear FMRP, leading one to speculate on how FMRP exits the nucleus efficiently in the rest of the cells. One possible explanation is that any residual Tap/NXF1 expression in cells after siRNA treatment facilitates export. It is also possible that other export factors facilitate the export of FMRP. NXF2, another NXF family member, has highly conserved architecture and is also capable of mRNA export (79). In fact, NXF2 has been shown to associate with FMRP and is also present in testes and brain (79, 87). NXF2 has also been proposed to destabilize Tap/NXF1 mRNA when associated with FMRP (87). Perhaps in cells where FMRP and NXF2 are expressed, a reduction in Tap/NXF1 expression is desirable to either increase the nuclear accumulation of FMRP or permit the association of FMRP with NXF2 in the absence of Tap/NXF1. Primarily found in the brain and testes and not highly expressed in cells used in tissue culture, NXF2 may perform tissue-specific functions that likely have not influenced the function of Tap/NXF1 in our experiments.

FMRP and Tap/NXF1 functionally associate.

In addition to that shown in our study, a functional association between Tap/NXF1 and FMRP has already been shown to occur during Drosophila development (59). The small bristles gene encodes the Drosophila ortholog of Tap/NXF1 (85). During cleavage furrow formation, blocking Tap/NXF-1 expression using the conditional small bristles mutant results in a dramatic change in the cytoplasmic state of Drosophila FMRP. In the absence of exported zygotic transcripts, Drosophila FMRP moves from relatively diffuse punctate structures to large polymorphic structures. Thus, the cytoplasmic particles containing Drosophila FMRP are dynamic in response to new transcripts (59).

In the studies mentioned earlier, it was suggested that FMRP interacts with the Tap/NXF family member NXF2 but not with Tap/NXF1 (51, 87). This conclusion was drawn in part from the inability to coimmunoprecipitate Tap/NXF1 with FMRP. Our study differs from that work in two ways: (i) we used a robust FMRP-immunoprecipitating antibody, 7G1-1, to capture FMRP

complexes (12) in contrast to the antibody used for the studies described previously (51, 87), which has been characterized as working only for immunostains and Western blots (14, 19, 22), and (ii) we suspect that the association with FMRP is transient and likely mediated by RNA. We found that FMRP and Tap/NXF1 do indeed associate in an mRNA-containing complex that is captured using cross-linking and disrupted upon RNase treatment. More importantly, in addition to demonstrating a physical association, we show a functional effect of the loss of Tap/NXF1 on FMRP localization in cells.

FMRP's NLS.

We showed that the reduction of Tap/NXF1 in cells expressing EGFP-FMRP resulted in the nuclear accumulation of FMRP and that the removal of both Tap/NXF1 and the NES led to the majority of cells expressing some FMRP in the nucleus. Thus, FMRP's endogenous NLS is functional, as has been reported before (24); however, the SV40 NLS is much more efficient at directing FMRP into the nucleus. One explanation for the relative weakness of FMRP's NLS might be that it requires additional factors to be activated. Perhaps cell-type or cell-cycle-specific proteins facilitate the nuclear import of FMRP under specific conditions, as in the early stages of Xenopus and zebrafish development when FMRP is primarily nuclear (9, 81). In contrast, the removal of FMRP's NLS led to an improperly functioning protein that could not be evaluated for its ability to traffic in cells. Naturally occurring splice variants of FMRP retain normal protein function after the removal of some domains like the RGG box and the NES (5, 26), suggesting that FMRP behaves more modularly in the C terminus.

In conclusion, prior studies established that FMRP resides in the nucleus under certain conditions, although it was not known what its function was there. It has been long speculated that FMRP binds its mRNA cargoes in the nucleus, but the evidence has been lacking. By demonstrating a functional and physical association with the primary RNA exporter Tap/NXF1 and also by visualizing FMRP association with the LBCs, we provide the first evidence that FMRP can enter the nucleus to bind its mRNA cargoes.

2.5 Figures.

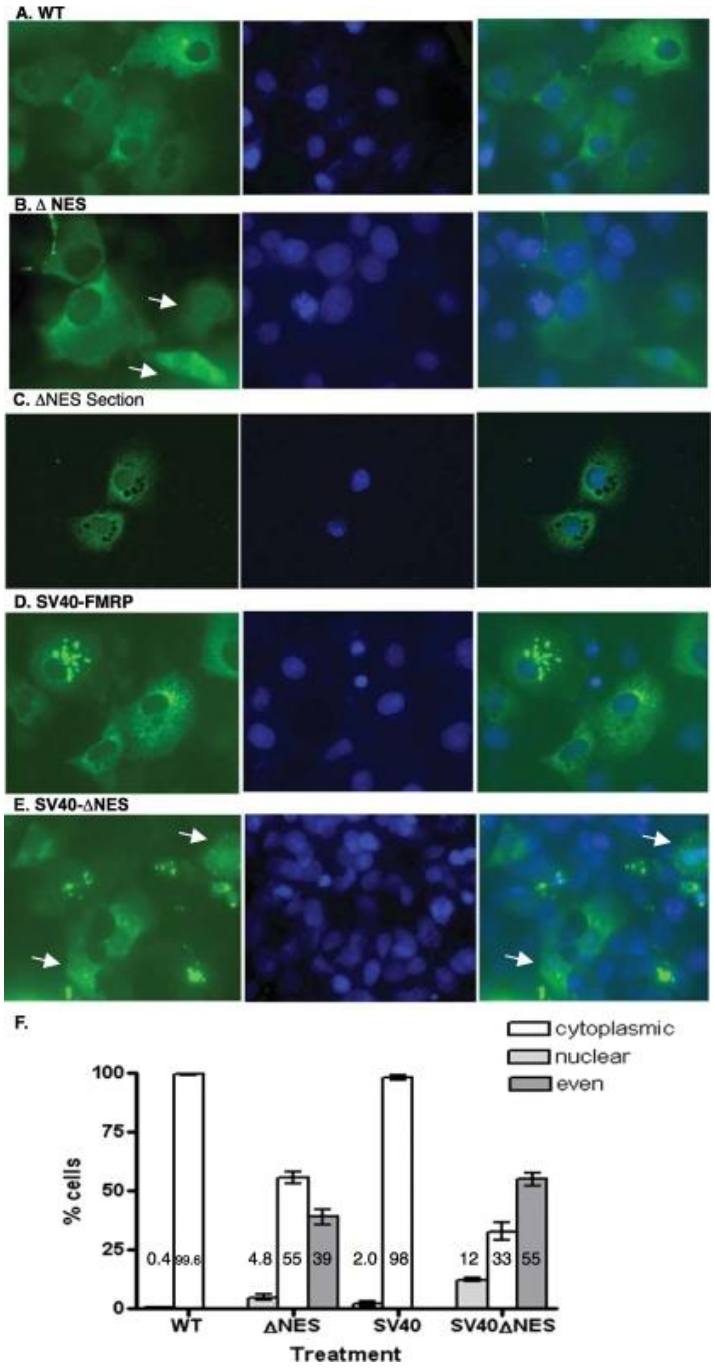

Figure 2.1. FMRP is efficiently exported from the nucleus in the absence of an NES and in the presence of the SV40 NLS. Cos-7 cells were plated and transfected with constructs expressing EGFP-FMRP (WT) (A); EGFP-FMRP with the NES deleted (ΔNES) (B, C); EGFP-SV40-FMRP (SV40-FMRP) (D); and EGFP-SV40-ΔNES (SV40-ΔNES), fixed in DAPI-containing mounting medium and imaged for the expression of EGFP-FMRP (green, left panels) and nuclei (blue DAPI stain, middle panels) and for the merged EGFP and DAPI images (right panels) (E). The arrows in panel B indicate cells expressing ΔNES in the nucleus. Panel C shows

ΔNES-expressing cells examined by optical sectioning as described in Materials and Methods. The arrows in panel E indicate cells expressing comparable amounts of SV40-ΔNES in the nucleus and cytoplasm. (F) Cos-7 cells expressing EGFP-FMRP (WT), ΔNES, SV40-FMRP (SV40), and SV40-ΔNES were scored for the percentage of cells with a nuclear accumulation of FMRP. The results of individual experiments, where over 100 cells were scored each time, were averaged to find the percentage of cells with nuclear accumulation of FMRP for each construct. The WT and SV40 constructs were scored for primarily nuclear FMRP, while ΔNES and EGFP-SV40-ΔNES were scored for cells that demonstrated primarily nuclear, primarily cytoplasmic, or evenly distributed FMRP between the nucleus and cytoplasm (even).

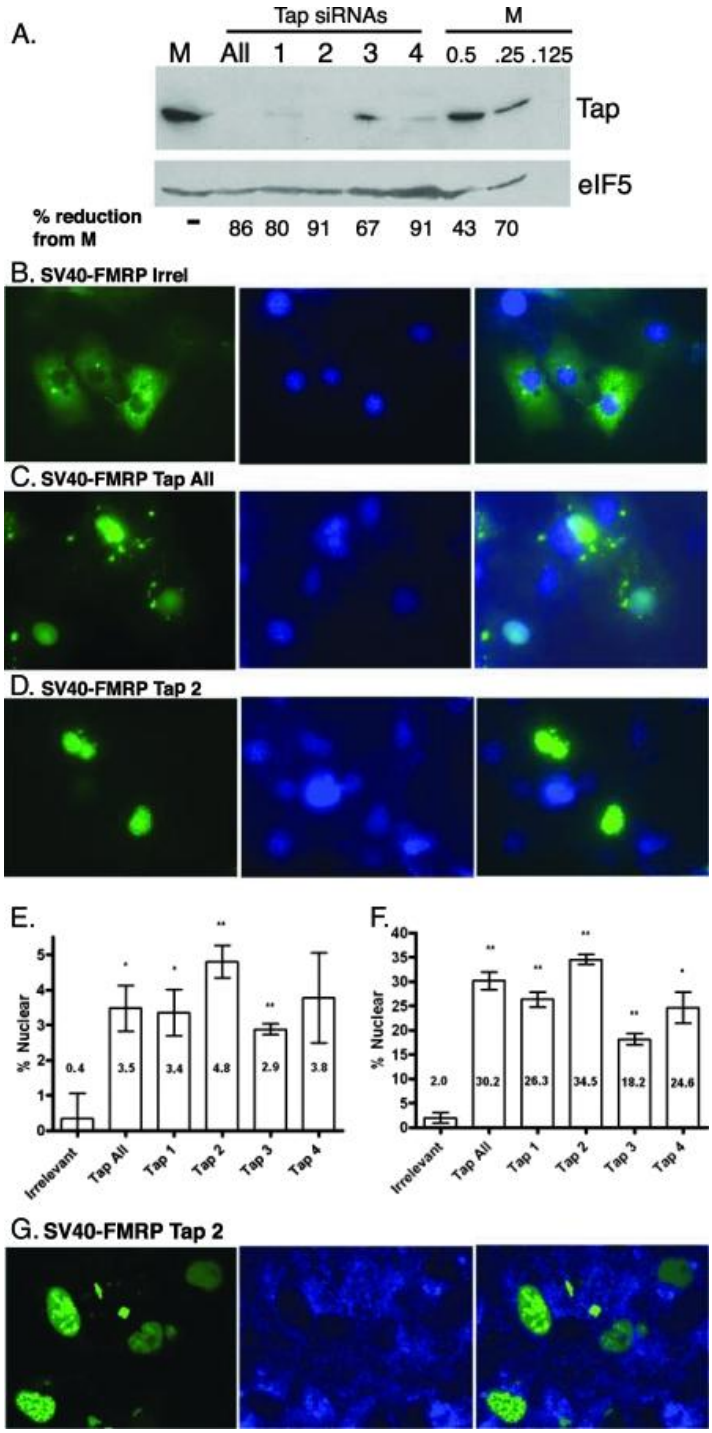

Figure 2.2. The reduction of Tap/NXF1 expression results in the nuclear accumulation of EGFP-FMRP and SV40-FMRP. (A) Cos-7 cells were mock treated with an irrelevant siRNA (M) or treated with a mixture of the four siRNAs against Tap/NXF1 (All) at a final concentration of 100 nM or individually with each of the four Tap/NXF1 siRNAs (1 to 4). Forty-eight hours later, the lysates were prepared and 75 µg of each were resolved on 7.5% SDS-polyacrylamide gel electrophoresis gels. The last three lanes contain dilutions of the mock: 50% (37.5 µg), 25%

(18.8 μg), and 12.5% (9.4 μg). The blot was probed with affinity-purified anti-Tap antisera and reprobed with anti-eIF-5 as a loading control. The amount of Tap per lane was calculated using NIH Image and shown as the percent reduction from the mock. (B to D) Cos-7 cells were transfected with SV40 FMRP and the siRNAs indicated as follows: an irrelevant siRNA (B), a mixture of the four Tap/NXF1 siRNAs (Tap All) (C), and Tap/NXF1-2 siRNA (D). The cells were imaged for the expression of EGFP (green, left panels) and nuclei (blue DAPI stain, middle panels), and the EGFP and DAPI images were merged (right panels). (E, F) Cos-7 cells transfected with either EGFP-FMRP (E) or EGFP-SV40-FMRP (F) and treated with either the irrelevant siRNA, a mixture of the four Tap/NXF1 siRNAs (Tap All), or the individual Tap/NXF1 siRNAs (Tap 1 to 4) for 48 h and scored for the percentage of cells with a primarily nuclear accumulation of FMRP. The percentage of cells expressing FMRP in the nucleus is indicated by each bar. The results were plotted using GraphPad Prism 4. Significance was calculated using a one-tailed Student's t test. A single star indicates a P of <0.05, and two stars indicate a P of <0.01. (G) Cos-7 cells were transfected with SV40 FMRP and the Tap/NXF1-2 siRNA. Twenty-four hours later, the cytoplasmic counterstain CellTrace BODIPY TR methyl ester (Invitrogen) was added, and the cells were live imaged with a confocal microscope at ×63 magnification with oil for EGFP (green, left panels) and cytoplasm stain (blue, middle panels), and the EGFP and BODIPY images were merged (right panels).

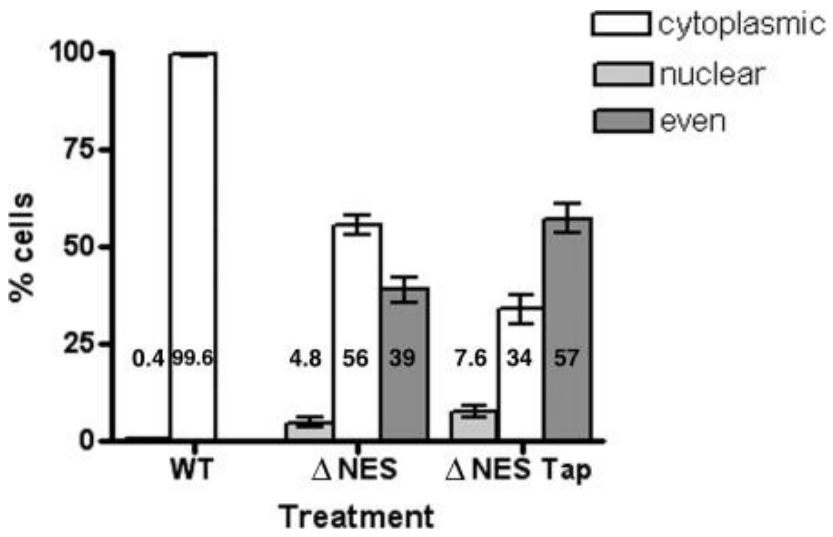

Figure 2.3. The endogenous NLS of FMRP directs a significant amount of EGFP-ΔNES into the nucleus. Cos-7 cells were transfected with either EGFP-FMRP (WT) or ΔNES with irrelevant siRNA (ΔNES) or with Tap/NXF1-2 siRNA (ΔNES Tap). The cells were imaged and scored for nuclear, cytoplasmic, or even distribution between the nucleus and cytoplasm. Five independent experiments were scored and plotted using GraphPad Prism 4.

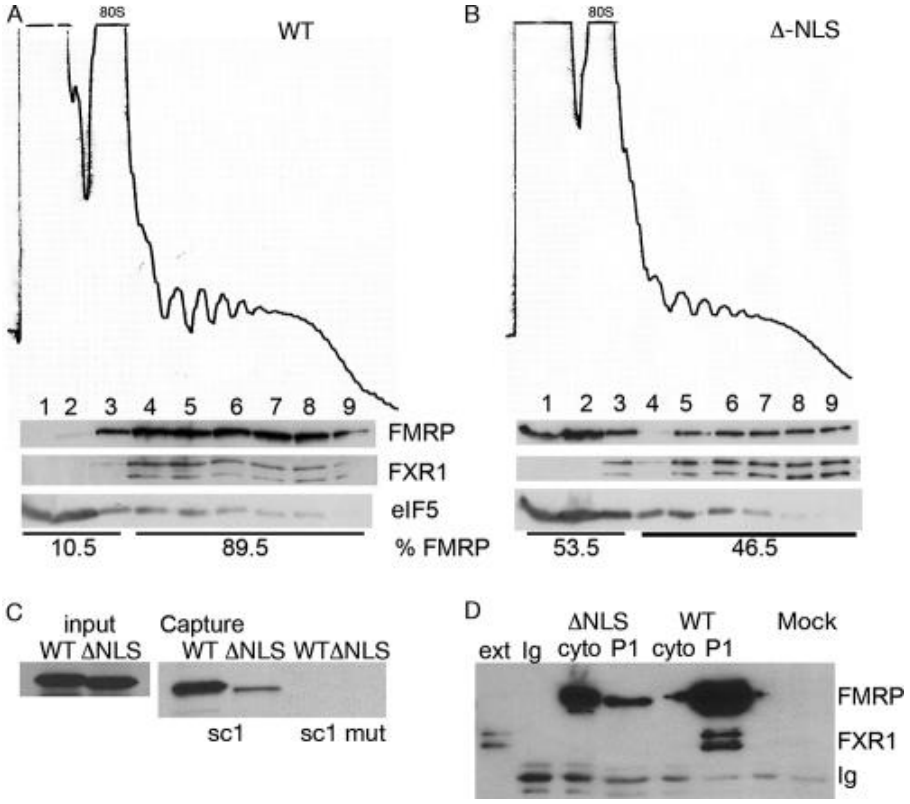

Figure 2.4. Removal of the NLS impairs the function of FMRP. Immortalized Fmr1 knockout fibroblast cells (STEK) (57a) were transfected with EGFP-FMRP (WT) (A) or EGFP-FMRP in which the endogenous NLS has been removed (ΔNLS) (B), treated with cycloheximide, and fractionated on a linear 15 to 45% sucrose gradient. Profiles are shown as the absorbance at 254 nm, and the position of the 80S monosome is indicated at the top of each gradient. Fractions were analyzed on 7.5% gels, transferred to polyvinylidene difluoride and probed with the anti-FMRP antibody 1a to visualize transgene expression (top row), FXR1 (middle row), or eIF5 (bottom row). The amount of FMRP in each fraction was quantified using NIH Image. Removal of the NLS led to a loss of ~50% of the polyribosome-associated FMRP. (C) EGFP-FMRP or ΔNLS expressed in pSport were transcribed and translated in vitro and used in a biotinylated RNA capture assay (75). sc1 is an RNA encoding a G quartet, and the sc1 mutant (sc1 mut) is an RNA encoding a G quartet mutant unable to bind the RGG box of FMRP (18). (D) STEK cells transfected with either EGFP-FMRP (WT) or ΔNLS transgenes were fractionated into either a postnuclear supernatant (cyto) or pelleted again (P1). FMRP was immunoprecipitated from each fraction and blotted for FXR1 or FMRP as indicated on the right. STEK extract was loaded as a control (ext), and the immunoprecipitating immunoglobulin chains (Ig) are indicated.

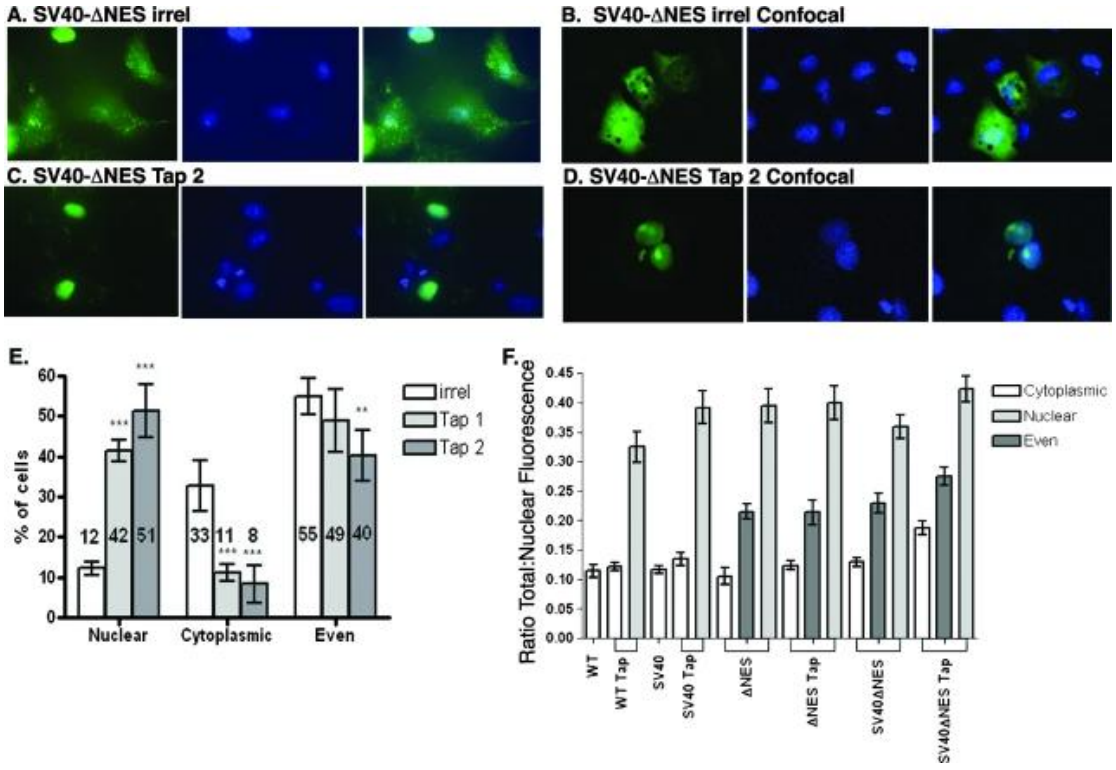

Figure 2.5. Tap/NXF1 knockdown increases the nuclear accumulation of SV40-ΔNES. (A to D) Cos-7 cells were plated and transfected with SV40-ΔNES and the siRNAs indicated and imaged for the expression of EGFP-SV40-ΔNES (green, left panels) and nuclei (blue DAPI stain, middle panels); the EGFP and DAPI images were merged (right panels) by inverted fluorescence microscopy (A, C) and by confocal microscopy (B, D). (E) Three independent experiments were scored for cells that expressed transgene primarily in the nucleus (nuclear), primarily in the cytoplasm (cytoplasmic), or evenly distributed between the nucleus and cytoplasm (even) after treatment with an irrelevant siRNA (irrel) or Tap 1 or 2 siRNA. The average percentage of cells is given at the bottom of the bar. The results were plotted using GraphPad Prism 4. Significance was calculated using a one-tailed Student's t test. A single star indicates a P of <0.05, two stars indicate a P of <0.01, and three stars indicate a P of <0.005. (F) Consistency of cell scoring was evaluated by calculating the ratio of total nuclear fluorescence to total cellular fluorescence and performing a one-way analysis of variance using an α value of 0.05. Cells scored as cytoplasmic had an average nuclear fluorescence of 12.93% ± 2.12%, while cells scored as even had an average nuclear fluorescence of 23.37% ± 4.57% and nuclear cells had average nuclear fluorescence of 38.29% ± 3.65%. All P values were less than 0.05, and many were less than 0.001, with the exception of the SV40-ΔNES cells treated with Tap/NXF1.

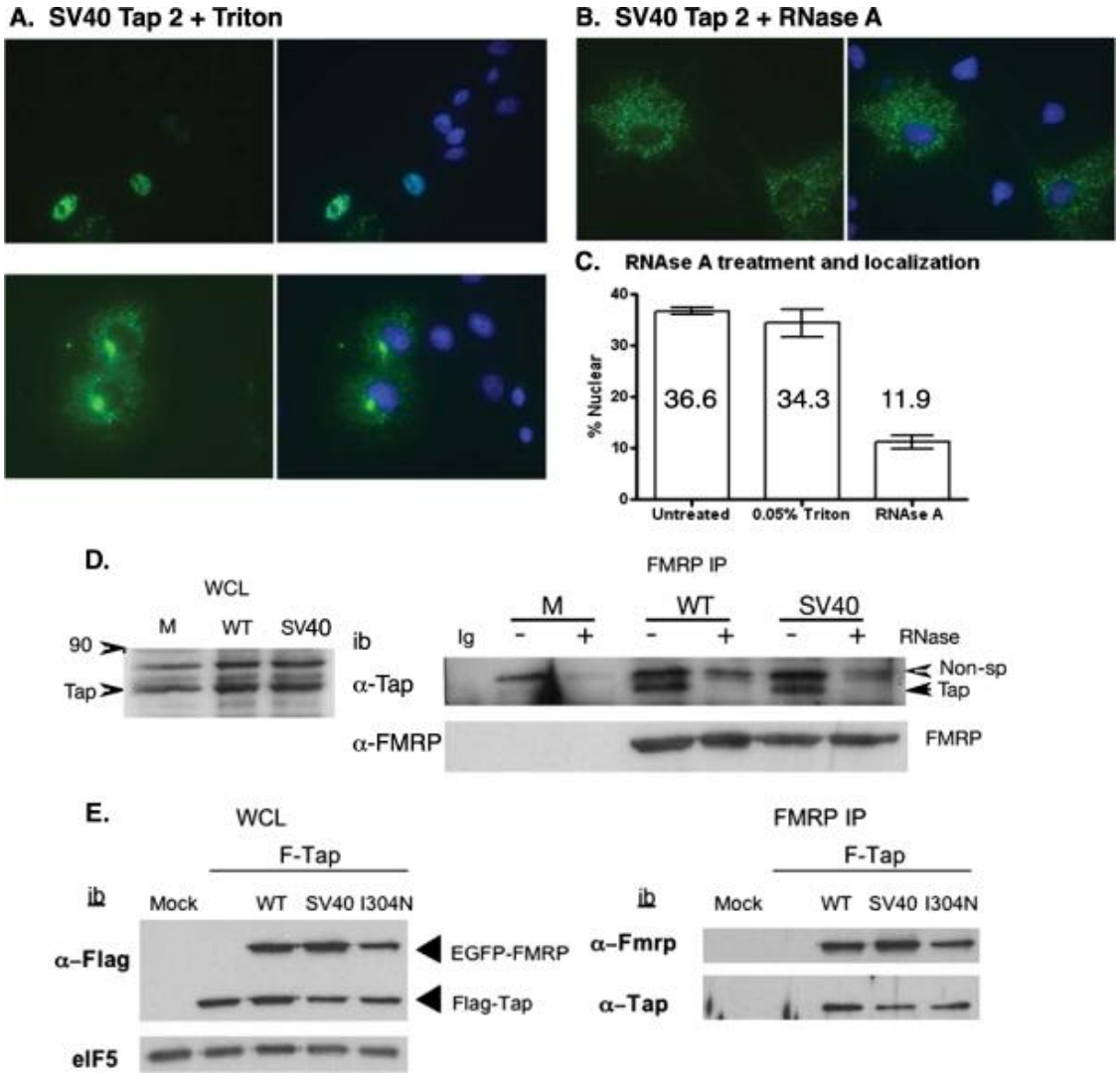

Figure 2.6. The retention of EGFP-FMRP in the nucleus in the absence of Tap/NXF1 is RNA dependent. Cos-7 cells were plated and transfected with SV40-FMRP and Tap/NXF1-2 siRNA, permeabilized with 0.05% Triton (A) (top, cells expressing SV40-FMRP in the nucleus; bottom, cells expressing SV40-FMRP in the cytoplasm), and treated with RNase (B). (C) The percentage of cells expressing FMRP in the nucleus is indicated by each bar. The results were plotted using GraphPad Prism 4. (D) Cos-7 cells were either untransfected (M) or transfected with EGFP-FMRP (WT) or SV40-FMRP (SV40) (WCL, whole cell lysate [50 μg/lane]), immunoprecipitated (IP) with the anti-FMRP antibody 7G1-1, washed with buffer containing RNase (+) or not (−) and immunoblotted for endogenous Tap/NXF1 (Tap) coimmunoprecipitation and FMRP transgene (bottom). Non-sp, reactivity to an irrelevant protein; Ig, immunoprecipitating antibody alone; ib, immunoblot. (E) Cos-7 cells were either mock transfected (M) or transfected with Flag-Tap/NXF1 (F-Tap) alone or with Flag-Tap/NXF1 and one of the following constructs: FMRP (WT), SV40-FMRP (SV40), or I304N. Cells were treated with 0.5% formaldehyde and sonicated as described in Materials and Methods. Left panel, 35 μg of the lysates were loaded, resolved, and probed for transfection efficiency with the anti-Flag antibody (M2; Sigma) to visualize EGFP-FMRP expression (these constructs contain the Flag

epitope) and Flag-Tap/NXF1; the eIF5 immunoblot (ib) shows equal loading. Right panel, immunoprecipitation with the anti-murine FMRP antibody 7G1-1. Immunoprecipitated FMRP was visualized using the anti-FMRP antibody K1, and Flag-Tap coimmunoprecipitation was visualized by a rabbit anti-Tap antibody.

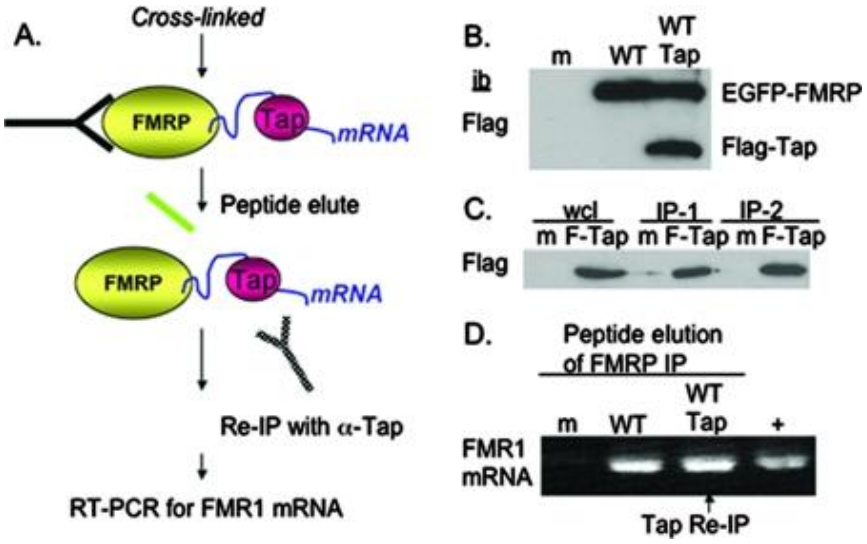

Figure 2.7. Tap/NXF1 associates with FMRP in a complex with FMR1 mRNA. (A) Schematic showing the reimmunoprecipitation experiment. Transfected cells were treated with formaldehyde (cross-linked) and then immunoprecipitated with the anti-FMRP antibody 7G1-1. Immunoprecipitated complexes were eluted with the 7G1-1 peptide and reimmunoprecipitated (Re-IP) with an anti-Tap antibody. RNA was extracted and analyzed from the complex. (B) Cos-7 cells were mock-transfected (m) or transfected with EGFP-FMRP (WT) or EGFP-FMRP and Flag-Tap (WT Tap) and immunoblotted (ib) with an anti-Flag antibody (Flag). (C) The anti-Tap/NXF1 antibodies immunoprecipitate with ~15% efficiency. Cos-7 cells were mock transfected (m) or transfected with Flag-Tap (F-Tap); 50 μg was loaded per lane (wcl, whole cell lysate). Two different anti-Tap/NXF1 antibodies (IP-1 and IP-2) were used to immunoprecipitate extracts from mock or Flag-Tap-expressing cells. (D) FMRP immunoprecipitations (IP) from mock-treated Cos-7 cells (m), EGFP-FMRP-expressing Cos-7 cells (WT), or EGFP-FMRP- and Flag-Tap/NXF1-expressing Cos-7 cells (WT Tap) were peptide eluted. RNA was extracted from mock and WT peptide elutions. The peptide elution from WT Tap was reimmunoprecipitated with the anti-Tap/NXF1 antibody from which the RNA was extracted. First-strand synthesis was performed, followed by PCR for FMR1 mRNA. +, RT-PCR from Cos-7 cell total RNA.

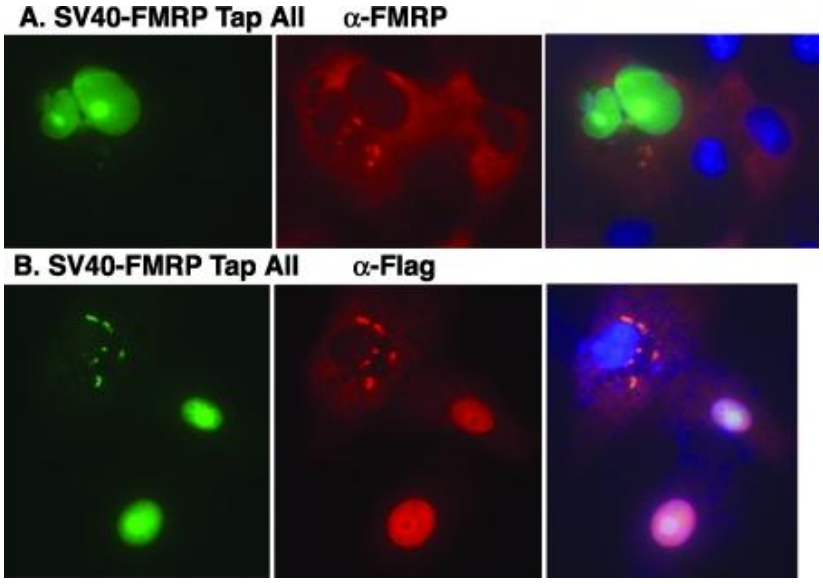

Figure 2.8. Nuclear EGFP-SV40-Flag-FMRP is not recognized by the anti-FMRP antibody 1a. Cos-7 cells were transfected with SV40-FMRP and Tap siRNAs (Tap All), fixed, and permeabilized as described previously (57). The cells were stained with either the anti-FMRP antibody 1a (22) (A) or the anti-Flag antibody (M2) (B). Nuclear EGFP SV40-FMRP was observed using the green channel (left images) and by Flag staining (middle image in panel B); however, it was not detected by antibody 1a (middle image in panel A). Right images show merged DAPI staining with EGFP and anti-mouse rhodamine (red).

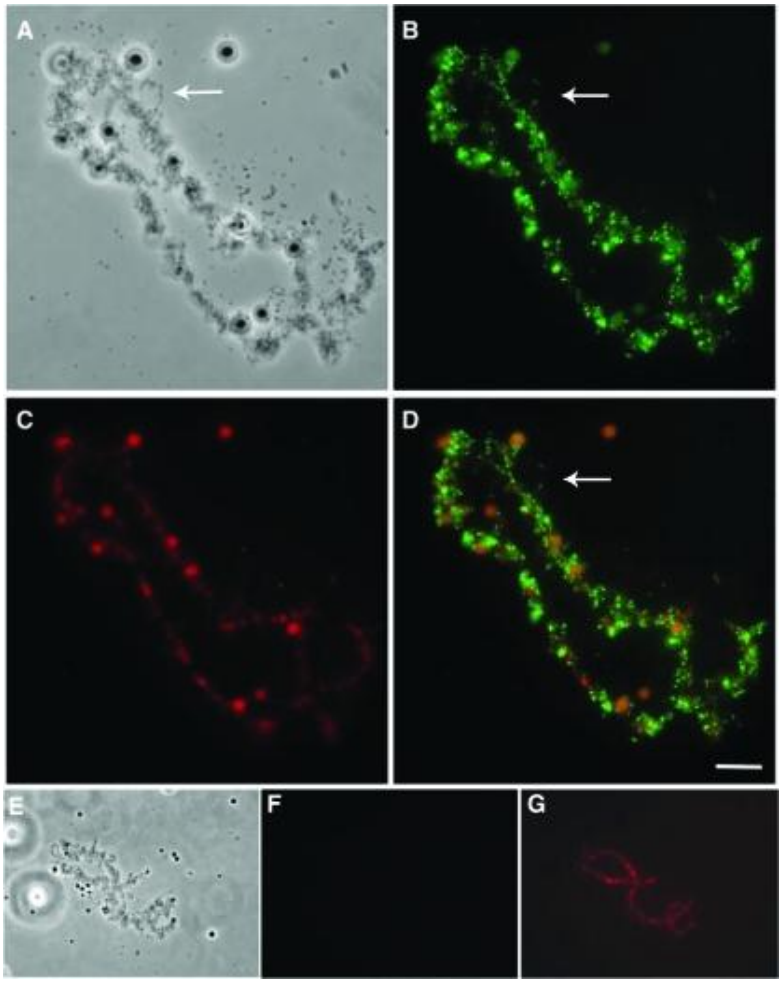

Figure 2.9. FMRP associates with LBCs in the nucleus. Stage V Xenopus laevis oocytes were injected with HA-SV40-WT FMRP cRNA. Nuclear spreads were prepared 24 to 48 h after injection, and the localization of FMRP was visualized using fluorescence microscopy. (A) The phase contrast image shows an LBC and associated proteins. (B) Chromosomal spreads were incubated with anti-HA antibody and visualized by fluorescence microscopy. FMRP is localized along the DNA axis and is also seen along chromosomal loops (arrows) in green. (C) Chromosomes were counterstained using DAPI and false colored in red. (D) Merged images of chromosomes and FMRP localization demonstrate that FMRP is associated with the LBCs and along a subset of chromosomal loops. The scale bar represents 5 mm. (E) Uninjected control oocytes were prepared in parallel to injected oocytes. The phase contrast image shows a single chromosome. (F) Anti-HA antibody staining. (G) Counterstaining using DAPI and false coloring in red.

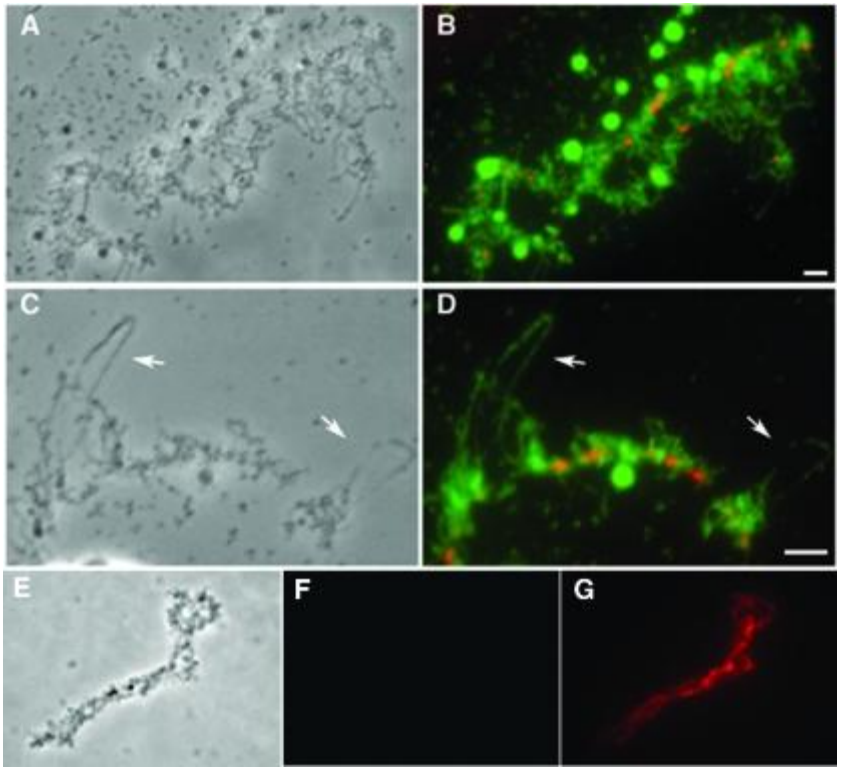

Figure 2.10. Endogenous FMRP associates with nascent transcripts in the nucleus. Xenopus oocytes were stained with the anti-Xenopus FMRP antibody K1. (A) A ×40 magnification of a single chromosome visualized in phase contrast. (B) FMRP (green) is localized with the LBCs. The DNA axis is shown in red. (C) A ×100 magnification shows single-stranded loops (indicated by arrows) of DNA extending off the axis in phase contrast. Scale bar represents 2 mm. (D) FMRP (green) is localized with the LBCs. The DNA axis is shown in red. Phase contrast of an LBC (E), stained with rabbit preimmune antisera (F), and counterstained using DAPI and false colored in red (G).

2.6 Experimental Procedures

Cell lines, transfections, and DNA constructs.

Cells were grown at 37°C in 5% CO2 in Dulbecco's minimal essential medium containing 10% fetal calf serum supplemented with 10 mM HEPES, 1× nonessential amino acids (Biowhittaker, Walkersville, MD) (complete medium). Cotransfections of small interfering RNAs (siRNAs) and plasmids were performed as described previously (27). Briefly, 5 × 104 Cos-7 cells were plated in 1 ml per chamber of a four-chamber culture slide (BD Falconwell) or in 1 well of a 24-well dish. The next day, siRNAs were resuspended in 1× Dharmacon RNA buffer at 0.2 to 0.28 μg/ml (20 μM): 1 μl of siRNA was mixed with 0.8 μg of sterile transgene in 50 μl of Optimem (Gibco). At the same time, 2 μl of Lipofectamine 2000 were added to 50 μl of Optimem and allowed to sit for 5 min. The Lipofectamine dilution was then mixed with siRNA/transgene and incubated for 20 min at room temperature. The complete medium was removed and replaced with 0.5 ml of Optimem, and the mixture of siRNA/transgene and Lipofectamine was added for 4 h, after which time it was removed and replaced with complete medium until the slides were analyzed.

The simian virus 40 (SV40) NLS was introduced into the enhanced green fluorescent protein (EGFP)-Flag-FMRP construct (75) N terminal to Flag (hereafter referred to as SV40-FMRP) (24) using the QuikChange XL site-directed mutagenesis kit (Stratagene) and the following primers from Invitrogen that were polyacrylamide gel electrophoresis purified: SV40-F, GACGACGATGACAAGCCAAAAAAGAAGAGAAAGGTAGAGCTGGTGGTGGAAG, and SV40-R, CTTCCACCACCAGCTCTACCTTTCTCTTCTTTTTTGGCTTGTCATCGTCGTC. The primers for the removal of the nuclear export sequence (NES), as defined in references 24 and 31, containing amino acids 428 to 437 (QLRLERLQID) were as follows: F-CTATTTAAAGGAAGTAGACGAGCAGTTGCGAC and R-GTCGCAACTGCTCGTCTACTTCCTTTAAATAG. The primers for the removal of the NLS as defined in reference 24 containing amino acids 111 to 152 were as follows: F-CCGAATTCGTGAGGATGATAAAGGGTGAG and R-CCGGATCCGGTGACTTCATTGATGGA.

An N-terminal hemagglutinin (HA) tag was introduced into the SV40-FMRP construct behind a T3 promoter by a two-step PCR. The constructs were cloned using the Invitrogen TA cloning kit. The forward primers for the addition of the HA tag followed by the addition of the T3 promoter

were as follows: HA, GCCGCCACCATGGGGTACCCATACGACGTGCCAGACTACGCTCCAAAAAAGAAGAG AAAGGTAGAG, and T3, GCAATTAACCCTCACTAAAGGGAACAAAAGGCCGCCACCATGGGGTACCCATACGA CGTGCCAGAC. The SV40-FMRP reverse primer was TTAGGGTACTCCATTCACCAGCGGTTCCAGCCCATCTACGCTGTC.

siRNAs.

The following siRNAs were obtained from Dharmacon (only the sense sequence will be given although the siRNAs were administered as a duplex): Tap/NXF1-1, CGAGAUCGCAUUCAUGUUAUU; Tap/NXF1-2, GCACACGCGUCUCAACGUUUU; Tap/NXF1-3, GGCUAUGUAUUGUAAAUGAUU; and Tap/NXF1-4, GCGAACGAUUUCCCAAGUUUU. The irrelevant siRNAs were derived from human FBX011, a putative protein arginine methyltransferase (16) that has no effect on the methylation status of FMRP (data not shown).

Fluorescence microscopy and imaging.

The cells were fixed with 4% (wt/vol) formaldehyde in phosphate-buffered saline (PBS; 137 mM NaCl, 2.7 mM KCl, 10 mM Na2HPO4, 1.76 mM KH2PO4 [pH 7.4]) containing 4% (wt/vol) sucrose for 10 min at room temperature, as described previously (54). The cells were mounted in DAPI (4′,6-diamidino-2-phenylidole)-containing mounting medium (1× PBS [pH 9], 15% polyvinyl alcohol, 23% glycerol, 2% 1,4-Diaza-bicyclo[2.2.2]octane, and 1 μg/ml DAPI), coverslipped, and examined by fluorescence microscopy using a Zeiss Axiovert 200 M inverted microscope at either ×40 or ×60 magnification using oil. For immunostaining, after the fixation procedure described above, the cells were stained with either anti-Flag (1/1,000) (Sigma, St.Louis, MO) or the anti-FMRP antibody (1a) (undiluted hybridoma supernatant) for 2 to 4 h, washed, and then incubated with 1/800 of cy3-coupled anti-mouse antibody (Jackson ImmunoResearch Laboratories, West Grove, PA), mounted, and visualized as described above.

Confocal microscopy and optical sectioning.

For live imaging by confocal microscopy, the cells were plated at 2.5 × 105 cells/ml on 35-mm glass-bottom microwell dishes that were poly-d-lysine-coated (MatTek Cultureware, Ashland, MA). The next day, they were transfected as described above. Twenty-four hours later, the cells were counterstained by the addition of CellTrace BODIPY TR methyl ester (Invitrogen) at a 1/5,000 dilution and cultured for 15 min in 5% CO2 at 37°C, and the medium was replaced with fresh complete medium. The cells were imaged at ×63 magnification with a Zeiss LSM510 confocal microscope using the fluorescein isothiocyanate and Cy5 settings.

The cells prepared for fluorescence microscopy were examined by confocal microscopy using the Leica SP2 laser-scanning confocal with the Argon (Ar+) laser line at 488 nm for GFP and the 785-nm line from an fs pulse Ti-sapphire laser (two-photon microscopy) for DAPI imaging. The cells were prepared for fluorescence microscopy and fixed in DAPI containing mounting medium. Optical sections of cells expressing FMRP constructs were taken using the Zeiss Axiovert 200 M inverted microscope with the Zeiss Apotome structured illumination system to increase the wide-field fluorescence contrast and for optical sectioning.

RNase A treatment.

Cos-7 cells transfected with SV40-FMRP and Tap 2 siRNA were treated with RNase A as described previously (67). Briefly, 36 h after transfection, the cells were preextracted in CSK buffer (10 mM PIPES [pH 6.8], 100 mM NaCl, 300 mM sucrose, 3 mM MgCl2) and incubated on ice with CSK containing 0.05% Triton X-100 for 2 to 3 min. The cells were washed twice with CSK buffer before being treated with RNase A (1 mg/ml; Sigma) for 5 to 10 min and then washed once in CSK, fixed in 4% paraformaldehyde for 15 min, and mounted as described with DAPI-containing mounting medium.

The cellular distribution of FMRP was scored for cytoplasmic or nuclear distribution by viewing multiple fields at ×20 magnification and counting between 100 and 200 cells with visible nuclei verified by the DAPI stain. The percentage of cells that expressed the EGFP-tagged FMRP construct (EGFP-FMRP) primarily in the nucleus was averaged from the results of three or four independent experiments, and the standard deviation was calculated. The numbers were analyzed and plotted in GraphPad Prism 4. The significance was calculated using Student's one-tailed t test.

Calculation of the ratios of total nuclear fluorescence to total cellular fluorescence.

The consistency of scoring was evaluated by determining the ratio of total nuclear fluorescence to total cellular fluorescence. Using images captured at ×20 magnification, 20 representative cells of the three categories of cellular distribution were selected from each treatment category. Nuclei were demarcated by DAPI nuclear staining, and the quantification of the fluorescence intensity in the compartments of each cell was determined using Axiovision software. Total fluorescence was determined by obtaining the average fluorescence of the selection multiplied by the area of the selection. This value was obtained for both nuclear and whole-cell measurements. Total nuclear fluorescence was then divided by total cellular fluorescence to obtain the ratio of nuclear to total cellular fluorescence in each scoring category. A one-way analysis of variance was performed on each treatment group to determine whether fluorescence was significantly different between the analyzed cells scored as cytoplasmic, nuclear, or evenly distributed. Each category of cellular localization was significantly different from the other. The cells scored as cytoplasmic were compared to wild-type (WT) EGFP-FMRP treated with TAP-irrelevant peptide and were not significantly different across treatments.

Antibodies and Western blotting.

The anti-FMRP antibody 1a obtained from Jean-Louis Mandel at the Institute of Genetics in Illkirch, France, was used as a hybridoma supernatant for immunoblotting at a 1/10 dilution. Antibody reactivity was visualized using an anti-mouse horseradish-peroxidase conjugate (Jackson Laboratories). The rabbit anti-Tap/NXF1 antibodies (mixed 1/800 each) used for the experiment for which the results are depicted in Fig. Fig.22 were obtained from Genway (San Diego, CA) and Protein Tech Group (Chicago, IL). These antibodies were also used in Fig. Fig.77 for immunoprecipitation. The rabbit anti-Tap/NXF1 used for the experiment for which the results are depicted in Fig. Fig.6D6D was provided by Marie Louise Hammarskjold and used at 1/1,000. The rabbit anti-Tap/NXF1 used for the experiment for which the results are depicted in Fig. Fig.6E6E was provided by Lyne Levesque and used at 1/1,000. The rabbit anti-FMRP K1 antibody was provided by Andre Hoogeveen and used at a 1/2,000 dilution. The antibody against eIF-5 was obtained from Santa Cruz and used at a concentration of 1/10,000. Reactivity was visualized using an anti-rabbit horseradish-peroxidase conjugate (Amersham) and developed with ECL (Amersham). Quantification was performed using NIH Image.

Coimmunoprecipitation.

A total of 107 Cos-7 cells/condition were plated in 150-mm dishes and transfected the following day with 25 μg of the indicated plasmid using Lipofectamine 2000 as per the manufacturer's instructions. Twenty-four hours later, the cells were harvested with trypsin and washed twice in PBS. The postnuclear supernatants were immunoprecipitated with the 7G1-1 antibody (12) and washed twice with lysis buffer and then once for 10 min with buffer containing 0.3 M NaCl-50 mM Tris-0.5% Triton X-100 and 30 mM EDTA. The samples were split and treated with RNase A (60 μg Sigma) for 20 min in lysis buffer at 4°C. For the reimmunoprecipitation experiment and other cross-linking experiments, the transfected cells were harvested with trypsin, washed twice in PBS, and then treated for 10 min with 0.5% formaldehyde (Sigma) at 37°C. The cross-linking reaction was quenched by the addition of glycine to 200 mM for 5 min at room temperature. The cells were washed twice in ice-cold PBS, lysed, and sonicated as described previously (63, 83). The postnuclear supernatants were immunoprecipitated with the 7G1-1 antibody (12) and washed twice with lysis buffer and then once for 10 min with buffer containing 0.3 M NaCl/50 mM Tris/0.5% Triton X-100 and 30 mM EDTA. For the reimmunoprecipitation experiment, the 7G1-1 immunoprecipitations were eluted with 75 μl of 10 mg/ml peptide—the sequence of which is described in reference 12—for 2 h at 4°C and then at 37°C for 10 min. The peptide elutions from the mock transfection and EGFP-FMRP transfections were saved and harvested for RNA as described below. The peptide elution from the EGFP-FMRP-Flag-Tap cotransfection was increased in volume to 0.5 ml with lysis buffer and reimmunoprecipitated overnight with 1 μg of anti-Tap/NXF1 antibody (Proteintech Group, Inc., Chicago, IL). After two washes, the cross-linking was reversed by adding sample buffer, incubating at 65°C for 40 min, and boiling for 5 min. All three peptide elutions were phenol-chloroform extracted and ethanol precipitated. Isolated RNA was reverse transcribed with oligodeoxyribosylthymine (Invitrogen) and Superscript III (Invitrogen) following the manufacturer's instructions. Half of the reverse transcription reaction was amplified for the FMR1 mRNA, and then 1/10 of that reaction was amplified again for FMR1 mRNA. The forward primer for the FMR1 amplification (exons 5 to 7) was F-CACCTCAAAGCGAGCACATA, and the reverse primer was R-CAATAGCAGTGACCCCAGGT.

Oocytes, microinjection, and nuclear spreads.

Fragments of Xenopus laevis ovary were surgically removed from adult female frogs anesthetized with 0.15% tricaine methanesulfonate (MS222; Sigma Chemical, St. Louis, MO). Stage IV to VI oocytes were manually separated using fine tweezers and maintained in saline buffer OR2 (82.5 mM NaCl, 2.5 mM KCl, 1 mM CaCl2, 1 mM MgCl2, 1 mM Na2PO4, 5 mM HEPES). Glass needles were prepared using a horizontal pipette puller (P-97; Sutter Instrument Co.). Capped cRNA was transcribed in vitro from SpeI-linearized HA-SV40-FMRP cDNA using the Stratagene T3 in vitro transcription kit. RNA was isolated by phenol-chloroform extraction followed by ethanol precipitation. All injections were performed under a dissecting microscope (S; Leica) using an injector (Nanojet II; Drummond). Oocytes were injected with 20 to 30 ng of HA-SV40-FMRP cRNA and maintained at 18°C in OR2 solution supplemented with 100 μg/ml streptomycin.

Chromosomal spreads.

Nuclear spreads were prepared as described in reference 66. The samples were fixed with 2% paraformaldehyde in PBS plus 1 mM MgCl2 for 1 h at room temperature. After fixation, the nuclear spreads were rinsed in PBS and blocked with 0.5% bovine serum albumin (Sigma-Aldrich) plus 0.5% gelatin (from cold-water fish) in PBS (blocking buffer) for 10 min. The immunodetection of newly made HA-tagged proteins was done using the anti-HA antibody mAb3F10 (Roche, Mannheim, Germany) as indicated in reference 66.

Images were captured on an upright LeicaDMR (Heidelberg, Germany), using a PL Fluotar 40× oil objective (numerical aperture, 1.0), a HCL FL Fluotar 100 oil objective (numerical aperture, 1.30), and a monochrome Retiga EXI charge-coupled device camera (Qimaging, Surrey, BC, Canada) driven by Invivo software (version 3.2.0; Media Cybernetics, Bethesda, MD). All images were captured at room temperature.

2.7 References

1. Adinolfi, S., C. Bagni, G. Musco, T. Gibson, L. Mazzarella, and A. Pastore. 1999. Dissecting FMR1, the protein responsible for fragile X syndrome, in its structural and functional domains. RNA 5:1248-1258.
2. Adinolfi, S., A. Ramos, S. R. Martin, F. Dal Piaz, P. Pucci, B. Bardoni, J. L. Mandel, and A. Pastore. 2003. The N-terminus of the fragile X mental retardation protein contains a novel domain involved in dimerization and RNA binding. Biochemistry 42:10437-10444.
3. Antar, L. N., R. Afroz, J. B. Dictenberg, R. C. Carroll, and G. J. Bassell. 2004. Metabotropic glutamate receptor activation regulates fragile X mental retardation protein and Fmr1 mRNA localization differentially in dendrites and at synapses. J. Neurosci. 24:2648-2655.
4. Arttamangkul, S., V. Alvarez-Maubecin, G. Thomas, J. T. Williams, and D. K. Grandy. 2000. Binding and internalization of fluorescent opioid peptide conjugates in living cells. Mol. Pharmacol. 58:1570-1580.
5. Ashley, C. T., J. S. Sutcliffe, C. B. Kunst, H. A. Leiner, E. E. Eichler, D. L. Nelson, and S. T. Warren. 1993. Human and murine FMR-1: alternative splicing and translational initiation downstream of the CGG-repeat. Nat. Genet. 4:244-251.
6. Ashley, C. T., K. D. Wilkinson, D. Reines, and S. T. Warren. 1993. FMR1 protein: conserved RNP family domains and selective RNA binding. Science 262:563-566.
7. Bardoni, B., A. Sittler, Y. Shen, and J. L. Mandel. 1997. Analysis of domains affecting intracellular localization of the FMRP protein. Neurobiol. Dis. 4:329-336.
8. Beenders, B., P. L. Jones, and M. Bellini. 2007. The tripartite motif of nuclear factor 7 is required for its association with transcriptional units. Mol. Cell. Biol. 27:2615-2624.
9. Blonden, L., S. van't Padje, L. A. Severijnen, O. Destree, B. A. Oostra, and R. Willemsen. 2005. Two members of the Fxr gene family, Fmr1 and Fxr1, are differentially expressed in Xenopus tropicalis. Int. J. Dev. Biol. 49:437-441.
10. Bor, Y., J. Swartz, A. Morrison, D. Rekosh, M. Ladomery, and M.-L. Hammarskjold. 2006. The Wilms' tumor 1 (WT1) gene (+KTS isoform) functions with a CTE to enhance translation from an unspliced RNA with a retained intron. Genes Dev. 20:1597-1608.
11. Braun, I. C., E. Rohrbach, C. Schmitt, and E. Izaurralde. 1999. TAP binds to the constitutive transport element (CTE) through a novel RNA-binding motif that is sufficient to promote CTE-dependent RNA export from the nucleus. EMBO J. 18:1953-1965.
12. Brown, V., P. Jin, S. Ceman, J. C. Darnell, W. T. O'Donnell, S. A. Tenenbaum, X. Jin, Y. Feng, K. D. Wilkinson, J. D. Keene, R. B. Darnell, and S. T. Warren. 2001. Microarray identification of FMRP-associated brain mRNAs and altered mRNA translational profiles in fragile X syndrome. Cell 107:477-487.
13. Ceman, S., V. Brown, and S. T. Warren. 1999. Isolation of an FMRP-associated messenger ribonucleoprotein particle and identification of nucleolin and the fragile X-related proteins as components of the complex. Mol. Cell. Biol. 19:7925-7932.
14. Ceman, S., F. Zhang, T. Johnson, and S. T. Warren. 2003. Development and characterization of antibodies that immunoprecipitate the FMR1 protein. Methods Mol. Biol. 217:345-354.
15. Conti, E., and E. Izaurralde. 2001. Nucleocytoplasmic transport enters the atomic age. Curr. Opin. Cell Biol. 13:310-319.
16. Cook, J. R., J.-H. Lee, Z.-H. Yang, C. D. Krause, N. Herth, R. Hoffmann, and S. Pestka. 2006. FBXO11/PRMT9, a new protein arginine methyltransferase, symmetrically dimethylates arginine residues. Biochem. Biophys. Res. Commun. 342:472-481.

17. Darnell, J. C., C. E. Fraser, O. Mostovetsky, G. Stefani, T. A. Jones, S. R. Eddy, and R. B. Darnell. 2005. Kissing complex RNAs mediate interaction between the fragile-X mental retardation protein KH2 domain and brain polyribosomes. Genes Dev. 19:903-918.
18. Darnell, J. C., K. B. Jensen, P. Jin, V. Brown, S. T. Warren, and R. B. Darnell. 2001. Fragile X mental retardation protein targets G quartet mRNAs important for neuronal function. Cell 107:489-499.
19. Davidovic, L., X. H. Jaglin, A.-M. Lepagnol-Bestel, S. Tremblay, M. Simonneau, B. Bardoni, and E. W. Khandjian. 2007. The fragile X mental retardation protein is a molecular adaptor between the neurospecific KIF3C kinesin and dendritic RNA granules. Hum. Mol. Genet. 16:3047-3058.
20. De Boulle, K., A. J. M. H. Verkerk, E. Reyniers, L. Vits, J. Hendrickx, B. Van Roy, F. Van den Bos, E. de Graaff, B. A. Oostra, and P. J. Willems. 1993. A point mutation in the FMR-1 gene associated with fragile X mental retardation. Nat. Genet. 3:31-35.
21. De Diego Otero, Y., L.-A. Severijnen, G. van Cappellen, M. Schrier, B. Oostra, and R. Willemsen. 2002. Transport of fragile X mental retardation protein via granules in neurites of PC12 cells. Mol. Cell. Biol. 22:8332-8341.
22. Devys, D., Y. Lutz, N. Rouyer, J.-P. Bellocq, and J.-L. Mandel. 1993. The FMR-1 protein is cytoplasmic, most abundant in neurons, and appears normal in carriers of the fragile X premutation. Nat. Genet. 4:335-340.
23. Didiot, M.-C., Z. Tian, C. Schaeffer, M. Subramanian, J.-L. Mandel, and H. Moine. 2008. The G-quartet containing FMRP binding site in FMR1 mRNA is a potent exonic splicing enhancer. Nucleic Acids Res. 36:4902-4912.
24. Eberhart, D. E., H. E. Malter, Y. Feng, and S. T. Warren. 1996. The fragile X mental retardation protein is a ribonucleoprotein containing both nuclear localization and nuclear export signals. Hum. Mol. Genet. 5:1083-1091.
25. Eberhart, D. E., and S. T. Warren. 1996. The molecular basis of fragile X syndrome. Cold Spring Harb. Symp. Quant. Biol. 61:679-687.
26. Eichler, E. E., S. Richards, R. A. Gibbs, and D. L. Nelson. 1993. Fine structure of the human FMR1 gene. Hum. Mol. Genet. 2:1147-1153.
27. Elbashir, S. M., J. Harborth, K. Weber, and T. Tuschl. 2002. Analysis of gene function in somatic mammalian cells using small interfering RNAs. Methods 26:199-212.
28. Farina, K. L., and R. H. Singer. 2002. The nuclear connection in RNA transport and localization. Trends Cell Biol. 12:466-472.
29. Feng, Y., D. Absher, D. E. Eberhart, V. Brown, H. Malter, and S. T. Warren. 1997. FMRP associates with polyribosomes as an mRNP, and the I304N mutation of severe fragile X syndrome abolishes this association. Mol. Cell 1:109-118.
30. Feng, Y., C.-A. Gutekunst, D. E. Eberhart, H. Yi, S. T. Warren, and S. M. Hersch. 1997. Fragile X mental retardation protein: nucleocytoplasmic shuttling and association with somatodendritic ribosomes. J. Neurosci. 17:1539-1547.
31. Fridell, R., R. Benson, J. Hua, H. Bogerd, and B. Cullen. 1996. A nuclear role for the fragile X mental retardation protein. EMBO J. 15:5408-5414.
32. Fu, Y.-H., D. P. Kuhl, A. Pizzuti, M. Pieretti, J. S. Sutcliffe, S. Richards, A. J. M. H. Verkerk, J. J. A. Holden, R. G. Fenwick, Jr., S. T. Warren, B. A. Oostra, D. L. Nelson, and C. T. Caskey. 1991. Variation of the CGG repeat at the fragile X site results in genetic instability: resolution of the Sherman paradox. Cell 67:1047-1058.

33. Fukuda, M., S. Asano, T. Nakamura, M. Adachi, M. Yoshida, M. Yanagida, and E. Nishida. 1997. CRM1 is responsible for intracellular transport mediated by the nuclear export signal. Nature 390:308-311.
34. Garber, K., K. T. Smith, D. Reines, and S. T. Warren. 2006. Transcription, translation and fragile X syndrome. Curr. Opin. Genet. Dev. 16:270-275.
35. Gonzalez-Reyes, A., H. Elliott, and D. St Johnston. 1995. Polarization of both major body axes in Drosophila by gurken-torpedo signalling. Nature 375:654-658.
36. Gruter, P., C. Tabernero, C. von Kobbe, C. Schmitt, C. Saavedra, A. Bachi, M. Wilm, B. K. Felber, and E. Izaurralde. 1998. TAP, the human homolog of Mex67p, mediates CTE-dependent RNA export from the nucleus. Mol. Cell 1:649-659.
37. Hachet, O., and A. Ephrussi. 2001. Drosophila Y14 shuttles to the posterior of the oocyte and is required for oskar mRNA transport. Curr. Biol. 11:1666-1674.
38. Hamilton, B. J., R. C. Nichols, H. Tsukamoto, R. J. Boado, W. M. Pardridge, and W. F. C. Rigby. 1999. hnRNP A2 and hnRNP L bind the 3′ UTR of glucose transporter 1 mRNA and exist as a complex in vivo. Biochem. Biophys. Res. Commun. 261:646-651.
39. Hodel, M. R., A. H. Corbett, and A. E. Hodel. 2001. Dissection of a nuclear localization signal. J. Biol. Chem. 276:1317-1325.
40. Hornstra, I. K., D. L. Nelson, S. T. Warren, and T. P. Yang. 1993. High resolution methylation analysis of the FMR1 gene trinucleotide repeat region in fragile X syndrome. Hum. Mol. Genet. 2:1659-1665.
41. Huang, Y., R. Gattoni, J. Stevenin, and J. A. Steitz. 2003. SR splicing factors serve as adapter proteins for TAP-dependent mRNA export. Mol. Cell 11:837-843.
42. Huang, Y., and J. A. Steitz. 2005. SRprises along a messenger's journey. Mol. Cell 17:613-615.
43. Huttelmaier, S., D. Zenklusen, M. Lederer, J. Dictenberg, M. Lorenz, X. Meng, G. J. Bassell, J. Condeelis, and R. H. Singer. 2005. Spatial regulation of β-actin translation by Src-dependent phosphorylation of ZBP1. Nature 438:512-515.
44. Izaurralde, E. 2002. A novel family of nuclear transport receptors mediates the export of messenger RNA to the cytoplasm. Eur. J. Cell Biol. 81:577-584.
45. Jin, L., B. W. Guzik, Y.-C. Bor, D. Rekosh, and M.-L. Hammarskjold. 2003. Tap and NXT promote translation of unspliced mRNA. Genes Dev. 17:3075-3086.
46. Jin, P., R. S. Alisch, and S. T. Warren. 2004. RNA and microRNAs in fragile X mental retardation. Nat. Cell Biol. 6:1048-1053.
47. Kalderon, D., W. D. Richardson, A. F. Markham, and A. E. Smith. 1984. Sequence requirements for nuclear location of simian virus 40 large-T antigen. Nature 311:33-38.
48. Kalderon, D., B. L. Roberts, W. D. Richardson, and A. E. Smith. 1984. A short amino acid sequence able to specify nuclear location. Cell 39:499-509.
49. Kang, Y., and B. R. Cullen. 1999. The human Tap protein is a nuclear mRNA export factor that contains novel RNA-binding and nucleocytoplasmic transport sequences. Genes Dev. 13:1126-1139.
50. Kataoka, N., J. Yong, V. N. Kim, F. Velazquez, R. A. Perkinson, F. Wang, and G. Dreyfuss. 2000. Pre-mRNA splicing imprints mRNA in the nucleus with a novel RNA-binding protein that persists in the cytoplasm. Mol. Cell 6:673-682.
51. Lai, D., D. Sakkas, and Y. Huang. 2006. The fragile X mental retardation protein interacts with a distinct mRNA nuclear export factor NXF2. RNA 12:1446-1449.

52. Le Hir, H., D. Gatfield, E. Izaurralde, and M. J. Moore. 2001. The exon-exon junction complex provides a binding platform for factors involved in mRNA export and nonsense-mediated mRNA decay. EMBO J. 20:4987-4997.
53. Le Hir, H., E. Izaurralde, L. E. Maquat, and M. J. Moore. 2000. The spliceosome deposits multiple proteins 20-24 nucleotides upstream of mRNA exon-exon junctions. EMBO J. 19:6860-6869.
54. Levesque, L., Y.-C. Bor, L. H. Matzat, L. Jin, S. Berberoglu, D. Rekosh, M.-L. Hammarskjold, and B. M. Paschal. 2006. Mutations in Tap uncouple RNA export activity from translocation through the nuclear pore complex. Mol. Biol. Cell 17:931-943.
55. Li, Y., Y.-C. Bor, Y. Misawa, Y. Xue, D. Rekosh, and M.-L. Hammarskjold. 2006. An intron with a constitutive transport element is retained in a Tap messenger RNA. Nature 443:234-237.
56. Mattaj, I. W., and L. Englmeier. 1998. Nucleocytoplasmic transport: the soluble phase. Ann. Rev. Biochem. 67:265-306.
57. Matzat, L. H., S. Berberoglu, and L. Levesque. 2007. Formation of a Tap/NXF1 homotypic complex is mediated through the amino-terminal domain of Tap and enhances interaction with nucleoporins. Mol. Biol. Cell 19:327-338.
57a. Mazroui, R., M. E. Huot, S. Tremblay, C. Filion, Y. Labelle, and E. W. Khandjian. 2002. Trapping of messenger RNA by Fragile X Mental Retardation protein into cytoplasmic granules induces translation repression. Hum. Mol. Genet. 11:3007-3017.
58. Miyashiro, K. Y., A. Beckel-Mitchener, T. K. Purk, K. G. Becker, T. Barret, L. Liu, S. Carbonetto, I. J. Weiler, W. T. Greenough, and J. Eberwine. 2003. RNA cargoes associating with FMRP reveal deficits in cellular functioning in Fmr1 null mice. Neuron 37:417-431.
59. Monzo, K., O. Papoulas, G. T. Cantin, Y. Wang, J. R. Yates, III, and J. C. Sisson. 2006. Fragile X mental retardation protein controls trailer hitch expression and cleavage furrow formation in Drosophila embryos. Proc. Natl. Acad. Sci. USA 103:18160-18165.
60. Morgan, G. T. 2002. Lampbrush chromosomes and associated bodies: new insights into principles of nuclear structure and function. Chromosome Res. 10:177-200.
61. Nakielny, S., and G. Dreyfuss. 1999. Transport of proteins and RNAs in and out of the nucleus. Cell 99:677-690.
62. Newport, J., and M. Kirschner. 1982. A major developmental transition in early Xenopus embryos. I. Characterization and timing of cellular changes at the midblastula stage. Cell 30:675-686.
63. Niranjanakumari, S., E. Lasda, R. Brazas, and M. A. Garcia-Blanco. 2002. Reversible cross-linking combined with immunoprecipitation to study RNA-protein interactions in vivo. Methods 26:182-190.
64. Oberlé, I., F. Rousseau, D. Heitz, C. Kretz, D. Devys, A. Hanauer, J. Boué, M. F. Bertheas, and J. L. Mandel. 1991. Instability of a 550-base pair DNA segment and abnormal methylation in fragile X syndrome. Science 252:1097-1102.
65. Ossareh-Nazari, B., F. Bachelerie, and C. Dargemont. 1997. Evidence for a role of CRM1 in signal-mediated nuclear protein export. Science 278:141-144.
66. Patel, S. B., N. Novikova, and M. Bellini. 2007. Splicing-independent recruitment of spliceosomal small nuclear RNPs to nascent RNA polymerase II transcripts. J. Cell Biol. 178:937-949.

67. Prasanth, K. V., S. G. Prasanth, Z. Xuan, S. Hearn, S. M. Freier, C. F. Bennett, M. Q. Zhang, and D. L. Spector. 2005. Regulating gene expression through RNA nuclear retention. Cell 123:249.
68. Rodrigues, J. P., M. Rode, D. Gatfield, B. J. Blencowe, M. Carmo-Fonseca, and E. Izaurralde. 2001. REF proteins mediate the export of spliced and unspliced mRNAs from the nucleus. Proc. Natl. Acad. Sci. USA 98:1030-1035.
69. Schaeffer, C., B. Bardoni, J. L. Mandel, B. Ehresmann, C. Ehresmann, and H. Moine. 2001. The fragile X mental retardation protein binds specifically to its mRNA via a purine quartet motif. EMBO J. 20:4803-4813.
70. Siomi, H., M. Choi, M. C. Siomi, R. L. Nussbaum, and G. Dreyfuss. 1994. Essential role for KH domains in RNA binding: impaired RNA binding by a mutation in the KH domain of FMR1 that causes fragile X syndrome. Cell 77:33-39.
71. Siomi, H., M. C. Siomi, R. L. Nussbaum, and G. Dreyfuss. 1993. The protein product of the fragile X gene, FMR1, has characteristics of an RNA binding protein. Cell 74:291-298.
72. Siomi, M. C., Y. Zhang, H. Siomi, and G. Dreyfuss. 1996. Specific sequences in the fragile X syndrome protein FMR1 and the FXR proteins mediate their binding to 60S ribosomal subunits and the interactions among them. Mol. Cell. Biol. 16:3825-3832.
73. Sittler, A., D. Devys, C. Weber, and J.-L. Mandel. 1996. Alternative splicing of exon 14 determines nuclear or cytoplasmic localisation of fmr1 protein isoforms. Hum. Mol. Genet. 5:95-102.
74. Stade, K., C. S. Ford, C. Guthrie, and K. Weis. 1997. Exportin 1 (Crm1p) is an essential nuclear export factor. Cell 90:1041-1050.
75. Stetler, A., C. Winograd, J. Sayegh, A. Cheever, E. Patton, X. Zhang, S. Clarke, and S. Ceman. 2006. Identification and characterization of the methyl arginines in the fragile X mental retardation protein Fmrp. Hum Mol. Genet. 15:87-96.
76. Stutz, F., A. Bachi, T. Doerks, I. C. Braun, B. Seraphin, M. Wilm, P. Bork, and E. Izaurralde. 2000. REF, an evolutionary conserved family of hnRNP-like proteins, interacts with TAP/Mex67p and participates in mRNA nuclear export. RNA 6:638-650.
77. Sutcliffe, J. S., D. L. Nelson, F. Zhang, M. Pieretti, C. T. Caskey, D. Saxe, and S. T. Warren. 1992. DNA methylation represses FMR-1 transcription in fragile X syndrome. Hum. Mol. Genet. 1:397-400.
78. Tamanini, F., C. Bontekoe, C. E. Bakker, L. van Unen, B. Anar, R. Willemsen, M. Yoshida, H. Galjaard, B. Oostra, and A. T. Hoogeveen. 1999. Different targets for the fragile X-related proteins revealed by their distinct nuclear localizations. Hum. Mol. Genet. 8:863-869.
79. Tan, W., A. S. Zolotukhin, I. Tretyakova, J. Bear, S. Lindtner, S. V. Smulevitch, and B. K. Felber. 2005. Identification and characterization of the mouse nuclear export factor (Nxf) family members. Nucleic Acids Res. 33:3855-3865.
80. Tran, E. J., and S. R. Wente. 2006. Dynamic nuclear pore complexes: life on the edge. Cell 125:1041-1053.
81. van′t Padje, S., B. Engels, L. Blonden, L. A. Severijnen, F. Verheijen, B. A. Oostra, and R. Willemsen. 2005. Characterisation of Fmrp in zebrafish: evolutionary dynamics of the fmr1 gene. Dev. Genes Evol. 215:198-206.
82. Varadi, A., and G. A. Rutter. 2002. Dynamic imaging of endoplasmic reticulum Ca2+ concentration in insulin-secreting MIN6 cells using recombinant targeted cameleons: roles of sarco(endo)plasmic reticulum Ca2+-ATPase (SERCA)-2 and ryanodine receptors. Diabetes 51:S190-S201.

83. Vasudevan, S., and J. A. Steitz. 2007. AU-rich-element-mediated upregulation of translation by FXR1 and Argonaute 2. Cell 128:1105-1118.
84. Verkerk, A. J. M. H., M. Pieretti, J. S. Sutcliffe, Y.-H. Fu, D. P. A. Kuhl, A. Pizutti, O. Reiner, S. Richards, M. F. Victoria, F. Zhang, B. E. Eussen, G. J. B. van Ommen, L. A. J. Blonden, G. J. Riggins, J. L. Chastain, C. B. Kunst, H. Galjaard, C. T. Caskey, D. L. Nelson, B. A. Oostra, and S. T. Warren. 1991. Identification of a gene (FMR-1) containing a CGG repeat coincident with a breakpoint cluster region exhibiting length variation in fragile X syndrome. Cell 65:905-914.
85. Wilkie, G. S., V. Zimyanin, R. Kirby, C. Korey, H. Francis-Lang, D. Van Vactor, and I. Davis. 2001. Small bristles, the Drosophila ortholog of NXF-1, is essential for mRNA export throughout development. RNA 7:1781-1792.
86. Zalfa, F., S. Adinolfi, I. Napoli, E. Kuhn-Holsken, H. Urlaub, T. Achsel, A. Pastore, and C. Bagni. 2005. Fragile X mental retardation protein (FMRP) binds specifically to the brain cytoplasmic RNAs BC1/BC200 via a novel RNA-binding motif. J. Biol. Chem. 280:33403-33410.
87. Zhang, M., Q. Wang, and Y. Huang. 2007. Fragile X mental retardation protein FMRP and the RNA export factor NXF2 associate with and destabilize Nxf1 mRNA in neuronal cells. Proc. Natl. Acad. Sci. USA 104:10057-10062.

Chapter 3. FMRP-associated MOV10 facilitates and antagonizes microRNA-mediated regulation

---

Miri Kim, Phillip J. Kenny, Radhika S. Khetani, Mary Luz Arcila, Hongjun Zhou, Kenneth S. Kosik, Stephanie Ceman

This work has been submitted and in review with Molecular Cell

3.1 Abstract

The fragile X mental retardation protein FMRP is an RNA binding protein that regulates translation of its bound mRNAs through incompletely defined mechanisms. FMRP has been linked to the microRNA pathway and we show here that it is associated with MOV10, a putative helicase that is also associated with the microRNA pathway. We show that FMRP associates with MOV10 in an RNA-dependent manner and facilitates MOV10-association with RNAs in brain. We identified the RNA sequences recognized by MOV10 using iCLIP and found an increased number of G-quadruplexes in the CLIP sites. We provide evidence that MOV10 facilitates microRNA-mediated translation regulation and also has the novel role of increasing the expression of a subset of RNAs by sterically hindering Argonaute2 association. In summary, we have identified a new mechanism for FMRP-mediated translational regulation through its association with MOV10.

3.2 Introduction

Fragile X syndrome (FXS) is described as a disease of aberrant protein production [1-3]. As a result, FXS patients are cognitively impaired and demonstrate behavioral abnormalities that include autistic-like features [4]. The fragile X mental retardation protein FMRP is absent in FXS, establishing that FMRP is required for normal cognition. FMRP is an RNA binding protein that binds ~4% of brain mRNAs and regulates their expression—either enhancing or suppressing translation—by an unknown mechanism [5]. FMRP is implicated in microRNA (miRNA)-mediated translational suppression [6-10], although the molecular basis for its role in this pathway is unknown.

MOV10 is a putative helicase that was initially identified in a screen of mouse embryos intentionally infected with the Moloney leukemia virus (MOV) [11, 12]. Like FMRP, MOV10 has been implicated in miRNA-mediated translational suppression [13-15]. We show here that a subset of MOV10- and FMRP-associated mRNAs is regulated through the 3'UTR. The 3'UTR is the primary site of miRNA-mediated regulation where Argonaute2 (Ago2) is the key effector of translational suppression [16, 17]. We propose a novel mechanism of translational regulation whereby MOV10 binding to the 3'UTR of Ago2 regulates accessibility for subsequent translational regulation.

3.3 Results

FMRP associates with MOV10

FMRP and MOV10 are both expressed in brain and co-localized to dendritic foci by immunostaining [3, 13, 18]. To demonstrate their physical association biochemically, we prepared an RNA sedimentation gradient on brain and HEK293T cells as described [19]. FMRP and MOV10 were present in fractions 7-15 in brain and 7-25 in HEK293T cells (Fig 1A and 1C). To show that FMRP and MOV10 are in the same complex in brain, we immunoprecipitated FMRP from brain lysate and found it associated with MOV10 (Fig 1B). To demonstrate that FMRP and MOV10 directly associate in fractions from the RNA sediment gradient (versus being present individually in similarly sized populations), we pooled the MOV10- and FMRP-containing fractions, immunoprecipitated FMRP and showed that MOV10 was associated with FMRP (Fig 1D).

FMRP also associates with translating ribosomes (polysomes) [20, 21]. Because we hypothesized that MOV10 interacts with FMRP to regulate translation, we examined its distribution on polysomes. FMRP and MOV10 are in the same fractions as the actively translating polyribosomes (Fig 1E right). Treatment with EDTA disrupts polysomes and removes MOV10 and FMRP from the heavier fractions, as has been described previously for FMRP [20, 21] (Fig 1F).

To characterize further the interaction between MOV10 and FMRP, anti-FLAG immunoprecipitations were performed on murine fibroblast L-M(TK-) cells that stably expressed either the empty FLAG vector (VC) or FLAG-FMRP [22]. MOV10 specifically associated with FMRP and this association was disrupted in 300 mM NaCl and was partially disrupted by

treatment with RNase A (Fig 1G). In the reverse experiment, immunoprecipitation of myc-tagged MOV10 demonstrated that endogenous FMRP co-immunoprecipitated in an RNA-dependent manner (Fig 1H). We conclude that FMRP association with MOV10 is RNA-dependent.

Identification of the cellular RNAs bound by MOV10

Because FMRP and MOV10 associated in an RNA-dependent manner, we next sought to identify the mRNAs associated with MOV10. RNAs associated with FMRP in brain and cell lines have been extensively characterized [5, 23-25]. To identify the RNAs that bound MOV10, we UV-cross-linked HEK293F cells and immunoprecipitated with an irrelevant antibody (ir) followed by a MOV10-specific antibody (MOV10) to isolate associated RNAs after stringent washing. We then prepared a library and a biological replicate for deep sequencing (Fig 2A, right). The top 20 RNAs associated with MOV10 are shown in the table in Figure 2B (the entire list is shown in Table S1). To identify the specific region of the RNA bound by MOV10, we performed individual-nucleotide resolution UV cross-linking and immunoprecipitation (iCLIP) as described [26, 27]. Radiolabeled RNA bound to MOV10 was visualized at ~135 kDa (Fig 2A, left) cut-out, along with a similarly sized region from the irrelevant immunoprecipitation as a control. 1,181 regions were found in both CLIP libraries at least twice: 1036 of these corresponded to regions identified as 3'UTRs, exons, introns and 5'UTRs (Table S2). This stringent number provided the most confidence that the RNAs identified were true MOV10 targets. Importantly, 90% of the annotated MOV10 CLIP targets were identified in the RNA IP (Figure 2A right, Figure 2B and Table S1).

Once the MOV10 CLIP sites were normalized to the length of each gene region, the 3'UTR was determined to be the primary MOV10 binding site (Figure 2C). We were interested in determining whether MOV10 regulated specific molecular functions. Gene Ontology (GO) analysis of the MOV10 CLIP targets showed a clear enrichment ($p \leq 0.05$) for certain categories of molecular function (Figure 2D). The MOV10 3'UTR CLIP RNAs were significantly enriched for nucleotide binding proteins, RNA binding proteins, and transcription factors compared to the MOV10 exon CLIP RNAs, which were enriched for RNAs encoding proteins with a ligase activity.

FMRP recruits MOV10 to target mRNAs in the brain

Because we found MOV10 and FMRP associated in an RNA-dependent manner, we wanted to identify the commonly bound RNAs. Accordingly, we compared previously published FMRP CLIP targets with our MOV10 CLIP sites and found a large number of overlapping mRNAs (Figure 3A). We examined the CLIP lists of FMRP isolated from HEK293 [23] and from brain polyribosomes [24] and found 69.5% overlap between the MOV10 CLIP targets and HEK293 FMRP CLIP targets and 23.6% overlap between the MOV10 CLIP targets and brain FMRP CLIP targets (Figure 3A and Table S3 for a complete list).

Since FMRP and MOV10 bind some of the same mRNAs, we hypothesized that FMRP binds the mRNA first and then recruits MOV10 for subsequent binding and translational regulation. We chose to address this question in brain because both FMRP and MOV10 are expressed in neurons [3, 13, 18]. To test this hypothesis and validate specific mRNAs found by deep sequencing, we selected three mRNA targets (GNB2L1, CALM3, and eEF2) that were identified independently using both strategies shown in Figure 2A. Importantly, CALM3 and eEF2 were also present in the FMRP brain CLIP list while GNB2L1 was not present in the FMRP CLIP list [24]. Thus, CALM3 and eEF2 associate with both FMRP and MOV10 while GNB2L1 only associated with MOV10. To examine whether FMRP facilitated association of MOV10 with RNAs in brain, we immunoprecipitated MOV10 from both WT and FMR1 knockout brains and quantified the associated RNAs. MOV10 association with eEF2 and CALM3 was significantly reduced in the absence of FMRP (Figure 3B) suggesting that FMRP was required for efficient loading of MOV10 onto its mRNAs. As expected, because GNB2L1 does not associate with FMRP, MOV10 bound equally well to GNB2L1 in both the presence and absence of FMRP in brain (Figure 3B). It is important to note that the levels of all three RNAs were the same in brains of both WT and FMR1 knockout (KO) mice (Figure 3C). Thus, FMRP is required for normal association of a subset of RNAs with MOV10, suggesting that FMRP binds a subset of mRNAs and recruits MOV10 to those RNAs.

FMRP and MOV10 recognize GQ structures

We next hypothesized that there were specific motifs or secondary structures in the RNA targets that were recognized by MOV10. The motifs recognized by FMRP have been extensively characterized [5, 23, 28, 29] and include G-quadruplexes (GQs) [30]. GQs are nucleic acid

structures formed by square coplanar arrays of four guanines (G-quartets) that are stabilized by Hoogsteen-type hydrogen bonds [31, 32]. Two or more G-quartets stack to form a GQ [33]. RNA GQs can be substrates for helicases, as is the case for G4R1/RHAU and DHX9—helicases that are primarily nuclear [34, 35].

GQs are found in a large number of RNAs [36, 37]. To examine the MOV10 CLIP sites for putative GQs, we used a GQ prediction program QGRS [37, 38] and found that 27.2% of the MOV10 3'UTR CLIP sites contained predicted GQs--nearly twice that predicted in a large-scale screen of 3'UTRs [36]. Accordingly, QGRS identified several putative GQs or clusters of GQs within or in proximity to the identified MOV10 binding sites in eEF2, CALM3, and GNB2L1 (Figure 3D). To ask directly whether MOV10 bound GQs, we tested its ability to bind the RNA sc1, which is a model GQ that binds FMRP with nanomolar affinity [28]. Like FMRP, MOV10 was able to specifically bind sc1 and was unable to bind the nucleotide-substituted sc1-mutant, in which formation of the GQ is disrupted (Fig 3E). Thus, both FMRP and MOV10 bind GQ structures.

MOV10 regulates mRNA expression through the 3'UTR and modulates Ago2 function.

MOV10 bound most CLIP targets in the 3'UTR (Fig 2C). Previous work demonstrated that MOV10 co-immunoprecipitated with Ago2 and was required for silencing of a reporter RNA [14, 39]. If MOV10 is indeed participating in miRNA-mediated silencing, then some of its target mRNAs should be degraded as a consequence of miRNA-mediated translation suppression [40-42]. Accordingly, knockdown of MOV10 should lead to an increase in expression of those same mRNAs.

To examine the effect of MOV10 on total mRNA levels, we treated HEK293F cells with MOV10 siRNAs for knockdown (KD), irrelevant siRNAs as a control (IR), or we overexpressed a MOV10 transgene (OE) and evaluated mRNA levels under each of these treatment conditions by RNA-Seq (Table S4). We identified 14,679 RNAs in the total RNA pool, and found that 6057 RNA levels changed significantly in the KD while 7593 targets changed in the OE. The changes in RNA levels in both the KD and OE were significant ($p<0.05$) compared to control treatment (Fig 4A). There were 3313 genes that showed significantly changed RNA expression in both treatment conditions. Of the genes in the intersection, 1216 RNAs changed in opposite

directions in the KD or OE of MOV10: more specifically, in the absence of MOV10, 604 RNAs increased while 612 decreased. In the OE, those same RNAs changed in the opposite direction. Many of these significantly changed RNAs are likely downstream of MOV10, rather than being directly bound and regulated by MOV10. In fact, the GO analysis indicated that transcription factors were directly regulated by MOV10 (Figure 2B). Thus, genes that are downstream targets of those transcription factors were likely affected in the KD and OE experiments. To focus on the fate of the RNAs that are directly bound by MOV10--as identified by iCLIP--we compared the fate of the MOV10 CLIP targets to the non-CLIP targets in Figure 4B. As would be expected, direct binding by MOV10 had a significant impact on the levels of mRNAs. The MOV10 CLIP targets were changed significantly in the KD ($p=0.0068$) and the OE ($p=1.833E-26$) experiment (Figure 4B and Table S5). The larger effect observed in the OE experiment likely reflects the fact that the MOV10 transgene was overexpressed (>30-fold [data not shown]). Thus, RNAs that are directly bound by MOV10 are more likely to have significantly altered expression levels in the absence of MOV10 or when MOV10 is overexpressed, than the RNAs that are not CLIP targets.

We next visualized the direction of change of the MOV10 CLIP targets by heat map (Fig 4C). The significantly changed MOV10 CLIP targets in KD, IR, and OE clustered in a very distinct manner, correlating with their treatment (Fig 4C). If MOV10 participates in miRNA-mediated silencing, as has been hypothesized [14, 15], then MOV10 KD would be predicted to lead to increased levels of its CLIP targets (red in Figure 4C) and decreased levels upon MOV10 OE (blue in Figure 4C), which occurred in the RNA cluster indicated by the yellow bar on the left. Importantly, there were also clusters of RNAs that demonstrated the opposite expression pattern: MOV10 KD resulted in decreased expression (blue) and MOV10 OE resulted in increased expression (red). These RNA clusters are indicated by orange and lime green bars in Figure 4C. These two patterns of expression suggest that MOV10 binding to target RNAs had two distinct fates: MOV10 increased the RNA levels of some CLIP targets and decreased the RNA levels of other CLIP targets.

Because of the hypothesized role of MOV10 in the microRNA pathway and the greater efficacy of miRNA silencing response elements in the 3'UTR [17, 43], we were particularly interested in the fate of the mRNAs in which MOV10 bound the 3'UTR. We examined the effect of MOV10 OE on non-CLIP RNAs and found that of the RNAs that were significantly changed,

25.05% decreased in expression and 26.9% increased in expression (Figure 4D left). In contrast, when examining MOV10 OE on RNAs that are 3'UTR CLIP targets, 47.2% were significantly decreased and 15.8% were increased (Figure 4D, center). The larger percentage of downregulated RNAs among the 3'UTR CLIP targets (47.2%) compared to the non-CLIP RNAs (25.05%), is consistent with a role for MOV10 in miRNA-mediated regulation and degradation, where increased levels of MOV10 drove decreases in target RNA levels. Examination of the intronic CLIP targets (presumably bound by MOV10 in the nucleus) revealed a fate more similar to that observed for the non-CLIP RNA (Figure 4D right). Thus, MOV10 OE leads to significantly decreased levels of the 3'UTR CLIP targets, supporting a role for MOV10 in microRNA-mediated translational suppression, accompanied by mRNA degradation.

Because direct binding of MOV10 to RNAs had a distinct effect on mRNA fate as shown in Figure 4B and 4C, we analyzed the 3'UTR CLIP targets for the presence of Ago2 CLIP sites [44], exploring the hypothesis that MOV10 binding modulates miRNA-mediated translation suppression by either facilitating or blocking Ago2 association. Of the Ago2-bound regions identified [44], 532 were overlapped with the 1,181 regions identified in the MOV10 CLIP libraries, supporting the hypothesis that MOV10 participates in miRNA-mediated translation regulation.

We observed three categories of RNAs with 3'UTR MOV10 CLIP sites: 1) RNAs with overlapping MOV10 and Ago2 CLIP sites (Figure 4E, left); 2) RNAs with MOV10 and Ago2 CLIP sites that did not overlap (Figure 4E, middle); 3) RNAs that contained no Ago2 CLIP sites in their 3'UTR (Figure 4E, right). When the MOV10 CLIP sites overlapped with the Ago2 CLIP sites, the percentage of RNAs that decreased upon MOV10 KD was significantly larger than the percentage of RNAs that decreased when there were no Ago2 CLIP sites (36% compared to 21.7%, $p=0.042$). This observation suggested a protective role for MOV10 on those RNAs where the MOV10 binding site overlaps with the Ago2 binding site such that loss of MOV10 led to decreased RNAs. Accordingly, the percentage of RNAs that increased upon MOV10 knockdown when the MOV10 and Ago2 sites overlapped was significantly reduced compared to the percentages of increased RNAs in the other two categories (10% compared to 26.% and 29.6%, $p<0.05$). Thus, when the MOV10 and Ago2 CLIP sites overlap, MOV10 binding antagonizes Ago2-mediated transcript reduction.

To evaluate the fate of MOV10 on steady-state protein levels encoded by individual CLIP targets, we examined the 3'UTR MOV10 CLIP targets whose RNAs were previously shown to be regulated by miRNAs in HEK293 cells [45]. MOV10 knockdown significantly increased the expression of endogenous Phactr2, TGFB1 and SAMHD1 (Figure 5A), as would be expected if MOV10 facilitated miRNA-mediated suppression. This translational regulation occurred through their respective 3'UTRs (Figure 5B). Thus, MOV10 facilitated miRNA-mediated translation suppression of the proteins encoded by these 3'UTR CLIP targets.

In contrast, endogenous protein levels of MAZ were decreased upon MOV10 KD (Figure 5A), suggesting that MOV10 functions to enhance MAZ expression. The effect of MOV10 on MAZ was localized to the 3'UTR based on luciferase reporter expression (Figure 5B). The dependence of MAZ on MOV10 was similar to those RNAs that decreased in the absence of MOV10 (Figure 4B, 4C and 4E), suggesting that MOV10 normally upregulates the mRNA and protein levels of a subset of CLIP targets.

In Figure 5C we show the spatial arrangement of the MOV10 CLIP sites, the Ago2 CLIP sites and the putative GQs in the 3'UTRs of the proteins on which MOV10 had opposing effects: MAZ, whose expression is enhanced by MOV10, and Phactr2 and SAMHD1—the expressions of which are suppressed by MOV10. We propose that when MOV10 binding occurs at Ago2 sites--perhaps facilitated through an increased density of GQs--Ago2 binding and consequently, miRNA-mediated silencing, is blocked and RNA and protein levels increase, as in the case for MAZ. In contrast, when MOV10 binding occurs near (but not coincident with) Ago2 sites, Ago2 binding is enhanced and miRNA-mediated silencing proceeds, resulting in decreased RNA and protein levels, as is the case for Phactr2 and SAMHD1. These results demonstrate that proximity of Ago2 and MOV10 binding sites is important for the regulatory effects of MOV10 on target mRNAs. More broadly, since FMRP recruits MOV10 to a subset of RNAs, this suggests that association with MOV10 is a new mechanism for FMRP-mediated translation regulation (Figure 5D).

3.4 Discussion

FMRP regulates the translation of its bound mRNAs--either activating or suppressing translation [5]; however, the mechanism of regulation is largely unknown, with a few exceptions [46, 47]. miRNAs are a potent mechanism for translational regulation and both FMRP and

MOV10 are implicated in the miRNA pathway [14, 39, 48, 49]. Recently, MOV10 was shown to participate in translational suppression of mRNAs important for neuronal development and function [13]. Here, we demonstrate that MOV10 does indeed influence mRNA levels and subsequently translation, through the 3'UTR, supporting a role for MOV10 in miRNA-mediated regulation. In addition to facilitating Ago2 association, which has previously been suggested [15, 39], MOV10 binding also blocks miRNA-mediated translation suppression and consequently mRNA degradation by interfering with Ago2 binding sites, similar to the novel function recently described for polypyrimidine tract binding protein PTB [44]. PTB suppressed or enhanced miRNA targeting by competitive binding on target mRNAs or altering local RNA secondary structure [44]. Like PTB, MOV10 joins the growing list of RNA binding proteins including HuR, Dnd1, CRD-BP and PUM1 that have been implicated in modulating miRNA targeting [50].

MOV10 demonstrates specificity for secondary structure, namely GQs, as determined through bioinformatic analysis of CLIP targets and an RNA capture assay using a known GQ, sc1. GQ structures create the highest thermodynamically stable structure per base pair found in nucleic acids, and have been reported to play important roles in translational regulation, acting in both the 5'UTR and the 3'UTR [35]. In fact, the 3'UTR of PSD-95—an FMRP target--also contains three GQ forming sequences, one of which contains a functional miRNA binding site [10].

At this point, we do not know if the GQ functions only to bind MOV10 and change the local environment of the RNA or if the GQ is also subsequently unwound by MOV10, as MOV10 is a putative helicase [11, 12]. Notably, there are 3'UTR CLIP targets where the MOV10 CLIP site overlapped with the Ago2 site and the mRNAs increased in the absence of MOV10, suggesting that MOV10 facilitated miRNA-mediated translational suppression of those RNAs—a fate opposite to that of MAZ. Significantly, in those RNAs, the MOV10 CLIP sites did not contain GQs, suggesting that MOV10 bound nearby to facilitate Ago2 mediated-suppression, which is what we suspect is occurring for SAMHD1 and Phactr2. Another important issue to consider may be the strength or stability of the GQ, which may determine the ultimate fate of MOV10 on the mRNA it binds.

While we explored the role of MOV10 binding and regulation in the 3'UTR, we observed that 36.9% of the MOV10 CLIP targets in the 3'UTR showed no change in RNA levels

upon either depletion or overexpression of MOV10 (Figure 4D, middle). This lack of an effect on mRNA levels is suggestive of other roles for MOV10 outside of the miRNA pathway. In fact, a recent study showed that MOV10 played a role in an Ago-independent mechanism of LINE RNA degradation [51]. MOV10 also has a nuclear role, participating in transcriptional silencing [52] and associating with spliceosomes [[53] Table S2], which could explain its binding to introns. In that study, MOV10 is named functional spliceosome-associated protein 113 (fSAP113). Finally, MOV10 has been demonstrated to play an important role in viral pathways, influencing the replication and infectivity of HIV and HDV [54, 55].

In summary, we have identified a novel functional partner for FMRP that modulates miRNA-mediated translation regulation by Ago2, giving insight into how FMRP regulates translation of a subset of its bound RNAs.

3.5 Experimental Procedures

Immunoprecipitations, immunoblotting, RNA capture assays and gradients.

Immunoprecipitating antibodies: anti-FMRP 7G1-1 [5] and anti-MOV10 (Bethyl), agarose conjugated anti-Myc (Sigma), irrelevant antibody (rabbit antibody specific for Zebra finch FMRP [56]). Immunoprecipitations and immunoblots were performed as previously described [57]. Additional antibodies used for immunoblot include anti-FMRP [58]), anti-FMRP (Abcam ab17722), anti-Phactr2 (Abcam ab85262), anti-MAZ (Santa Cruz sc-28745) anti SAMHD1 (Thermo Scientific PA5-27898) anti TGFb1 (Sigma AV37156-100UG), anti-eIF5 (Abcam), HRP-conjugated anti-rabbit and anti-mouse antibodies (Jackson Laboratories). RNA capture assays with sc1 and sc1 mutant were performed as described [59] Myc-MOV10 was transiently transfected into HEK293F cells and immunoprecipitated using anti-Myc conjugated beads (Sigma) and eluted with Myc peptide. 15-45% Polysome gradients were performed as described in [60]. 15-30% sucrose gradients were performed as described in [19]. Protein was isolated from 100-500 uL fractions using TCA.

RNA isolation and qRT-PCR

Total RNA was isolated from adult male mouse brains (WT FVB.129, FVB FMR1 knockout mice, or C57/BL6) and treated HEK293F cell lines using Trizol (Life Technology) following

manufacturer's instructions, treated with DNase I (Biolabs) and Phenol:chloroform extracted. qRT-PCR was performed with iQ SYBR Green supermix and run on a StepOnePlus RT PCR machine (Biosystems) in triplicate. Statistical analysis was performed using a Student's t-Test. The statistics for the RNA-seq analysis is described in the Supplemental Methods. See Table S6 for the list of PCR primers.

Transfections and Luciferase assays

HEK293T or HEK293F cells were transfected with irrelevant or MOV10 specific siRNAs (Dharmacon) using PEI (Sigma) for 6 hrs. 24 hrs later, a second transfection containing irrelevant or MOV10 specific siRNA, 900 ng eGFP, 100 ng Psicheck luciferase reporter was performed. 500 ng TGFB1 in PGL3 was transfected with 500 ng eGFP, and 10 ng renilla 24 hrs post MOV10 knockdown. Luciferase activity was measured using a dual-luciferase reporter assay kit (Promega) on a SynergyTM HT Multi-detection plate reader 24 hours post secondary transfection.

MOV10-RNA coIP

HEK293F cells were UV-cross-linked three times (Stratalinker), lysed in 0.3 M lysis buffer (50 mM Tris 7.5, 300 mM NaCl, 30 mM EDTA, 0.5% triton). Lysate was cleared by ultracentrifugation at 30K for 35 min and precleared with irrelevant antibody followed by MOV10 specific antibody. IP was treated with DNase followed by RNase and subsequent washing in high salt buffer followed by proteinase K treatment. RNA was eluted and isolated by phenol/chloroform extraction followed by ethanol precipitation. Library preparation and sequencing analysis was performed using reagents for SOLiD sequencing on a SOLiD 4.0.

iCLIP

A published iCLIP protocol was followed [26, 27] with the following exceptions: phosphatase treatment was performed using shrimp alkaline phosphatase (SAP), the irrelevant immunoprecipitation was performed with a rabbit affinity purified antibody to zebra finch FMRP, described in [56]. MOV10-CLIP libraries were sequenced by the UIUC sequencing core facility using the Illumina HiSeq2000 platform. Sequences were trimmed and evaluated for quality and aligned to human genome hg19 (see Supplemental Experimental Procedures).

RNA-Seq analysis

Raw FASTQ data was quality-trimmed from the 3' end using the program Trimmomatic (v 0.22; Lohse et al. 2012), using a minimal PHRED quality score of 20 and a minimal length of 30. Sequences were then aligned using TopHat v. 2.0.8 [61] and Bowtie 2.1.0 [62] as described in Supplemental experimental procedures.

The genome sequence index was hg19 from UCSC (http://hgdownload.soe.ucsc.edu/downloads.html#human). The raw read counts were input into R 3.0.0 [63]a for data pre-processing and statistical analysis using packages from Biocondutor [64] and analyzed as described in the supplemental experimental procedures.

Accession Numbers: All iCLIP data files and RNA-Seq files will be available for download from NCBI Omnibus (http://www.ncbi.nlm.gov/geo/) under an accession number yet to be assigned because the submission in in process.

Acknowledgements
We would like to thank Tri Cong Nguyen and Sheng Zhong for generously sharing adaptors and reagents for the iCLIP library preparation, Auinash Kalsotra for extensive advice and guidance on the iCLIP experiments and for critically reading this manuscript, lab mates Geena Skariah and Albert Himoe for thoughtful input on the experiments and manuscript, colleagues Tod Jebe, Todd Patrick and Kyle Chipman for assistance with data analysis, and John Martin for the kind gift of the TGFB1 luciferase constructs. This project was supported by the High-Throughput Sequencing and Genotyping Unit in the The Roy J. Carver Biotechnology Center at UIUC with the expert assistance of the Director of DNA Services Alvaro Hernandez, PhD and by Jenny Drnevich, PhD, the Functional Genomics Bioinformatics Specialist of the High Performance Biological Computing Unit. This project was supported by the National Institutes of Health grant R01 MH093661 [to S.C and K.S.K], National Institutes of Health, University of Illinois at Urbana-Champaign Cell and Molecular Biology Training Grant [to M.K.], University of Illinois at Urbana-Champaign Research Board Arnold O. Beckman award [to S.C.], the Spastic Paralysis Research Foundation of the Illinois-Eastern Iowa District of Kiwanis International and the estates of Catherine Mary Paulsen and Anita Feller [to S.C.]. Author contributions: M.K. performed experiments and cowrote the manuscript, P.K. performed real-time PCR and created most of the luciferase reporters. R.K. analyzed the CLIP sequence data, facilitated access to Ago2 data and guided genome browser analysis, K.K. supervised the library preparation by M.A. and the sequence analysis of the MOV10 IP by H.Z., S.C. supervised the project, performed experiments and cowrote the manuscript. There are no conflicts of interest.

3.6 Figures

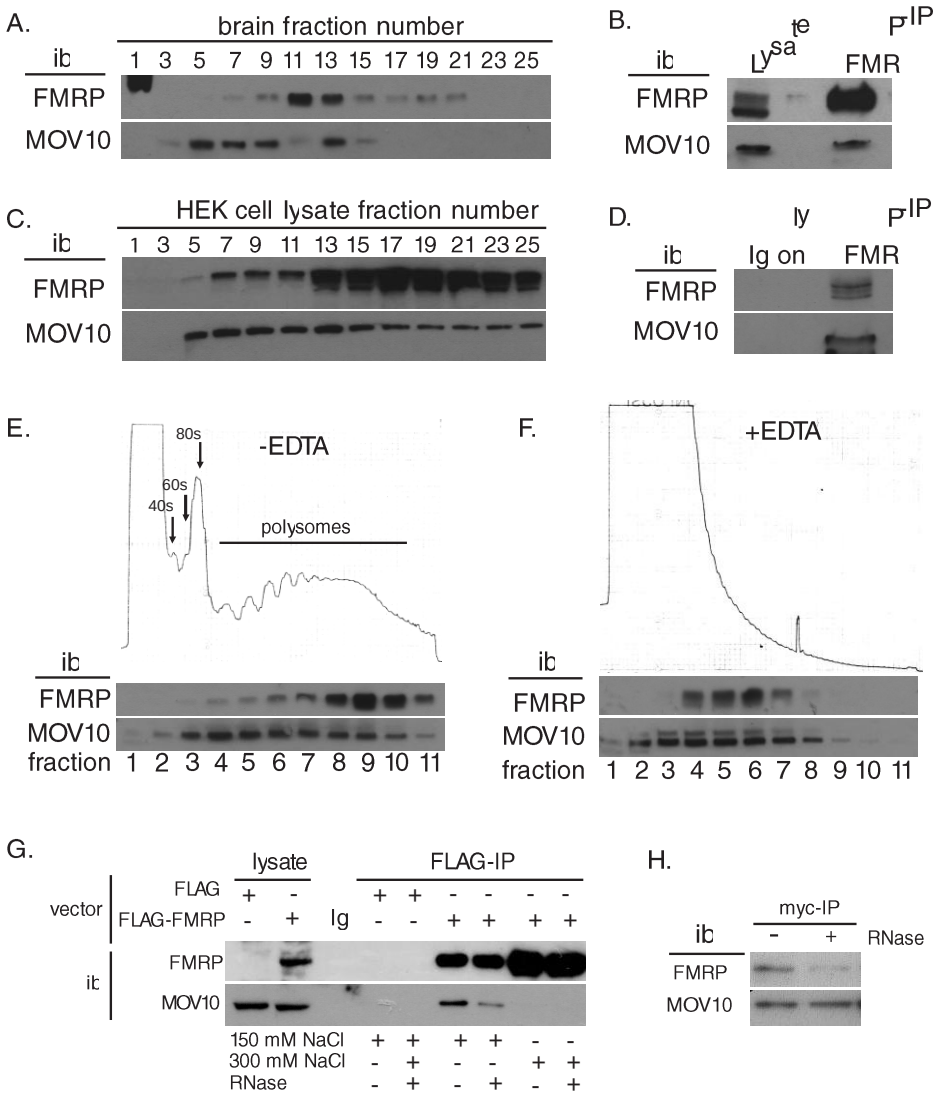

Figure 3.1. FMRP associates with MOV10 in brain and cell lines. **a)** Mouse brain extracts were analyzed by sucrose gradient centrifugation [19]. Odd numbered fractions (1-lightest-25-heaviest) were immunoblotted (ib) for FMRP and MOV10. **b)** FMRP was immunoprecipitated (IP) from whole brain lysate and immunoblotted for MOV10. **c)** HEK293F extracts were analyzed by sucrose gradient centrifugation as in A). **d)** Fractions containing both FMRP and MOV10 were pooled and immunoprecipiated for FMRP and immunoblotted for MOV10. **e)** HEK293T cells were fractionated on a sucrose gradient for polyribosome analysis: positions of the 40S and 60S subunits, the 80S ribosomes and mRNAs with multiple ribosomes (polysomes) are indicated. Fractions were immunoblotted for MOV10 and FMRP. **f)** EDTA treatment was used to disrupt polyribosomes, as described [20]. The small spike between fractions 7 and 8 is a technical artifact. **g)** FLAG-FMRP was immunoprecipitated from L-M(TK-) cells expressing the empty FLAG vector (VC) or stably expressing FLAG-FMRP (F-FMRP) [22] in the presence of high EDTA to disrupt polyribosomes, treated with RNase A (+) or not (-) and 150 mM or 300

mM NaCl, as described [22] and immunoblotted (ib) for MOV10 or FLAG (left). **h)** HEK293T cells were transfected with myc-tagged MOV10, immunoprecipitated for myc-tag, treated with RNase A and immunoblotted for endogenous FMRP [58] and myc.

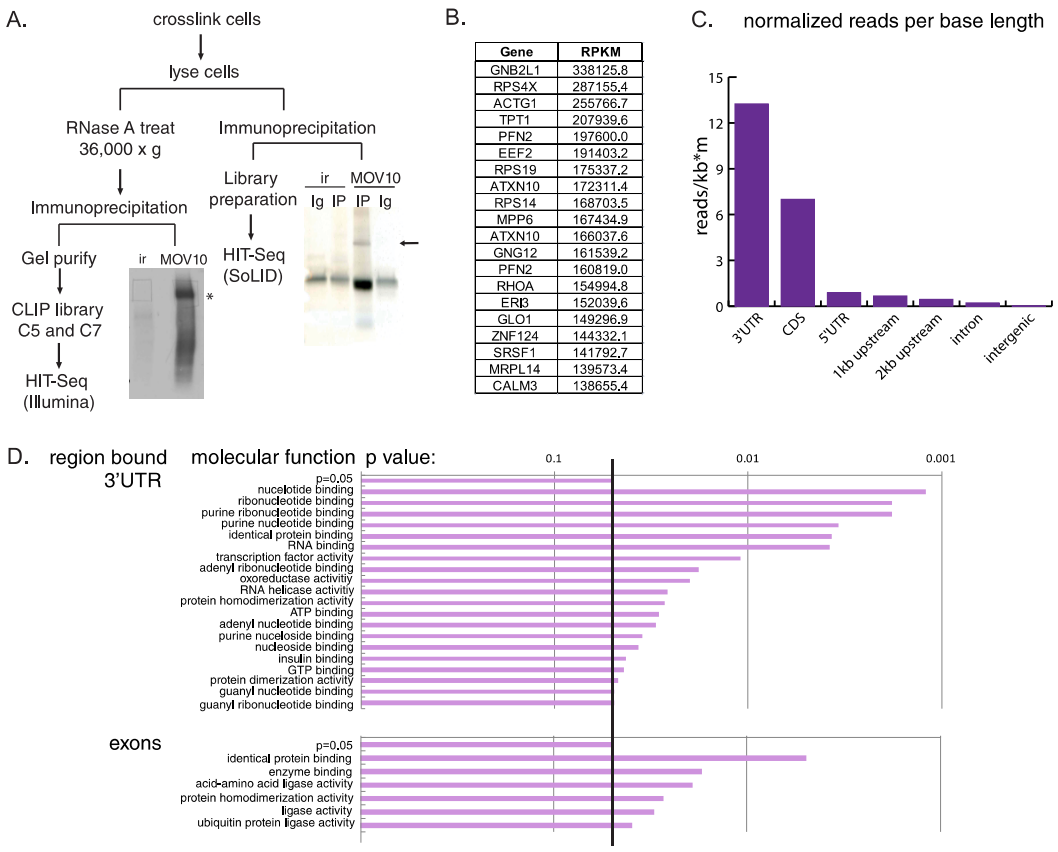

Gene	RPKM
GNB2L1	338125.8
RPS4X	287155.4
ACTG1	255766.7
TPT1	207939.6
PFN2	197600.0
EEF2	191403.2
RPS19	175337.2
ATXN10	172311.4
RPS14	168703.5
MPP6	167434.9
ATXN10	166037.6
GNG12	161539.2
PFN2	160819.0
RHOA	154994.8
ERI3	152039.6
GLO1	149296.9
ZNF124	144332.1
SRSF1	141792.7
MRPL14	139573.4
CALM3	138655.4

Figure 3.2. MOV10 binds a subset of mRNAs. a) Schematic of library preparations for MOV10 cross-linked immunoprecipitations (right) and CLIP (left). Right, silver stain of UV-cross-linked immunoprecipitations (IP), MOV10 (arrow); Left, autoradiography of [^{32}P]-labeled MOV10-RNA complex (star), C7 iCLIP library. Ir-irrelevant immunoprecipitation, Ig-immunoprecipitating antibody alone. **b)** Top 20 RNA targets in the UV-cross linked MOV10 IP. **c)** Distribution of MOV10 CLIP binding sites identified in both C5 and C7 libraries plotted as reads per kilobase per million reads. **d)** GO analysis of MOV10 CLIP targets based on region bound. Significance ($p<0.05$) is indicated by the black line.

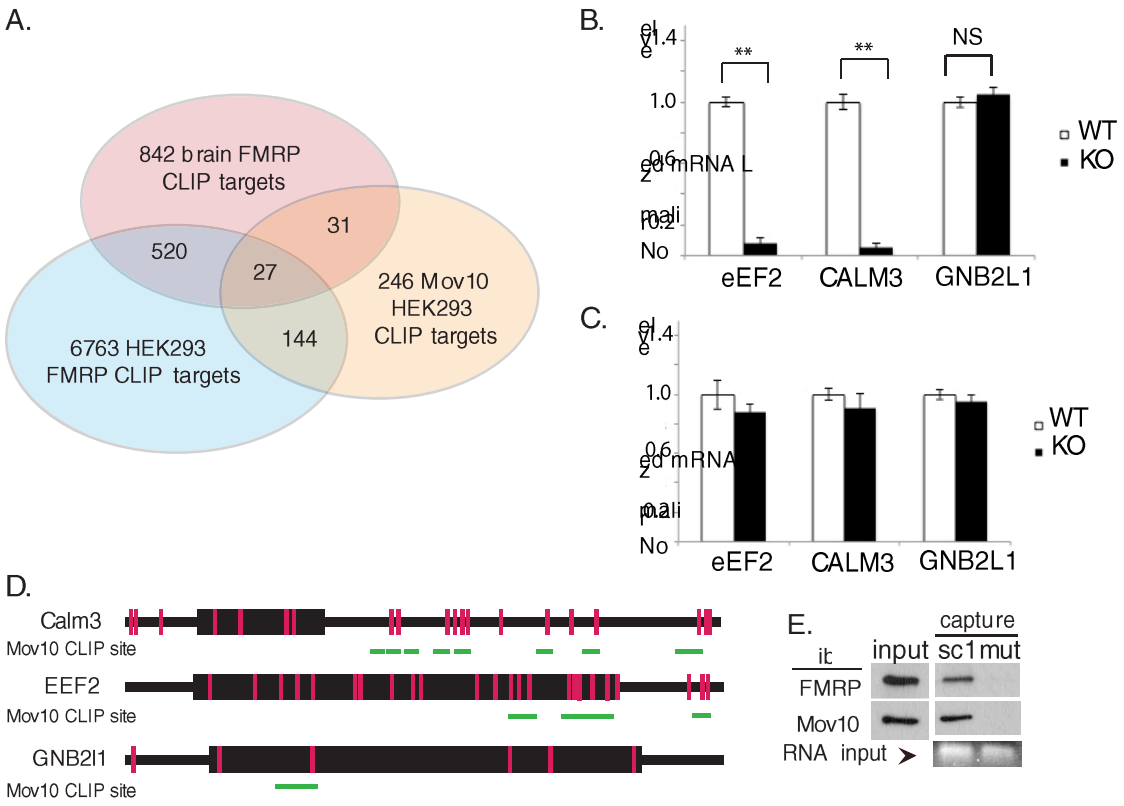

Figure 3.3. MOV10 recognizes a subset of RNAs bound by FMRP and GQs. a) Venn diagram showing overlap of MOV10 CLIP targets with previously published FMRP CLIP RNAs isolated from brain (Darnell et al., 2011) and FMRP isoform 1 CLIP RNAs isolated from transfected HEK293 cells (Ascano et al., 2012). **b)** Real-time PCR quantification of MOV10-associated RNAs (eEF2, CALM3 and GNB2L1) immunoprecipitated from WT and FMR1 knockout (ko) brains (n=3). **c)** Real-time PCR quantification of indicated RNAs from WT and FMR1 knockout brains (n=3). **d)** Schematic showing predicted GQs (pink bars) in CALM3, eEF2, and GNB2L1 (UTRs are thin lines; coding sequence is thick line) and MOV10 clip sites (green bars). **e)** Immunoblots (ib) of *in vitro* synthesized FMRP and purified recombinant MOV10 in RNA capture assays using the GQ sc1 and sc1 mutant (RNAs shown by ethidium stain of an agarose gel).

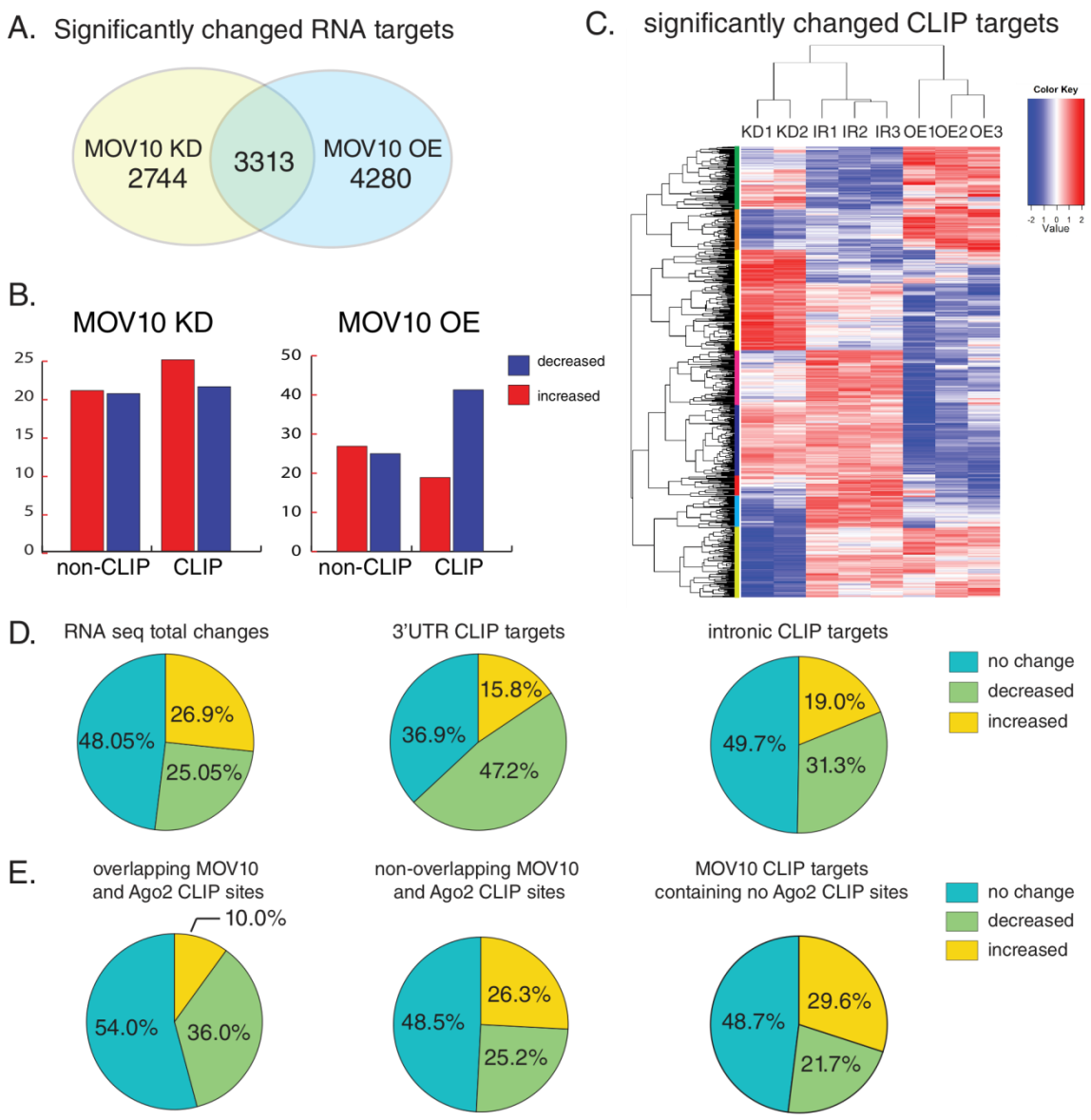

Figures 3.4. MOV10 affects mRNA levels of CLIP targets. a) Venn diagram of significantly changed RNAs ($p<0.05$) in MOV10 knockdown (KD) (6057 RNAs) or overexpression (OE) experiments (7593 RNAs). 3313 RNAs were common to both treatments. **b)** CLIP targets in the MOV10 knockdown (KD) were significantly changed compared to the non CLIP RNA under knockdown conditions (non-CLIP) (left, $p=0.0068$); CLIP targets in the MOV10 overexpression (OE) were significantly changed (CLIP) compared to the non-CLIP RNA (right, $p=1.83E-26$). **c)** Heatmap of significantly changed CLIP RNAs in MOV10 knockdown (KD), irrelevant siRNA (IR), and transgene overexpression (OE) experiments. Colored bars indicate discrete clusters of RNAs. Individual experiments are indicated on the top. **d)** Distribution of RNAs in MOV10 overexpression experiments that did not change (blue), significantly decreased (green) or significantly increased (yellow) for total RNA (left), for RNAs containing 3'UTR CLIP targets (center) or RNAs containing intronic CLIP targets (right). **e)** Distribution of RNAs in MOV10

knockdown experiments that did not change (blue), significantly decreased (green) or significantly increased (yellow) that had overlapping MOV10 and Ago2 CLIP sites in the 3' UTR (left, 50 RNAs), non-overlapping MOV10 and Ago2 CLIP sites in the 3'UTR (center, 167 RNAs) or no Ago2 CLIP sites in the 3'UTR (right, 115 RNAs)**.** Decreased: 36% vs. 22% is significant (X^2= 2.9752, df = 1, p-value = 0.04228) (1-tailed). Increased: 10% vs. 26% = X2 = 4.9842, df = 1, p-value = 0.01279 (1-tailed); 10% vs. 30% = X2 = 6.3465, df = 1, p-value = 0.005881 (1-tailed).

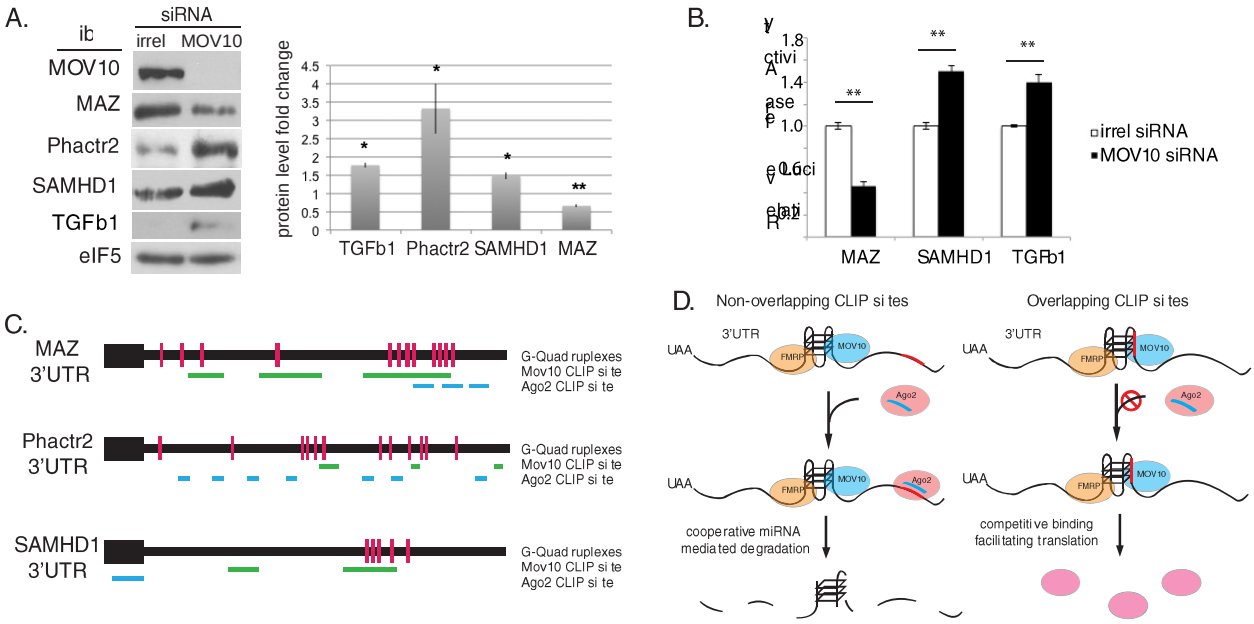

Figure 3.5. Effect of MOV10 on miRNA-regulated protein expression. a) Immunoblots (ib) for indicated endogenous proteins in HEK293T cells treated with irrelevant siRNAs (Irrel) or MOV10 siRNAs. eIF5 is a loading control. Right, fold-change of proteins in three independent experiments, * $p<0.05$, ** $p<0.01$ (right). **b)** 3'UTRs of MAZ, SAMHD1 and TGFB1 were subcloned into luciferase reporter plasmids and the effect of MOV10 loss examined. * $p<0.05$, ** $p<0.01$. **c)** 3'UTRs of MAZ, Phactr2 and SAMHD1, showing the relationship between GQs (pink bars), MOV10 CLIP sites (green bars), and Ago2 CLIP sites (blue bars). **d)** Model for FMRP-associated, MOV10-mediated translation regulation. FMRP binds mRNAs and recruits MOV10 to GQs. MOV10 binding facilitates the availability of nearby miRNA binding site (red) for Ago2-mediated translation suppression/RNA degradation through bound miRNA (blue) **(left)**. If the miRNA binding site is within the GQ, MOV10 binding precludes Ago2 association, leading to an increase in stability of the RNA and subsequent translation **(right).**

3.7 Supplemental Methods and Tables

Supplementary Files

Supplemental figures and legends, tables, Experimental Procedures, and references (in this order).

Table S1, related to Figure 3.2 . SOLiD sequencing platform results

Table S2, related to Figure 3.2. Identified MOV10 CLIP sites.

Table S3, related to Figure 3.3. Overlapping targets with Darnell and Ascanano CLIP lists

Table S4, related to Figure 3.4. Results of RNA seq analysis

Table S5, related to Figure 3.4. Significantly changed mRNA targets from RNA seq analysis.

Table S4

FileName	group	Label	total_reads	trim_reads	pct_map_genome	pct_map_genes	gene_mapped_read	gene_used_reads	norm.fact
Irrel_kd_1_CGATGT.counts	IR	IR.1	36,070,585	35,477,852	94.67%	63.95%	22,687,366	22,673,597	0.995762
Irrel_kd_2_TGACCA.counts	IR	IR.2	30,842,628	30,312,549	94.71%	63.94%	19,381,680	19,369,548	0.999486
Irrel_kd_3_ACAGTG.counts	IR	IR.3	23,917,772	23,523,421	94.27%	63.61%	14,962,754	14,953,196	1.003414
Mov10_kd_1_AGTCAA.counts	KD	KD.1	38,597,808	37,926,417	94.72%	60.66%	23,007,640	22,991,391	0.973383
Mov10_kd_2_AGTTCC.counts	KD	KD.2	52,680,333	51,731,846	94.60%	63.46%	32,826,936	32,808,876	0.968029
Mov10_kd_3_ATGTCA.counts	KD	KD.3	31,115,286	30,586,827	94.18%	63.30%	19,360,003	19,349,488	0.978172
Myc_mov10_1_GCCAAT.counts	OE	OE.1	39,971,841	39,277,123	90.59%	59.70%	23,447,317	23,430,488	1.025301
Myc_mov10_2_CAGATC.counts	OE	OE.2	37,102,084	36,457,707	89.90%	59.56%	21,713,289	21,698,007	1.031843
Myc_mov10_3_CTTGTA.counts	OE	OE.3	21,204,527	20,880,312	91.53%	61.00%	12,737,889	12,729,478	1.026916

Table S4. Total RNA seq analysis of MOV10 knockdown, overexpression, or irrelevant siRNA treatment.

Supplemental Experimental Procedures.

Transfectons and total RNA isolation and RT-PCR

HEK293T cells were transfected with irrelevant or MOV10 specific siRNAs (Dharmacon), or myc-MOV10 using PEI (Sigma) for 6 hours. siRNA transfections were performed at 24 hr intervals for 72 hours. Myc-MOV10 overexpression transfection was performed once and harvested 48 hrs later. Cells were lysed and RNA was isolated using Trizol (Life Technology) following manufacturer's instructions, treated with DNase I (Biolabs) and Phenol:chloroform extracted. qRT-PCR was performed with iQ SYBR Green supermix and run on a StepOnePlus RT PCR machine (Biosystems) in triplicate. Statistical analysis was performed using a Student's t-Test.

Primers used for RT-PCR:

Name	Sequence (5' to 3')
CALM3 F	CTTCGACAAGGATGGAGATGG
CALM3 R	AACTCTGGGAAGTCAATGGTC
Eef2 F	ACATTCTCACCGACATCACC
Eef2 R	GAACATCAAACCGCACACC
GNB2L1 F	AATACTGTGGGTGTCTGCAAG
GNB2L1 R	TTAGCCAGATTCCACACCTTG
GAPDH F	CTTTGTCAAGCTCATTTCCT
GAPDH R	CTTGCTCAGTGTCCTTGC
MAZ F	GCCGCTCGAGGTGATCCGTGGTGTTTCTCCTG
MAZ R	CATCAGCAAGGCGGCCGCGGCAGTTCTTAGTGAGGGCAA
SAMHD1 F	GCCGCTCGAGTGGGTGGTCCTAATTTCAGCA
SAMHD1 R	CATCAGCAAGGCGGCGCCAAAATCCAACTCGCCTCCG

Comparison of RNA lists

VLookup was used to compare FMRP CLIP lists from FMRP iso1 (ascano) and polysomal FMRP (darnell)

RNA-Seq analysis

Raw FASTQ data was quality-trimmed from the 3' end using the program Trimmomatic (v 0.22; Lohse et al. 2012), using a minimal PHRED quality score of 20 and a minimal length of 30. Sequences were then aligned using TopHat v. 2.0.8 [61] and Bowtie 2.1.0 [62] using the following parameters:

tophat2 --coverage-search -p 8 -N 7 --read-edit-dist 7 --library-type fr-firststrand -o <SAMPLE_NAME> <REFERENCE_DATABASE> <TRIMMED_FASTQ>

The genome sequence index (<REFERENCE_DATABASE>) was hg19 from UCSC (http://hgdownload.soe.ucsc.edu/downloads.html#human). The BAM alignments were first changed to SAM format using samtools (v 0.1.18, Li et al. 2009) and then raw read counts were tabulated for each sample at the gene level using the GTF gene model file <GTF_FILE> for hg19 from UCSC and htseq-count, from HTSeq v0.5.3p9 (http://www-huber.embl.de/users/anders/HTSeq/doc/index.html) using the default "exon" feature type, "gene_id" attribute and the following parameters:

htseq-count -s reverse -m intersection-nonempty - <GTF_FILE>

The raw read counts were input into R 3.0.0 [63]a for data pre-processing and statistical analysis using packages from Biocondutor [64] as indicated below. Initial quality control analysis indicated that one of the three KD replicates was an outlier and it was removed from the analysis. Genes without 1 Count Per Million (CPM) mapped reads in at least one of the 8 samples were filtered out due to unreliable data in any sample; 14,615 of the 23,368 genes passed this filter and were analyzed using edgeR 3.2.1 [65]. The raw count values were used in a negative bionomial statistical model that accounted for the total library size for each sample and an extra TMM normalization factor [66] for any biases due to changes in total RNA composition of the samples. Pairwise comparison for KD vs. IR and OE vs. IR were pulled from the model and separately adjusted for multiple testing using the False Discovery Rate method [67]; genes with FDR $p < 0.05$ were considered significantly different. For sample clustering and heatmaps, comparable expression values were generated from the read counts using edgeR's modified log2 CPM values. Additional annotation information (gene names, descriptions, Gene Ontology terms and pathways) was obtained from Bioconductor's org.Hs.eg.db package (v. 2.9.0; based on NCBI's Entrez database) using the transcript IDs provided in the GTF gene model file instead of the gene symbols. To compare with the CLIP data, the genomic regions showing CLIP targets for MOV10 were annotated to the closest gene using gene symbols for hg19 from Ensembl and assigned to a region of the gene (e.g., 3' UTR, exon, intron, etc.). Due to discrepancies between gene symbols from UCSC, NCBI and Ensembl, and multiple gene symbols for some CLIP targets, only 947 of the original 1049 CLIP targets could be matched to genes from the RNA-Seq data. This represented 779 different genes, as some genes had CLIP targets in more than one region and/or multiple CLIP targets within a region. Not counting multiple targets per region but allowing more than one region per gene, there were 360 genes with CLIP targets in the 3' UTR, 269 genes with CLIP targets in exons and 163 genes with CLIP targets in introns. For the KD vs. IR and OE vs. IR comparisons, the number of significantly up-regulated, down-regulated and non-significant genes among the 779 genes with CLIP targets were compared with the rest of the 13,863 genes using a Pearson's chi-squared test. Within each region, a similar comparison between the numbers of up, down and no-change genes with CLIP targets versus the rest of the genes without targets in that region was done with separate Pearson's chi-squared tests for each region.

MOV10-RNA coIP and iCLIP

HEK293F cells were UV-cross linked three times (Stratalinker), lysed in 0.3 M lysis buffer (50 mM Tris 7.5, 300 mM NaCl, 30 mM EDTA, 0.5% triton). Lysate was cleared by ultracentrifugation at 30K for 35 min and precleared with irrelevant antibody followed by MOV10 specific antibody. IP was treated with DNase followed by RNase and subsequent washing in high salt buffer followed by proteinase K treatment. RNA was eluted and isolated by

phenol/chloroform extraction followed by ethanol precipitation. Library preparation and sequencing analysis was performed using reagents for SOLiD sequencing on a SOLiD 4.0. iCLIP: A published iCLIP protocol was followed [26, 27] with the following exceptions: phosphatase treatment was performed using shrimp alkaline phosphatase (SAP), the irrelevant immunoprecipitation was performed with a rabbit affinity purified antibody to zebra finch FMRP, described in [56]. MOV10-CLIP libraries were sequenced by the UIUC sequencing core facility using the Illumina HiSeq2000 platform. Sequences were trimmed and evaluated for quality and aligned to human genome hg19

3.8 References

1. Bolduc, F.V., et al., *Excess protein synthesis in Drosophila Fragile X mutants impairs long-term memory.* Nat Neurosci, 2008. **11**(10): p. 1143.
2. Kelleher, R.J., 3rd and M.F. Bear, *The autistic neuron: troubled translation?* . Cell, 2008. **135**: p. 401-406.
3. Liu-Yesucevitz, L., et al., *Local RNA Translation at the Synapse and in Disease.* The Journal of Neuroscience, 2011. **31**(45): p. 16086-16093.
4. Hagerman, R.J., et al., *Advances in the Treatment of Fragile X Syndrome.* Pediatrics %R 10.1542/peds.2008-0317, 2009. **123**(1): p. 378-390.
5. Brown, V., et al., *Microarray identification of FMRP-associated brain mRNAs and altered mRNA translational profiles in fragile X syndrome.* Cell, 2001. **107**(4): p. 477-87.
6. Ishizuka, A., M.C. Siomi, and H. Siomi, *A Drosophila fragile X protein interacts with components of RNAi and ribosomal proteins.* Genes Dev, 2002. **16**(19): p. 2497-508.
7. Caudy, A.A., et al., *Fragile X-related protein and VIG associate with the RNA interference machinery.* Genes Dev, 2002. **16**(19): p. 2491-6.
8. Jin, P., et al., *Biochemical and genetic interaction between the fragile X mental retardation protein and the microRNA pathway.* Nat Neurosci, 2004. **7**(2): p. 113-7.
9. Edbauer, D., et al., *Regulation of Synaptic Structure and Function by FMRP-Associated MicroRNAs miR-125b and miR-132.* Neuron, 2010. **65**(3): p. 373.
10. Muddashetty, R.S., et al., *Reversible Inhibition of PSD-95 mRNA Translation by miR-125a, FMRP Phosphorylation, and mGluR Signaling.* Molecular Cell, 2011. **42**(5): p. 673-688.
11. Jaenisch, R., et al., *Chromosomal position and activation of retroviral genomes inserted into the germ line of mice.* Cell, 1981. **24**(2): p. 519.
12. Mooslehner, K., et al., *Structure and expression of a gene encoding a putative GTP-binding protein identified by provirus integration in a transgenic mouse strain.* Mol Cell Biol, 1991. **11**(2): p. 886-93.
13. Banerjee, S., P. Neveu, and K.S. Kosik, *A Coordinated Local Translational Control Point at the Synapse Involving Relief from Silencing and MOV10 Degradation.* Neuron, 2009. **64**(6): p. 871.
14. Meister, G., et al., *Identification of novel argonaute-associated proteins.* Curr Biol, 2005. **15**(23): p. 2149-55.
15. Sievers, C., et al., *Mixture models and wavelet transforms reveal high confidence RNA-protein interaction sites in MOV10 PAR-CLIP data.* Nucleic Acids Research, 2012.
16. Bartel, D.P., *MicroRNAs: Genomics, Biogenesis, Mechanism, and Function.* Cell, 2004. **116**(2): p. 281.
17. Bartel, D.P., *MicroRNAs: Target Recognition and Regulatory Functions.* Cell, 2009. **136**(2): p. 215.
18. Wulczyn, F.G., et al., *Post-transcriptional regulation of the let-7 microRNA during neural cell specification.* The FASEB Journal, 2007. **21**(2): p. 415-426.
19. Kanai, Y., N. Dohmae, and N. Hirokawa, *Kinesin transports RNA: isolation and characterization of an RNA-transporting granule.* Neuron, 2004. **43**: p. 513 - 525.
20. Feng, Y., et al., *FMRP associates with polyribosomes as an mRNP, and the I304N mutation of severe fragile X syndrome abolishes this association.* Mol Cell, 1997. **1**(1): p. 109-18.

21. Khandjian, E.W., et al., *The fragile X mental retardation protein is associated with ribosomes.* Nat Genet, 1996. **12**(1): p. 91-3.
22. Ceman, S., V. Brown, and S.T. Warren, *Isolation of an FMRP-associated messenger ribonucleoprotein particle and identification of nucleolin and the fragile X-related proteins as components of the complex.* Mol Cell Biol, 1999. **19**(12): p. 7925-32.
23. Ascano, M., et al., *FMRP targets distinct mRNA sequence elements to regulate protein expression.* Nature, 2012. **492**(7429): p. 382-386.
24. Darnell, J.C., et al., *FMRP Stalls Ribosomal Translocation on mRNAs Linked to Synaptic Function and Autism.* Cell, 2011. **146**(2): p. 247-261.
25. Miyashiro, K.Y., et al., *RNA cargoes associating with FMRP reveal deficits in cellular functioning in Fmr1 null mice.* Neuron, 2003. **37**(3): p. 417-31.
26. Konig, J., et al., *iCLIP reveals the function of hnRNP particles in splicing at individual nucleotide resolution.* Nat Struct Mol Biol, 2010. **17**(7): p. 909-915.
27. Konig, J., et al., *iCLIP - Transcriptome-wide Mapping of Protein-RNA Interactions with Individual Nucleotide Resolution.* J Vis Exp, 2011(50): p. e2638.
28. Darnell, J.C., et al., *Fragile X mental retardation protein targets G quartet mRNAs important for neuronal function.* Cell, 2001. **107**(4): p. 489-99.
29. Chen, L., et al., *The fragile x mental retardation protein binds and regulates a novel class of mRNAs containing u rich target sequences.* Neurosci., 2003. **120**(4): p. 1005-1017.
30. Phan, A.T.n., et al., *Structure-function studies of FMRP RGG peptide recognition of an RNA duplex-quadruplex junction.* Nat Struct Mol Biol, 2011. **18**(7): p. 796-804.
31. Kostadinov, R., et al., *GRSDB: a database of quadruplex forming G-rich sequences in alternatively processed mammalian pre-mRNA sequences.* Nucleic Acids Research, 2006. **34**(suppl 1): p. D119-D124.
32. Arthanari, H. and P.H. Bolton, *Functional and dysfunctional roles of quadruplex DNA in cells.* Chemistry & Biology, 2001. **8**(3): p. 221-230.
33. Williamson, J.R., M.K. Raghuraman, and T.R. Cech, *Monovalent cation-induced structure of telomeric DNA: The G-quartet model.* Cell, 1989. **59**(5): p. 871-880.
34. Chakraborty, P. and F. Grosse, *Human DHX9 helicase preferentially unwinds RNA-containing displacement loops (R-loops) and G-quadruplexes.* DNA Repair, 2011. **10**(6): p. 654-65.
35. Creacy, S.D., et al., *G4 Resolvase 1 Binds Both DNA and RNA Tetramolecular Quadruplex with High Affinity and Is the Major Source of Tetramolecular Quadruplex G4-DNA and G4-RNA Resolving Activity in HeLa Cell Lysates.* Journal of Biological Chemistry, 2008. **283**(50): p. 34626-34634.
36. Beaudoin, J.-D. and J.-P. Perreault, *Exploring mRNA 3′-UTR G-quadruplexes: evidence of roles in both alternative polyadenylation and mRNA shortening.* Nucleic Acids Research, 2013. **41**(11): p. 5898-5911.
37. Kikin, O., L. D'Antonio, and P. Bagga, *QGRS Mapper: a web-based server for predicting G-quadruplexes in nucleotide sequences.* Nucleic Acids Research, 2006. **34**(web server issue): p. W676-W682.
38. Menendez, C., S. Frees, and P.S. Bagga, *QGRS-H Predictor: a web server for predicting homologous quadruplex forming G-rich sequence motifs in nucleotide sequences.* Nucleic Acids Research, 2012.

39. Liu, C., et al., *APOBEC3G Inhibits MicroRNA-mediated Repression of Translation by Interfering with the Interaction between Argonaute-2 and MOV10.* Journal of Biological Chemistry, 2012. **287**(35): p. 29373-29383.
40. Guo, H., et al., *Mammalian microRNAs predominantly act to decrease target mRNA levels.* Nature, 2010. **466**(7308): p. 835-840.
41. Lim, L.P., et al., *Microarray analysis shows that some microRNAs downregulate large numbers of target mRNAs.* Nature, 2005. **433**(7027): p. 769.
42. Baek, D., et al., *The impact of microRNAs on protein output.* Nature, 2008. **455**(7209): p. 64.
43. Eulalio, A., E. Huntzinger, and E. Izaurralde, *Getting to the Root of miRNA-Mediated Gene Silencing.* Cell, 2008. **132**(1): p. 9-14.
44. Xue, Y., et al., *Direct Conversion of Fibroblasts to Neurons by Reprogramming PTB-Regulated MicroRNA Circuits.* Cell, 2013. **152**(1,Äì2): p. 82-96.
45. Schmitter, D., et al., *Effects of Dicer and Argonaute down-regulation on mRNA levels in human HEK293 cells.* Nucleic Acids Research, 2006. **34**(17): p. 4801-4815.
46. Napoli, I., et al., *The Fragile X Syndrome Protein Represses Activity-Dependent Translation through CYFIP1, a New 4E-BP.* Cell, 2008. **134**(6): p. 1042.
47. Bechara, E.G., et al., *A novel function for fragile X mental retardation protein in translational activation.* PLoS Biol, 2009. **7**(1): p. e16.
48. Jin, P., R.S. Alisch, and S.T. Warren, *RNA and microRNAs in fragile X mental retardation.* Nat Cell Biol, 2004. **6**(11): p. 1048-53.
49. Wang, D.O., K.C. Martin, and R.S. Zukin, *Spatially restricting gene expression by local translation at synapses.* Trends in Neurosciences, 2010. **33**(4): p. 173-182.
50. van Kouwenhove, M., M. Kedde, and R. Agami, *MicroRNA regulation by RNA-binding proteins and its implications for cancer.* Nat Rev Cancer, 2011. **11**(9): p. 644-656.
51. Li, X., et al., *The MOV10 helicase inhibits LINE-1 mobility.* Journal of Biological Chemistry, 2013.
52. Messaoudi-Aubert, S.E., et al., *Role for the MOV10 RNA helicase in Polycomb-mediated repression of the INK4a tumor suppressor.* Nat Struct Mol Biol, 2010. **17**(7): p. 862-868.
53. Zhou, Z., et al., *Comprehensive proteomic analysis of the human spliceosome.* Nature, 2002. **419**: p. 182-185.
54. Wang, X., et al., *Moloney Leukemia Virus 10 (MOV10) Protein Inhibits Retrovirus Replication.* Journal of Biological Chemistry, 2010. **285**(19): p. 14346-14355
55. Furtak, V., et al., *Perturbation of the P-Body Component Mov10 Inhibits HIV-1 Infectivity.* PLoS ONE, 2010. **5**(2): p. e9081.
56. Winograd, C., D. Clayton, and S. Ceman, *Expression of fragile X mental retardation protein within the vocal control system of developing and adult male zebra finches.* Neuroscience, 2008. **157**(1): p. 132-42.
57. Ceman, S., et al., *Development and characterization of antibodies that immunoprecipitate the FMR1 protein.* Methods Mol Biol, 2003. **217**: p. 345-54.
58. Devys, D., et al., *The FMR-1 protein is cytoplasmic, most abundant in neurons, and appears normal in carriers of the fragile X premutation.* Nat Genet, 1993. **4**(4): p. 335-40.
59. Stetler, A., et al., *Identification and characterization of the methyl arginines in the fragile X mental retardation protein Fmrp.* Hum Mol Genet, 2006. **15**(1): p. 87-96.

60. Blackwell, E., X. Zhang, and S. Ceman, *Arginines of the RGG box regulate FMRP association with polyribosomes and mRNA*
Human Molecular Genetics, 2010. **19**(7): p. 1314-23.
61. Trapnell, C., L. Pachter, and S.L. Salzberg, *TopHat: discovering splice junctions with RNA-Seq.* Bioinformatics, 2009. **25**(9): p. 1105-1111.
62. Langmead, B. and S.L. Salzberg, *Fast gapped-read alignment with Bowtie 2.* Nat Meth, 2012. **9**(4): p. 357-359.
63. Team, R.C. *R: A language and environment for statistical computing.* R Foundation for Statistical Computing, 2013.
64. Gentleman RC, C.V., Bates DM, Bolstad B, Dettling M, Dudoit S, Ellis B, Gautier L, Ge Y, Gentry J, Hornik K, Hothorn T, Huber W, Iacus S, Irizarry R, Leisch F, Li C, Maechler M, Rossini AJ, Sawitzki G, Smith C, Smyth G, Tierney L, Yang JY, Zhang J., *Bioconductor: open software development for computational biology and bioinformatics.* Genome Biology, 2004. **5**(10): p. R80.
65. Robinson, M.D., D.J. McCarthy, and G.K. Smyth, *edgeR: a Bioconductor package for differential expression analysis of digital gene expression data.* Bioinformatics, 2010. **26**(1): p. 139-140.
66. Robinson, M.D. and A. Oshlack, *A scaling normalization method for differential expression analysis of RNA-seq data.* Genome Biology, 2010. **11**(3): p. R25.
67. Benjamini, Y. and Y. Hochberg, *Controlling the false discovery rate: a practical and powerful approach to multiple testing.* Journal of the Royal Statistical Society Series, 1995. **B**(57): p. 289-300.

Chapter 4. Single molecule studies of transcribed RNA

4.1 Abstract

MOV10 is a putative RNA helicase that has yet to be demonstrated to show ribonucleic acid remodeling abilities. In this chapter, we begin the process of analyzing the molecular mechanism by which MOV10 interacts with RNA molecules through the use of single molecule total internal fluorescence microscopy (sm-TIRF). Here, we show that synthesized sc1 RNA is a suitable substrate for single molecule imaging and folds in a salt dependent manner. We establish preliminary data to determine behavior of potential RNA targets for eventual study of how MOV10 acts on true RNA targets.

4.2 Introduction

Helicases are important for many functions--from DNA repair and replication to translation at the RNA level. Domains and structures have been well studied and a number of crystal structures have been established for helicases such as T7 and Upf1[1-3]. Helicases have been extensively studied using single molecule techniques. For example, Hepatitis C virus helicase NS3 is a well characterized helicase that has benefited greatly from single molecule studies. Optical tweezers have been used to study the unwinding of RNA hairpin substrates as well as determining the unwinding and stepping velocity of the protein [4-6]. This chapter outlines the potential and lays the groundwork for future studies to further understand the molecular mechanism of MOV10 on RNA secondary structures.

FMRP binds RNA G quadruplexes, with sc1 as one of the model GQs that is bound with high affinity [7]. We recently identified it as an RNA substrate for MOV10 (Chapter 3), however the structure of the molecule was resolved by NMR [8], making this an ideal starting point to pursue single molecule studies. Single molecule imaging is a powerful tool that allows us to visualize nuanced and unique events at the per-molecule level. FRET energy transfers can be used to visualize changes in distance between the two fluorophores from a range of 20-80 angstroms (reviewed in [9]). The resolution offered by these techniques offers science an amazing tool to study individual kinetic and structural changes, especially on RNA secondary structures such as G-quadruplexes [10].

4.3 Results:

in vitro transcribed and end labeled RNAs are suitable for smFRET

Due to the length of the RNA constructs of PSD95, hASH1, sc1 and sc1 mut, it was necessary to *in vitro* transcribe and label molecules manually. Constructs were generated based on location of G quadruplexes and also the strength of GQs. (Figure 1) and labeled. RNAs were annealed to a biotinylated tether that contained the Cy5 dye, therefore annealed tether+synthesized RNA is visualized as yellow. Annealed RNA migrated slower on an acrylamide gel compared to unannelead single stranded synthesized molecules indicating an increase in molecular weight.

We first analyzed the RNA molecules by smFRET to determine behavior in salt solution. Because these RNAs have never been previously studied, it was difficult to determine where the dye would be placed in addition to predicting how the molecules would behave at the single molecule level. Based on previously published work, we developed sc1, sc1 mutant constructs, PSD-95 and hASH1 mRNA constructs that contained GQ forming sequences validated by QGRS. We expected these mRNAs to be loosely folded at low salt and tightly folded with increasing salt concentrations. We tested sc1 RNA, titrating NaCl, KCl, and LiCl, which are known salts to stabilize and coordinate GQ formation [11]. In low salt solutions, the RNA molecules largely existed in low FRET states, ranging from 0.2-0.3, suggesting a loose and unstructured conformation. With increasing levels of monovalent cations, the population shifted to favor the high FRET state from 0.8-0.9, indicating that the two dyes are now in close proximity to each other (Fig 2).

We next performed salt titrations on the sc1 mutant, hASH1, and PSD-95 to determine whether the RNA constructs also behaved similarly to sc1. Compared to sc1, sc1 mutant did not fold as efficiently, suggesting that the nucleotide substitutions significantly affected secondary structure and RNA folding (Fig 3a). hASH1 GQs 1 and 2 demonstrated salt dependent folding. By 50mM KCl, the majority population of the RNA was in a high fret state (Fig 3b). We anticipated the same to be true for PSD-95 however the construct selected did not successfully fold even in the presence of 300 mM salt. This may be due to the length of the sequence, or the complexity of the secondary structure.

sc1 RNA folds to high FRET in the presence of RGG peptide

Sc1 is an interesting molecule because it was initially found in a screen of high affinity binding RNAs to FMRP [12]. In the presence of the FMRP RGG box, the peptide suddenly snapped the RNA into a structured GQ [8]. We wanted to determine whether or not we could mimic this effect at the single molecule level, so we incubated 1mm minimal RGG peptide required for sc1 folding and found that the FMRP RGG box induced folding of sc1 RNA, even in low salt conditions.

We next determined the time scale by which binding of RGG peptide influenced sc1 RNA folding. In a brief time course experiment, we found that sc1 RNA became folded within 30 seconds of peptide addition and remained folded for the remainder of the time course (Fig 4) suggesting a strong and stable association between the peptide and RNA.

4.4 Discussion

These introductory studies demonstrate that single molecule FRET of MOV10 and associated mRNAs are a promising avenue of research. Current studies of FMRP-mRNA interactions have been performed using bulk measurements and assays, making the analysis of individual molecule binding very difficult. sc1 RNA has been analyzed by circular dichroism and also by NMR studies [8, 13]. We are the first to demonstrate sc1 folding efficiency in salt solutions as well as single molecule interactions between the FMRP RGG peptide and sc1 RNA. Additionally, we have demonstrated that potential targets that are recognized by MOV10 and FMRP are also viable targets for single molecule studies.

Obtaining sufficient quantities of purified FMRP and MOV10 would be next steps toward understanding how these proteins interact with target RNAs.

Acknowledgements

Single molecule TIR experiments and data analysis were performed with the assistance of Helen Hwang in the Myong lab. Typhoon imaging and RGG peptide was synthesized from the protein facilities at the University of Illinois.

4.5 Experimental Procedures

***in vitro* transcription constructs, labeling, and RGG peptide and MOV10 purification**

DNA constructs were ordered from IDT

sc1 wt:

5’GCCTCGCTGCCGTCGCCCGCTGCGCAACCCGACCACTCCTTCCACACCGCAGCCCC
TATAGTGAGTCGTATTA3’

sc1 mut:

5’GCCTCGCTGCCGTCGCCCGCTGCGCAACCCGACCACTGGTTCCACACCGCAGCCCC
TATAGTGAGTCGTATTA3’

hASH1:

5’GCCTCGCTGCCGTCGCCACTCGCCCTCCCTGGCCGGATCCCTGTCGGTGCGCCTTC
CACGTTCCCTGGCCAGAAGCCCTATAGTGAGTCGTATTA3’

PSD-95:

5’GCCTCGCTGCCGTCGCCCCAACCCCTGACCCTTTGCCCCCTCCACATTCCCCACTCC
CCAGACCCATCCCTCCCCTTTTCCCCCCTATAGTGAGTCGTATTA3’

RNA was transcribed using T7 RNA polymerase as per manufactures instructions. Transcribed RNA was labeled using the EndTag Nucle Acid Labeling system (Vector annealed by slow cooling from 95C at a 1:1.5 ratio of tether to synthesized RNA.

Minimal RGG peptide was synthesized by the protein facilities at the University of Illinois Urbana Champaign Protein Services Facility and resuspended at 1uM in water. The peptide sequence is the minimal RGG peptide established in [8].

HEK293F cells were grown to 5x10^5 cells/mL and transfected with myc-MOV10 using PEI (Sigma). 24-48 hrs after transfection, cells were harvested and lysed and myc-MOV10 was immunoprecipitated using myc-conjugated agarose beads (Sigma) and eluted with myc peptide after immunoprecipitation.

Single molecule imaging and experimental setup

Slides were prepared as described in [14]. Briefly, quarts slides and coverslips were cleaned and treated with methanol, acetone, KOH, burned and treated with aminosilane followed by a coating of 3% biotin PEG and 97% PEG.

Heteroduplex RNA/DNA constructs were immobilized on the slide surface. Unbound molecules were washed with buffer containing 1 mg/mL glucose oxidase, .4% (w/v) D glucose, 0.04 mg/mL catalase, and 1% v/v 2- mercaptoethanol.

Prism type total internal reflection microscopy was used to acquire single molecule FRET as described in [15]. A 532-nm Nd:YAG laser was guided through a prism to generate an evanescent field of illumination. A water-immersion objective was used to collect the signal and a 550-nm long pass filter was used to remove the scattered light. Cy3 signals were collected using a 630-nm dichroic mirror and sent to a charge-coupled device camera. Data were recorded with a time resolution of 100 ms as a stream of imaging frames and analyzed with scripts written in interactive data language.

4.6 Figures.

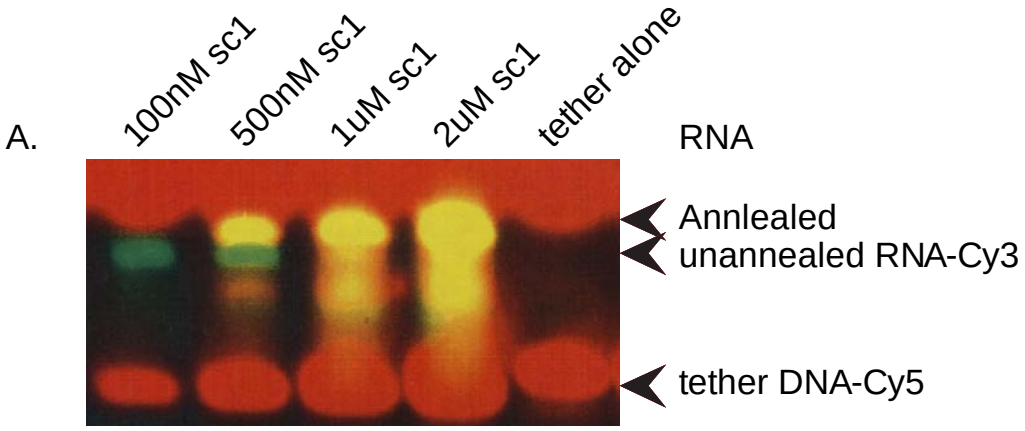

Figure 4.1. Typhoon image of synthesized RNAs. Increasing concentrations of sc1 RNA facilitated more efficient annealing (yellow) of tether DNA (red) to the synthesized mRNA (green).

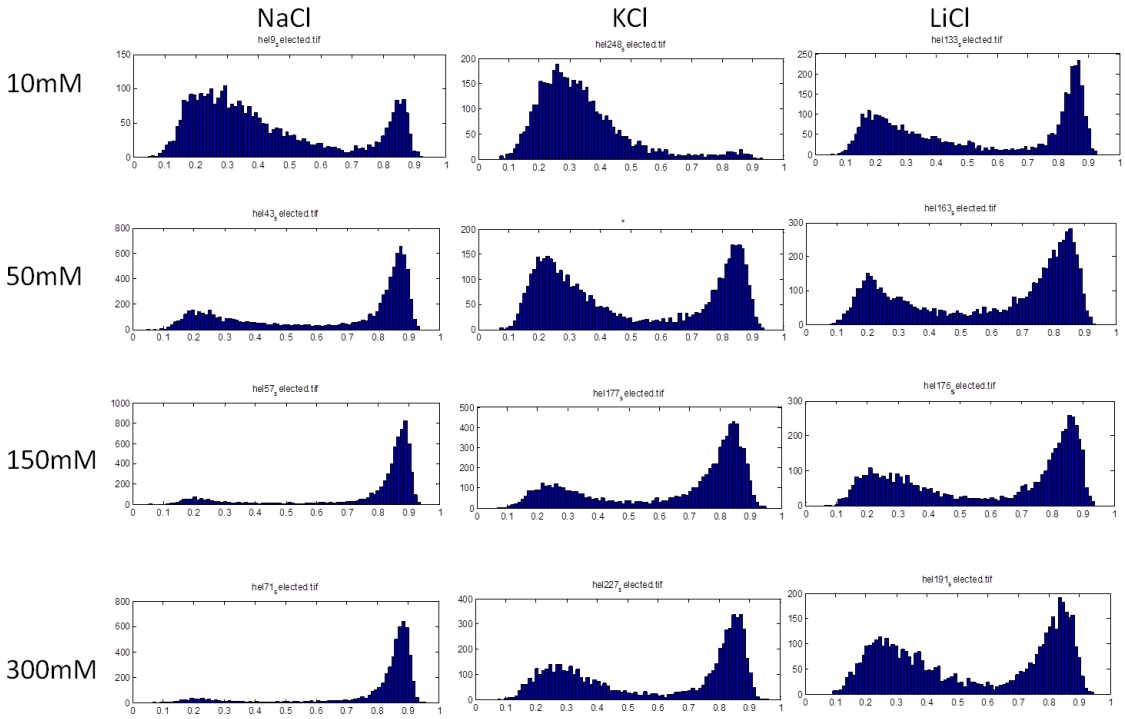

Figure 4.2. Salt titrations on sc1 RNA. NaCl, KCl, and LiCl salt solutions were used titrated at 10, 50, 150, and 300 mM concentrations. High fret was demonstrated most efficiently with NaCl followed by KCl, and LiCl.

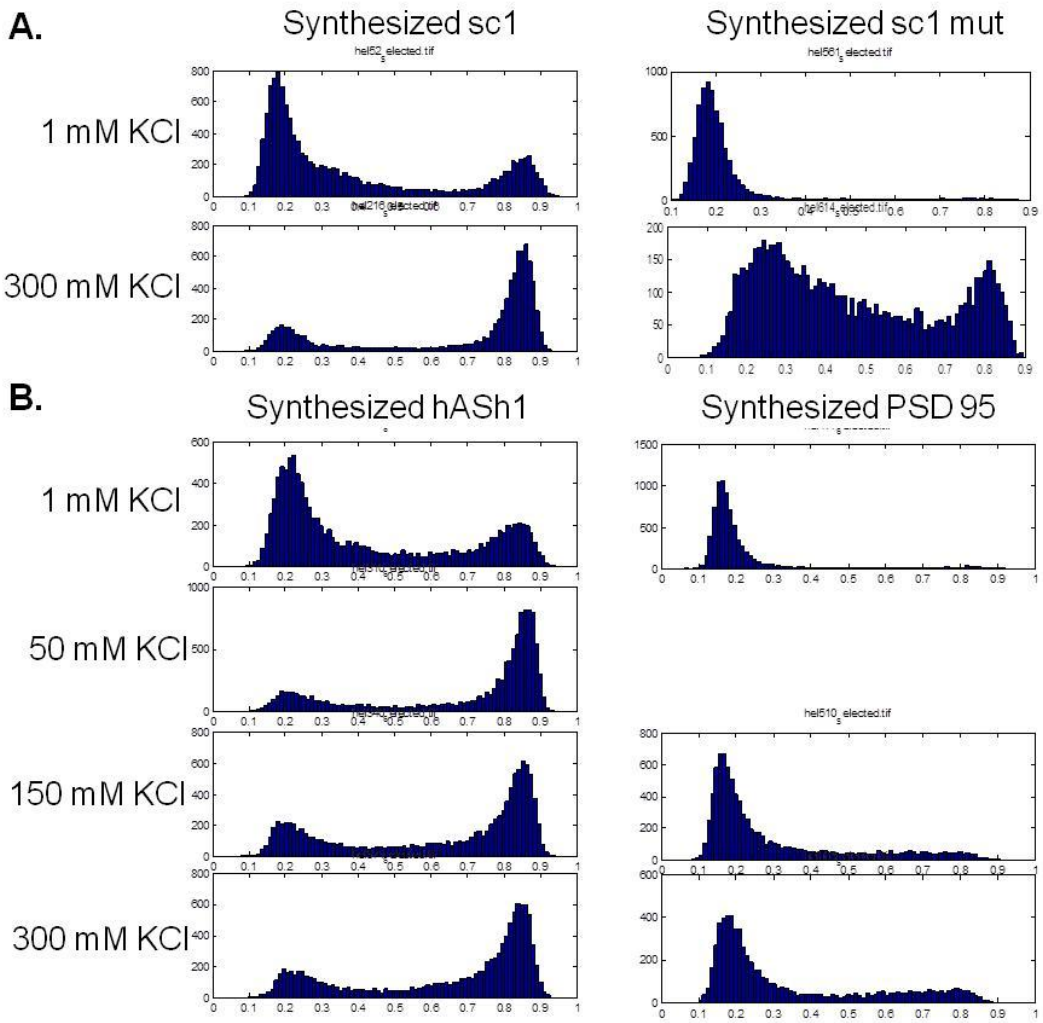

Figure 4.3. Salt titrations of synthesized RNA constructs. A. sc1 folds in high salt concentrations, however sc1 mutant remains largely low-mid fret with a small high fret peak even in 300 mM KCl. B. Synthesized hASH1 folds in the presence of salt, existing in largely high fret states at 50mM KCl. PSD-95 however, did not fold successfully even in high salt concentrations.

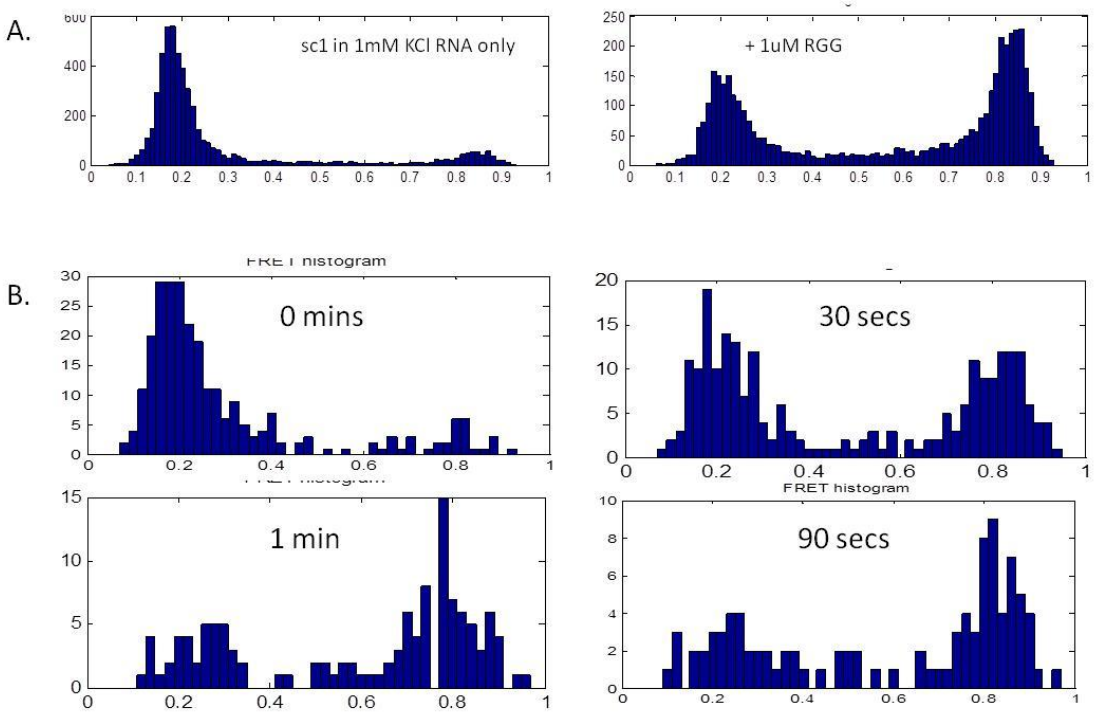

Figure 4.4. RGG peptide induces folding of sc1 RNA in low salt conditions. A. The addition of 1uM RGG peptide induced folding of sc1 RNA at 1mM KCl salt solution. B. sc1 folding occurs within the first 30 seconds of RGG peptide addition.

4.7 References

1. Satapathy, A.K., et al., *Promiscuous usage of nucleotides by the DNA helicase of bacteriophage T7: determinants of nucleotide specificity.* J Biol Chem, 2009. **284**(21): p. 14286-95.
2. Clerici, M., et al., *Unusual bipartite mode of interaction between the nonsense-mediated decay factors, UPF1 and UPF2.* EMBO J, 2009. **28**(15): p. 2293-306.
3. Kadlec, J., et al., *Crystal structure of the UPF2-interacting domain of nonsense-mediated mRNA decay factor UPF1.* RNA, 2006. **12**(10): p. 1817-24.
4. Cheng, W., et al., *Single-base pair unwinding and asynchronous RNA release by the hepatitis C virus NS3 helicase.* Science, 2011. **333**(6050): p. 1746-9.
5. Cheng, W., et al., *NS3 helicase actively separates RNA strands and senses sequence barriers ahead of the opening fork.* Proc Natl Acad Sci U S A, 2007. **104**(35): p. 13954-9.
6. Dumont, S., et al., *RNA translocation and unwinding mechanism of HCV NS3 helicase and its coordination by ATP.* Nature, 2006. **439**(7072): p. 105-8.
7. Darnell, J.C., et al., *Kissing complex RNAs mediate interaction between the Fragile-X mental retardation protein KH2 domain and brain polyribosomes.* Genes Dev, 2005. **19**(8): p. 903-18.
8. Phan, A.T.n., et al., *Structure-function studies of FMRP RGG peptide recognition of an RNA duplex-quadruplex junction.* Nat Struct Mol Biol, 2011. **18**(7): p. 796-804.
9. Yodh, J.G., M. Schlierf, and T. Ha, *Insight into helicase mechanism and function revealed through single-molecule approaches.* Q Rev Biophys, 2010. **43**(2): p. 185-217.
10. Kruger, A.C. and V. Birkedal, *Single molecule FRET data analysis procedures for FRET efficiency determination: Probing the conformations of nucleic acid structures.* Methods, 2013.
11. Sen, D. and W. Gilbert, *A sodium-potassium switch in the formation of four-stranded G4-DNA.* Nature, 1990. **344**(6265): p. 410-4.
12. Brown, V., et al., *Microarray identification of FMRP-associated brain mRNAs and altered mRNA translational profiles in fragile X syndrome.* Cell, 2001. **107**(4): p. 477-87.
13. Zanotti, K.J., et al., *Thermodynamics of the Fragile X Mental Retardation Protein RGG Box Interactions with G Quartet Forming RNA,Ä†.* Biochemistry, 2006. **45**(27): p. 8319-8330.
14. Hwang, H., H. Kim, and S. Myong, *Protein induced fluorescence enhancement as a single molecule assay with short distance sensitivity.* Proc Natl Acad Sci U S A, 2011. **108**(18): p. 7414-8.
15. Hwang, H., et al., *POT1-TPP1 regulates telomeric overhang structural dynamics.* Structure, 2012. **20**(11): p. 1872-80.

Chapter 5. MOV10 in the 5'UTR

5.1 Abstract

MOV10 was found to bind and regulate mRNAs through studies presented in chapter 3; however its role in the 5'UTR was not yet elucidated. In this chapter, we describe a novel role for MOV10 in regulating translation of mRNA targets through modification of secondary structure. hASH1 is an mRNA target bound and regulated by FMRP. This upregulation is mediated through the 5'UTR and also dependent on the presence of MOV10.

5.2 Introduction

G-Quadruplexes in nucleic acids

G-quadruplexes (GQs) are very stable secondary structures formed by nucleic acids, formed by the stacking of guanine tretrads. These bases bond in non-Watson Crick pairs, but rather through Hoogsteen base pairing where each guanine acts as a donor and acceptor for hydrogen bonds. G quadruplexes can also form between multiple strands making these *inter*- versus *intra*-molecular structures. GQs are stabilized by monovalent cations, preferring K^+ < Na^+ < Li^+[1]. GQs have been implicated in a number of regulatory functions from nuclear transcription to cytoplasmic translation.

DNA G-Quadruplexes

In DNA, GQs are most familiarly present at the telomere, which is rich in hexameric TTAGGG repeats [2, 3], in addition to many promoter regions in DNA. These molecules take on several conformations from parallel to anti-parallel, basket types to inter and intra molecular structures (reviewed in [4]). This variability in sequence and structure makes G quadruplexes interesting secondary structures that act as regulatory switches in nucleic acids. Telomeres form stable GQs and protect the end of chromosomes and inhibit the action of telomerase, which is activated in a large percentage of cancers. Many cancers (expand a little more). Additionally DNA GQs are involved in regulation of gene transcription. Several loci are tightly regulated such as c-MYC, KRAS, and hTERT, where the prevalence of GQs within the promoter regions can regulate gene transcription [5, 6]. At the level of DNA, these secondary structures are

important for the first steps in regulation, potentially becoming novel therapeutic targets for diseases such as cancers [7].

RNA G-Quadruplexes

RNA structures demonstrate more structural flexibility due to their single stranded nature and therefore can form more stable and stronger GQs [8]. In RNA molecules, GQs can serve as translational regulators acting both in the 3'and 5'UTRs as well as signals that may act as a localization signal as have been described for CamKII and PSD-95 [9].

In translation, the 5'UTR plays a variety of roles in initiation, scanning, and elongation. The presence of strong secondary structures near the 5'cap or even potentially masking the AUG start codon are all factors which may affect states of translation (reviewed in [10]). Some examples of strong secondary structure inhibiting translation have been demonstrated in NRAS, where GQ structures present closer to the 5'cap are more inhibitory compared to if they were located more centrally in the UTR [11, 12]. The same is true for a number of other genes such as the matrix metalloproteinase (MT3) and also BCL-2 [13, 14]. However, GQ structures may also play a role in facilitating translation by acting as an internal ribosome entry site (IRES), permitting cap-independent translation which is the case for VEGF, where a G quadruplex structure is important for facilitating translation [15]. These studies demonstrate that localization of the GQs in the 5'UTR play an important regulatory role in mRNAs.

Despite the prevalence of GQ structures throughout the cell, only a small handful of proteins have been demonstrated to specifically bind and unwind GQ secondary structure. RHAU, the RNA helicase associated with AU-rich elements is a DEAH-box RNA helicase that has been found to bind and also resolve G quadruplex RNA structures at the end of telomeres [16]. RHAU has also been published to resolve tetrameric G-quadruplexes as well as associate with a number of RNAs containing GQ sequences [17, 18].

FMRP and GQs

FMRP binds and recognizes RNA GQ structures, sc1 being one example of a high affinity binder as was reviewed in Chapter 1. An interesting target that FMRP binds and regulates its own transcript through GQs found in its own transcript, FMR1 [19]. The G-quadruplex region of FMRP acts as an exonic splicing enhancer, regulating the splicing of exon

15 of the FMR protein, further describing important roles for both the GQ binding abilities of FMRP and also the secondary structure of the RNA. FMRP, besides binding its own transcript, is also required for proper localization of two neuronal transcripts: PSD-95 and CAMKII mRNAs to the neurites [20]. PSD-95 and CAMKII have been well studied to be regulated and bound by FMRP [21-23]. These two mRNAs contain G quadruplex forming sequences as confirmed by reverse transcription and RNase protection assays. PSD-95 contained three tandem GQs while CAMKII only contained one, however removing these specific structures resulted in the loss of neurite localization of these transcripts.

5.3 Results

MOV10 associates with GQ containing sequences in the 5'UTR

In chapter 3, we found that MOV10 demonstrated specificity for GQ binding. Co-incidentally, this is a pattern we found in a number of the CLIP targets. What became interesting was the fact that MOV10 bound mRNA targets both in the 3'UTR as was studied in Chapter 3. While there were less targets bound in the 5'UTR, we found that of the 14 targets bound, 6 of them contained GQ forming sequences in the CLIP site, with STK11 containing three potential GQ forming patterns. Interestingly, the GQ containing sequences also had a high percentage of guanine composition compared to the non-GQ containing CLIP sites. What was strikingly different between the two was that the average length of the 5'UTR was about 7 times longer in the GQ containing CLIP sites (1659.5 bases) compared to the non GQ containing CLIP sites in the 5'UTR (224.4 bases if PCDH19 is excluded) (Table 1). This led us to further investigate the role of MOV10 in the 5'UTR.

FMRP requires MOV10 for upregulation of hASH1 mRNA

In 2009, FMRP was found to bind and regulate hASH1 mRNA through its 5'UTR [24]. hASH1, which is a transcription factor for development, was an interesting target due to the unusual length of the 5'UTR (571 nucleotides) as well as the presence of many different motifs: AU rich regions, poly U tracts and two tandem GQ forming sequences located centrally in the UTR. We analyzed the full 5'UTR of hASH1 using QGRS and found two additional G quadruplexes located immediately 3' to the cap, with GQ scores of 18 and 20, comparable to sc1

(Fig 1A). We were interested in using hASH1 as a potential target for studying the role of FMRP and MOV10 binding on a true neuronal target.

FMRP has been demonstrated to bind and increase translational regulation of hASH1, however hASH1 binding was mediated through the U rich region, which we were able to reproduce (Fig 1b left). Because MOV10 demonstrated GQ binding capabilities, we next sought to determine whether MOV10 had an impact on FMRP mediated translational upregulation. We found that knockdown of MOV10 through siRNA treatment inhibited FMRP mediated upregulation, suggesting that FMRP somehow requires MOV10 to regulate hASH1 translation (Fig 1b). Knockdown of MOV10 was efficient, indicating that the effects were mediated by the presence of MOV10. Similar to other brain mRNA targets such as CALM3 and eEF2, hASH1 may potentially require MOV10 to recruit the target to FMRP.

We next sought to determine the RNA binding capabilities of MOV10. MOV10 binds sc1 RNA with specificity, since disruption of the GQ prevented MOV10 association (Chapter 3). MOV10 demonstrated RNA binding ability of sc1 but not sc1 mutant in 5, 75, and 200mM KCl solutions (Fig 2a). Interestingly, MOV10 also demonstrated specificity for poly G beads, but not poly A, C, or U (Fig 2b). hASH1 mRNA was in vitro synthesized and also assessed for MOV10 binding. We found that full length, middle GQ deletion, and poly U tract (DU) all demonstrated binding by MOV10. The polyU deletion (DU) demonstrated less binding by FMRP as was described [24]. Both MOV10 and FMRP specifically bound sc1 but not the sc1 mutant (Fig 2c).

The presence of two tandem GQs present near the 5'cap of the hASH1. Because FMRP bound hASH1 in the polyU tract, and MOV10 demonstrated specificity for GQ structures, we hypothesized that MOV10 could bind and unwind these two tandem structures to facilitate ribosome loading and scanning on the hASH1 mRNA. Thus, we removed the GQs and compared translation in a reticulolysate assay to determine whether the tandem GQs were in fact inhibitory for translation. Upon removal of the GQs, we found that translation of the luciferase construct increased, suggesting that the quadruplexes were inhibiting translation (Fig 3b).

5.4 Discussion

The work presented in this chapter introduces a role for MOV10 in the 5'UTR, especially in mRNA transcripts that have long and highly structured 5'UTRs. Many GQ binding proteins have not yet been elucidated, yet these mRNA secondary structures are prevalent throughout the

genome and transcriptome. Taken together, these studies suggest a potential role for MOV10 in the 5'UTR. MOV10 has been published to be involved in miRNA pathways and also associated with Ago2 [25-27], a role in translation regulation through the 5'UTR has not been well studied. Here, we demonstrate a novel role for translational regulation by MOV10.

These studies suggest that MOV10 is involved in binding of long, highly structured 5'UTRs and may act by facilitating unwinding of secondary structure or somehow enhancing translation of target mRNAs.

5.5 Experimental Procedures

Western blots

The anti-FMRP antibody 1a obtained from Jean-Louis Mandel at the Institute of Genetics in Illkirch, France, was used as a hybridoma supernatant for immunoblotting at a 1/10 dilution. Anti-MOV10 antibody (Bethyl) was used at a 1:1000 dilution for 1 hr at rt or over night at 4C. Antibody reactivity was visualized using an anti-mouse horseradish-peroxidase conjugate (Jackson Laboratories).

Capture assays

RNA capture assays were performed as described [28]. Briefly, purified protein was incubated with biotin-tagged RNA at 30C for 20 minutes and captured on streptavidin coated beads (Dynabeads) for 2 hours at room temperature. Beads were washed and boiled in SDS sample buffer and analyzed by western blot.

Luciferase Transfections and Luciferase assays.

HEK293T cells were plated in 24 well plates at 10^4 cells/well and transfected using PEI (Sigma), and MOV10 specific siRNA or irrelevant siRNA. 24 hrs post transfection, cells were retransfected with siRNA, 100 ng/well luciferase construct and 10ng/well renilla. 24 hrs after, cells were lysed and assayed for luciferase activity. For in vitro transcription translation reactions, hASH1 5'UTR-Luc was transcribed using the MEGAscript T7 kit (Invitrogen). Translation assay was performed as described in [29]. Luciferase assay was carried out using the dual-luciferase reporter assay kit (Promega) as per manufacturer's instructions and measured on a LUMIstar OPTIMA luminometer, programmed with OPTIMA softer v 2.00.

5.6 Tables and Figures

A.

Position	Length	QGRS	G-Score
6	19	GGCCAGGGAACGUGGAAGG	18
36	18	GGAUCCGGCCAGGGAGGG	20
311	14	GGAGGGGAGGGAGG	21
326	20	GGAGGCGGCGUGCAGGGAGG	17

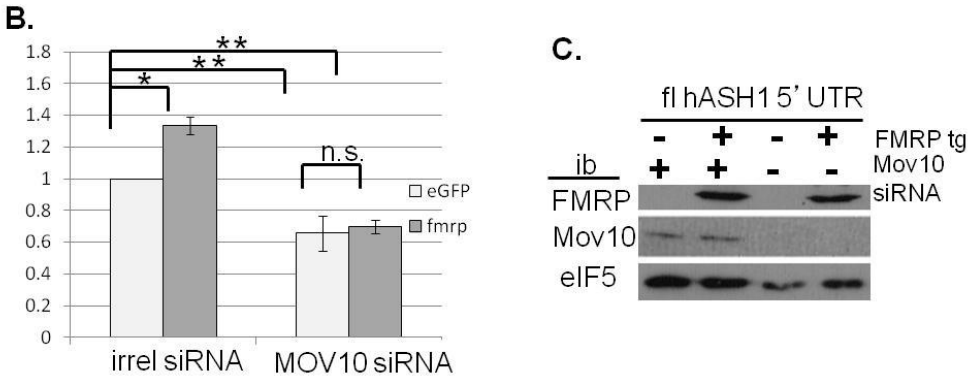

Figure 5.1. FMRP requires MOV10 to upregulate translation of hASH1 mRNA. A. GQRS analysis of the 571nt 5'UTR of hASH1 mRNA. B. FMRP upregulates translation of hASH1 reporter constructs. Knockdown of MOV10 blocks translation upregulation mediated by FMRP. $p<0.05$ is denoted by (*), $p<0.01$ is denoted by (**). C. Western blot confirmation of transfections.

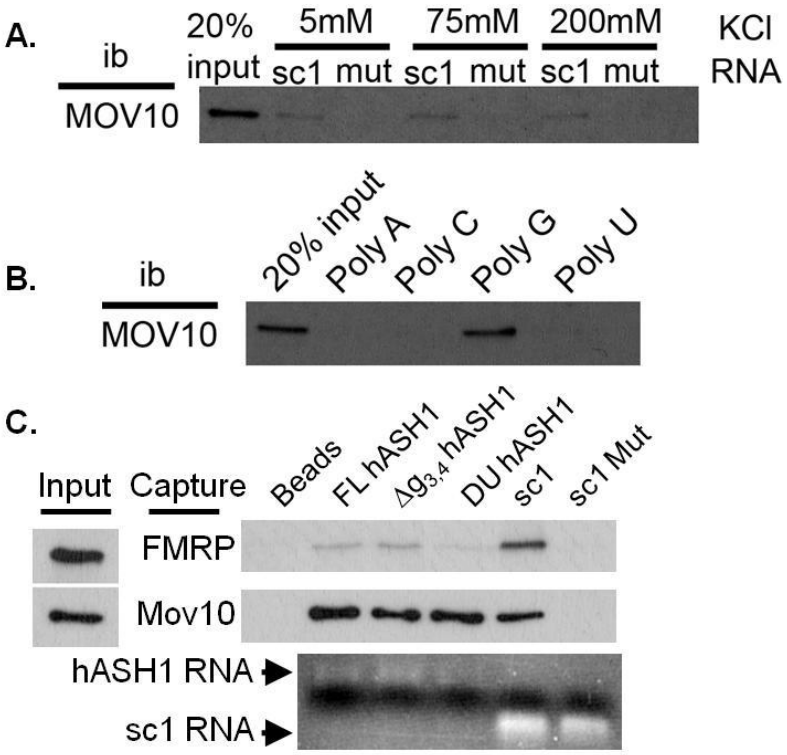

Figure 5.2. MOV10 and FMRP specifically bind similar RNAs. A. MOV10 binds sc1 but not sc1 mutant in RNA capture assays of varying KCl concentrations. B. MOV10 demonstrates specificity for polyG sequences. C. MOV10 and FMRP capture assays demonstrate hASH1 binding. FMRP binding is reduced in the DU mutant, and FMRP and MOV10 binding is disrupted in the sc1 mutant construct.

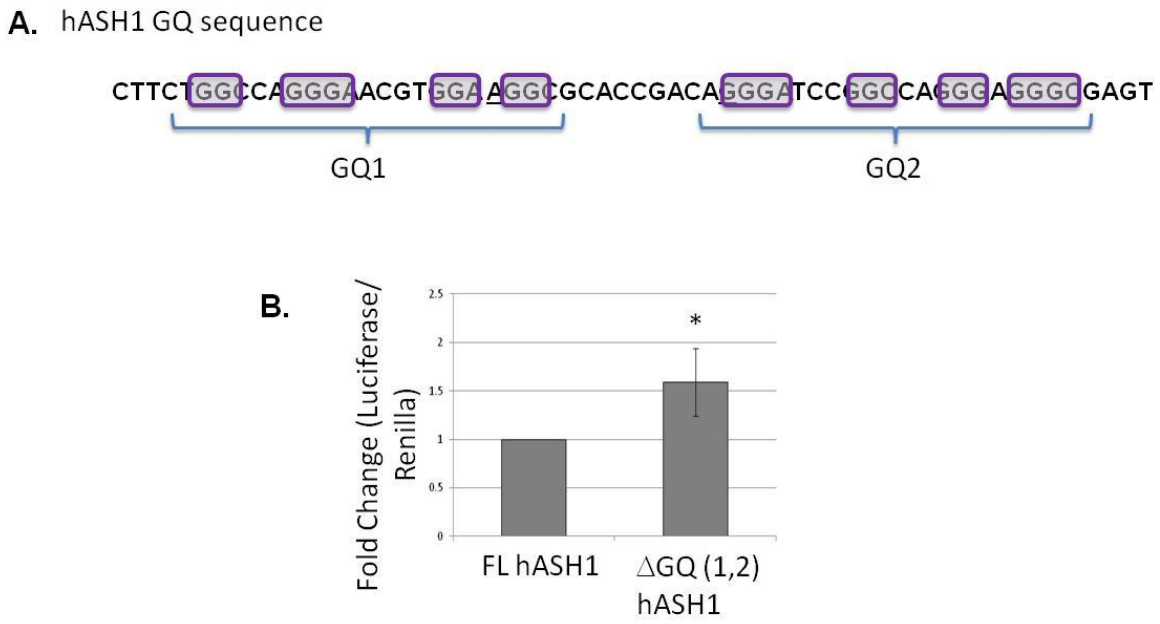

Figure 5.3. 5' tandem hASH1 GQ(1,2) sequence is translationally inhibitory. A. hASH1 sequence of the two tandem 5' GQ sequences, highlighting the GQ forming sequences identified by QGRS. B. in vitro translation assay of the full length hASH1 (FL) compared to the GQ deletion. $p<0.05$ is denoted by (*).

Gene ID	GQ	GQ score	%G	UTR length	avg length
STK11	yes, 3	21	57.50%	1115	1659.5
BRD2	yes	17	47.80%	1701	
HCFC1	yes	20	47.60%	528	
C9orf45	yes	20	45.20%	non-coding	
TULP4	yes	20	43.40%	1357	
LRP5L	yes	11	29.60%	2465	
ZKSCAN1	no		51.90%	219	405.9 (224.4 excluding PCDH19)
PRELID2	no		27.80%	53	
PASK	no		27.50%	133	
OAF	no		25.40%	241	
PCDH19	no		24.60%	1676	
COX7C	no		16%	89	
ZFAND3	no		14%	415	
ZNF219	no		8.60%	421	

Table 5.1. Analysis of 5'UTR CLIP targets bound by MOV10.

5.7 References

1. Sen, D. and W. Gilbert, *A sodium-potassium switch in the formation of four-stranded G4-DNA.* Nature, 1990. **344**(6265): p. 410-4.
2. Moyzis, R.K., et al., *A highly conserved repetitive DNA sequence, (TTAGGG)n, present at the telomeres of human chromosomes.* Proc Natl Acad Sci U S A, 1988. **85**(18): p. 6622-6.
3. Wang, Y. and D.J. Patel, *Solution structure of the human telomeric repeat d[AG3(T2AG3)3] G-tetraplex.* Structure, 1993. **1**(4): p. 263-82.
4. Chen, Y. and D. Yang, *Sequence, stability, and structure of G-quadruplexes and their interactions with drugs.* Curr Protoc Nucleic Acid Chem, 2012. **Chapter 17**: p. Unit17 5.
5. Brooks, T.A., S. Kendrick, and L. Hurley, *Making sense of G-quadruplex and i-motif functions in oncogene promoters.* FEBS J, 2010. **277**(17): p. 3459-69.
6. Huppert, J.L. and S. Balasubramanian, *G-quadruplexes in promoters throughout the human genome.* Nucleic Acids Res, 2007. **35**(2): p. 406-13.
7. Balasubramanian, S., L.H. Hurley, and S. Neidle, *Targeting G-quadruplexes in gene promoters: a novel anticancer strategy?* Nat Rev Drug Discov, 2011. **10**(4): p. 261-75.
8. Zhang, A.Y. and S. Balasubramanian, *The kinetics and folding pathways of intramolecular G-quadruplex nucleic acids.* J Am Chem Soc, 2012. **134**(46): p. 19297-308.
9. Subramanian, M., et al., *G-quadruplex RNA structure as a signal for neurite mRNA targeting.* EMBO Rep, 2011. **12**(7): p. 697-704.
10. Kozak, M., *Regulation of translation via mRNA structure in prokaryotes and eukaryotes.* Gene, 2005. **361**: p. 13-37.
11. Kumari, S., A. Bugaut, and S. Balasubramanian, *Position and stability are determining factors for translation repression by an RNA G-quadruplex-forming sequence within the 5' UTR of the NRAS proto-oncogene.* Biochemistry, 2008. **47**(48): p. 12664-9.
12. Kumari, S., et al., *An RNA G-quadruplex in the 5' UTR of the NRAS proto-oncogene modulates translation.* Nat Chem Biol, 2007. **3**(4): p. 218-21.
13. Shahid, R., A. Bugaut, and S. Balasubramanian, *The BCL-2 5' untranslated region contains an RNA G-quadruplex-forming motif that modulates protein expression.* Biochemistry, 2010. **49**(38): p. 8300-6.
14. Morris, M.J. and S. Basu, *An unusually stable G-quadruplex within the 5'-UTR of the MT3 matrix metalloproteinase mRNA represses translation in eukaryotic cells.* Biochemistry, 2009. **48**(23): p. 5313-9.
15. Morris, M.J., et al., *An RNA G-quadruplex is essential for cap-independent translation initiation in human VEGF IRES.* J Am Chem Soc, 2010. **132**(50): p. 17831-9.
16. Lattmann, S., et al., *The DEAH-box RNA helicase RHAU binds an intramolecular RNA G-quadruplex in TERC and associates with telomerase holoenzyme.* Nucleic Acids Res, 2011. **39**(21): p. 9390-404.
17. Creacy, S.D., et al., *G4 resolvase 1 binds both DNA and RNA tetramolecular quadruplex with high affinity and is the major source of tetramolecular quadruplex G4-DNA and G4-RNA resolving activity in HeLa cell lysates.* J Biol Chem, 2008. **283**(50): p. 34626-34.

18. Vaughn, J.P., et al., *The DEXH protein product of the DHX36 gene is the major source of tetramolecular quadruplex G4-DNA resolving activity in HeLa cell lysates.* J Biol Chem, 2005. **280**(46): p. 38117-20.
19. Didiot, M.-C., et al., *The G-quartet containing FMRP binding site in FMR1 mRNA is a potent exonic splicing enhancer.* Nucl. Acids Res. , 2008. **36**(15): p. 4902-4912.
20. Subramanian, M., et al., *G-quadruplex RNA structure as a signal for neurite mRNA targeting.* EMBO Rep, 2011. **12**(7): p. 697-704.
21. Muddashetty, R.S., et al., *Reversible Inhibition of PSD-95 mRNA Translation by miR-125a, FMRP Phosphorylation, and mGluR Signaling.* Molecular Cell, 2011. **42**(5): p. 673-688.
22. Zalfa, F., et al., *A new function for the fragile X mental retardation protein in regulation of PSD-95 mRNA stability.* Nat Neurosci, 2007. **10**(5): p. 578-87.
23. Kao, D.I., et al., *Altered mRNA transport, docking, and protein translation in neurons lacking fragile X mental retardation protein.* Proc Natl Acad Sci U S A, 2010. **107**(35): p. 15601-6.
24. Fahling, M., et al., *Translational Regulation of the Human Achaete-scute Homologue-1 by Fragile X Mental Retardation Protein.* J. Biol. Chem. , 2009. **284**(7): p. 4255-4266.
25. Chendrimada, T.P., et al., *MicroRNA silencing through RISC recruitment of eIF6.* Nature, 2007. **447**(7146): p. 823-8.
26. Meister, G., et al., *Identification of novel argonaute-associated proteins.* Curr Biol, 2005. **15**(23): p. 2149-55.
27. Sievers, C., et al., *Mixture models and wavelet transforms reveal high confidence RNA-protein interaction sites in MOV10 PAR-CLIP data.* Nucleic Acids Research, 2012.
28. Stetler, A., et al., *Identification and characterization of the methyl arginines in the fragile X mental retardation protein Fmrp.* Hum Mol Genet, 2006. **15**(1): p. 87-96.
29. Chiang, P.W., L.E. Carpenter, and P.J. Hagerman, *The 5'-untranslated region of the FMR1 message facilitates translation by internal ribosome entry.* J Biol Chem, 2001. **276**(41): p. 37916-21.

Chapter 6. Conclusions and future directions

6.1 Concluding remarks

Through my thesis work, I have demonstrated in Chapter 2 that FMRP binds nascent mRNAs in the nucleus and subsequently exports these target mRNAs out into the cytoplasm. Through a novel mechanism described in Chapter 3, we show that MOV10, a putative RNA helicase and Argonaute2 are key components in regulation of FMRP bound mRNA targets. As these cellular mechanisms were slowly revealed, we began to observe RNA and protein behavior by turning to single molecule resolution in Chapter 4. Through these efforts, we have traveled with an mRNA molecule from transcription until its fate in degradation and sought to clarify the means by which these proteins work together to make a cell function normally. In chapter 5, I discuss preliminary work demonstrating a role for MOV10 in the 5'UTR. These UTRs are long and highly structured suggesting a necessity for unwinding assistance. Future experiments to better understand the mechanism of how FMRP utilizes associated proteins to function as a regulator of translation are presented in this chapter.

Summary 1.

In chapter 2, we discuss the mechanism by which FMRP binds and recognizes its mRNA transcript. Through the use of the *Xenopus laevis* oocyte system, we were able to demonstrate that FMRP binds and recognizes nascent mRNA transcripts in the nucleus. FMRP bound in the nucleus is then exported via Tap/Nxf1 and then processed further in the cytoplasm for subsequent translation.

Future work for Summary 1.

1. **Identify the mechanism by which FMRP is selected for import into the nucleus.** Currently, it is largely unknown is how FMRP shuttles in and out of the nucleus. We demonstrated that Tap/Nxf1 is important for nuclear export; however import into the nucleus is understudied. The nuclear localization sequence of FMRP is a non-canonical NLS that contains many lysines and arginines [1, 2]. Recently, in a screen of developmentally delayed males without CGG repeat expansion, the traditional mechanism of FMR1 silencing, several

mutations in the FMR1 gene were identified. One notable mutation was found within the nuclear localization sequence, R138Q, which alters a conserved residue in the FMRP NLS, highlighting the importance of nuclear shuttling by FMRP for normal cognitive development [3]. Understanding what proteins are important for nuclear import as well as determining which splice variants of FMRP are involved in nuclear shuttling is a largely understudied area of research.

2. **Determine methylation patterns important for binding nascent mRNA in the nucleus**. Previous work has found that FMRP is methylated on several arginine residues, and that FMRP methylation confers some amount of RNA specificity as well as association of FMRP with mRNAs and polyribosomes [4, 5]. Further exploring the role of these post translational modifications and its impact on RNA binding specificity through polysome and binding assays would be an interesting area to study. While it is understood that FMRP is an RNA binding protein, determining how FMRP binds and recognizes specific mRNA targets whether it be for nuclear export, translational regulation, or mRNA localization is a key to understanding the complex disease process of fragile X syndrome.

Summary 2.

Chapter 3 described a novel associated protein, MOV10—a largely uncharacterized putative RNA helicase, and how the two proteins bind and regulate translation of mRNA through competition or facilitation of Ago2 mediated miRNA regulation. We found that FMRP and MOV10 both associated in similar granules in brain and in cells and are also present along polyribosomes. Interestingly, we also discovered that MOV10 specifically recognizes and binds RNA GQs, which is a structure that FMRP has also been published to bind. We found that mRNA targets specifically bound by MOV10 had different fates in MOV10 knockdown versus overexpression. These changes in fate were namely mediated through the 3'UTR, suggesting a role in miRNA mediated regulation.

We identified several mRNAs that contained MOV10 CLIP sites which overlapped with Ago2 binding sites suggesting a miRNA mediated mechanism of regulation. We found that the presence of secondary structure, namely G-Quadruplexes may act as a landing site for MOV10 such that binding of MOV10 would compete with Ago2 if the binding sites were overlapping. In these cases, MOV10 acted in a protective manner, preventing Ago2 from mediating RNA

degradation. In the absence of MOV10, Ago2 binding sites were then exposed, allowing Ago2 to destabilize the bound mRNA.

Future work for summary 2.

1. **Identify how GQ sequences influence MOV10 binding and Ago2 mediated translational regulation.** We described a few targets, Phact2, TGFB1, MAZ, and SamHD1, which are regulated by miRNAs and also affected by the presence or absence of MOV10. Further pursing the role of miRNAs and MOV10 binding would be interesting to develop by performing mutational analysis to tease apart whether it is the presence of secondary structure or miRNA binding that is influencing regulation. One interesting target that is currently being pursued is MAZ which we found to be a candidate example of MOV10 inhibiting miRNA mediated degradation that contains both miRNAs and GQs in the CLIP binding sites. By mutating the seed sequence without hindering the GQ s and also disrupting the GQ structure without affecting the miRNA binding site for MAZ as well as other mRNA targets would help us determine how MOV10 either helps or inhibits regulation.
2. **Determine whether phosphorylation status of FMRP influences MOV10 association**. FMRP, in addition to being methylated on arginine residues, is also phosphorylated on serine residues, influencing translation state of polyribosomes [6]. In addition to modulating translation, phosphorylation also acts as a switch to modulate its interactions with Dicer [7]. Determining whether or not MOV10 association with FMRP is dependent on phosphorylation status of FMRP would shed light on what aspects of miRNA mediated regulation the two proteins are involved.

Summary 3.

In this chapter, we begin to explore the possibility of studying MOV10 and FMRP together at the single molecule level to begin understanding the dynamics between FMRP and MOV10. We found that the model GQ sc1 folded in a salt dependent manner that was detectable by FRET. These studies have never before been validated at the single molecule level, making this an exciting avenue to explore. We tested the G quadruplexes of hASH1 in addition to PSD-95 and also the sc1 mutant. Similar to previous work [8], sc1 became highly structured in the presence of the RGG peptide as observed by single molecule FRET.

Future work for summary 3.

1. **Demonstrate MOV10 helicase activity using smFRET.** Chapter 4 sets the groundwork to study the physical mechanism by which MOV10 interacts with target mRNAs. We now have identified the specific region that MOV10 binds from CLIP data presented in Chapter 3. These sequences can be analyzed for GQ formation and subsequently used to design novel RNA substrates to be used for single molecule studies. Because we now know specific targets, we can use these mRNAs to answer the questions: Does MOV10 translocate or unwind GQ structures? Does MOV10 require ATP? Does MOV10 displace FMRP on mRNA? Amongst other questions. To begin these studies, full length functional MOV10 must be available, either through the use of insect cell purification or mammalian cell purification, which has been marginally successful. While mammalian cell purification has been successful in generating enough full length protein to pursue basic capture assays, it has not been in high enough concentrations to successfully perform the proposed studies. Through purification via sf9 insect cell culture, full length protein may be generated for these studies.
2. **How do FMRP and MOV10 act together on the same mRNA?** FMRP and MOV10 bind similar mRNA targets, however the proximal localization and binding specificities of these two proteins on the same mRNA is unknown. By also isolating full length FMRP through insect cultures, we can begin to answer the question of whether or not binding of the two proteins act cooperatively or competitively.

Summary 4.

Chapter 5 describes a role for MOV10 in the 5'UTR. We studied the role of MOV10 in the miRNA pathway, regulating protein and mRNA levels via the 3'UTR. However, MOV10 plays a broad role in the fate of RNAs as it is implicated in the infectivity and also replication of RNA viruses such as HIV and Hepatits D [9-11] and recently also involved in long the inhibition of retrotransposon LINE1 mobility throughout the genome as well as associating with the LINE1 RNA and regulating its stability [12]. From analysis of the CLIP data, we found several mRNA targets where MOV10 bound the 5'UTR. Interestingly, those CLIP targets that contained a GQ within the binding site also had very long 5'UTRs. hASH1, a recently described target of FMRP,

also had a long 5'UTR as well as two tandem GQ sequences at the 5'cap, which are inhibitory for translation.

Future work for summary 4.

1. **Does MOV10 affect translation initiation and efficient ribosome loading on highly structured 5'UTRs?** MOV10 demonstrated an interesting pattern of binding in the 5'UTR. CLIP targets that contained GQ sequences in the binding site had considerably longer 5'UTR lengths than the mRNA targets that did not contain GQ sequences in the CLIP site. Understanding the role of MOV10 in influencing protein levels of each target and separating the role of MOV10 in the 5'UTR from the 3'UTR is a promising area of study. Currently, there are few known helicases that modify GQ structures on mRNAs, and identifying the mechanism by which MOV10 influences secondary structure on target mRNAs will elucidate a novel mechanism of translational regulation that is independent of the miRNA pathway.

Conclusions

FMRP is important for proper neuronal development as the absence of FMRP is the cause of fragile X syndrome. By understanding how FMRP binds and recognizes target mRNAs as well as identifying mechanisms by which FMRP and associated proteins are capable of exerting regulatory functions on these mRNA targets is a first step towards more clearly understanding the disease process of fragile X.

6.2 Figures

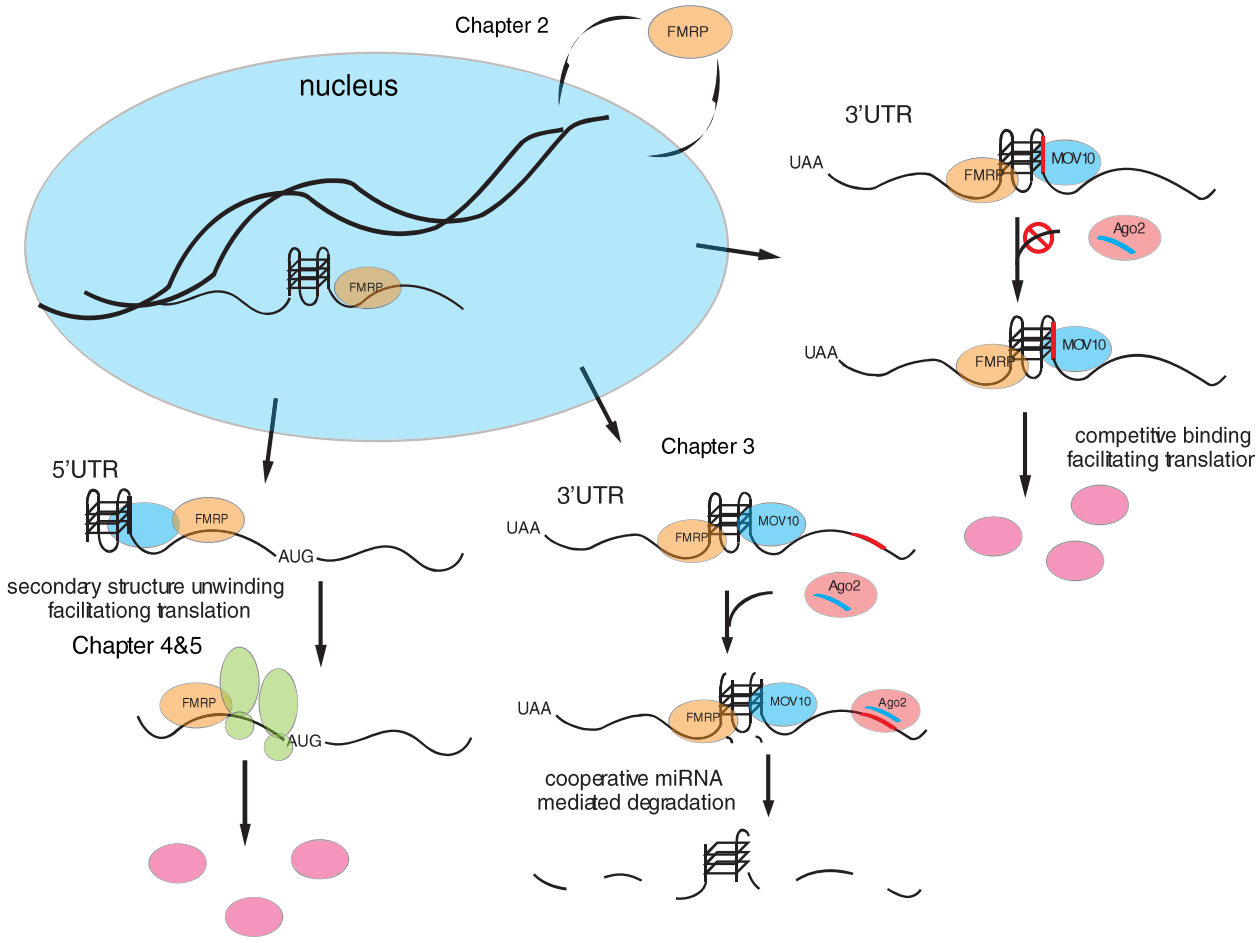

Figure 6.1. Model summary of work performed.

6.3 References

1. Bardoni, B., et al., *Analysis of Domains affecting intracellular localization of the FMRP protein.* Neurobiol. Dis., 1997. **4**: p. 329-336.
2. Eberhart, D.E., et al., *The fragile X mental retardation protein is a ribonucleoprotein containing both nuclear localization and nuclear export signals.* Hum Mol Genet, 1996. **5**(8): p. 1083-91.
3. Collins, S.C., et al., *Identification of novel FMR1 variants by massively parallel sequencing in developmentally delayed males.* Am J Med Genet A, 2010. **152A**(10): p. 2512-20.
4. Blackwell, E., X. Zhang, and S. Ceman, *Arginines of the RGG box regulate FMRP association with polyribosomes and mRNA.* Human Molecular Genetics, 2010. **19**(7): p. 1314-23.
5. Stetler, A., et al., *Identification and characterization of the methyl arginines in the fragile X mental retardation protein Fmrp.* Hum Mol Genet, 2006. **15**(1): p. 87-96.
6. Ceman, S., et al., *Phosphorylation influences the translation state of FMRP-associated polyribosomes.* Hum Mol Genet, 2003. **12**(24): p. 3295-305.
7. Cheever, A. and S. Ceman, *Phosphorylation of FMRP inhibits association with Dicer.* RNA, 2009. **15**(3): p. 362-9.
8. Phan, A.T.n., et al., *Structure-function studies of FMRP RGG peptide recognition of an RNA duplex-quadruplex junction.* Nat Struct Mol Biol, 2011. **18**(7): p. 796-804.
9. Burdick, R., et al., *P Body-Associated Protein Mov10 Inhibits HIV-1 Replication at Multiple Stages.* J. Virol. , 2010. **84**(19): p. 10241-53.
10. Furtak, V., et al., *Perturbation of the P-Body Component Mov10 Inhibits HIV-1 Infectivity.* PLoS ONE, 2010. **5**(2): p. e9081.
11. Wang, X., et al., *Moloney Leukemia Virus 10 (MOV10) Protein Inhibits Retrovirus Replication.* Journal of Biological Chemistry, 2010. **285**(19): p. 14346-14355
12. Li, X., et al., *The MOV10 Helicase Inhibits LINE-1 Mobility.* J Biol Chem, 2013. **288**(29): p. 21148-60.